Dissertations   Theses and Dissertations

1978

The Interaction of Thioxanthenones with Nucleic Acids

Laszlo Bodoni
Loyola University Chicago

Recommended Citation

THE INTERACTION OF

THIOXANTHENONES WITH

NUCLEIC ACIDS

by

Laszlo Bodoni

A Dissertation

Submitted to the Faculty of the Graduate School

of Loyola University of Chicago in Partial Fulfillment

of the Requirements for the Degree of

Doctor of Philosophy

May

1978

ACKNOWLEDGEMENTS

VITA

The author, Laszlo Bodoni, is the son of Laszlo Bodoni and Margit (Henter) Bodoni. He was born August 14, 1939, in Szeged, Hungary.

His elementary education was obtained in the public schools of Szeged, Hungary, and secondary education at the Radnóti Miklós High School, Szeged, Hungary, where he graduated in 1957.

In September, 1958, he entered the University of Szeged, and in June 1963, received a Diploma with a major in physical chemistry.

He joined the Department of Biochemistry and Biophysics of Loyola University of Chicago in the fall of 1971.

TABLE OF CONTENTS

LIST OF TABLES

CHAPTER I

INTRODUCTION

A number of thioxanthenone derivatives are known to possess
schistosomicidal, carcinostatic, and bacteriostatic activities.
Miracil D, as one of the most potent thioxanthenones, and its congeners
have been the subject of intense investigations for nearly three
decades. The majority of the investigations have been concerned
mainly with the biological effects of these compounds. Their mode of
action at the molecular level is not understood yet. This dissertation
represents an effort to correlate some of the physicochemical and bio-
logical properties of two thioxanthenones (see section I.8).

I.1. The Structure of Thioxanthenone

Thioxanthenone (Figure 1) has a permanent electric dipole moment
of 2.59 Debeyes in benzene at 25 $^\circ$C (Aroney et al., 1971). Assuming the
participation of the d-orbitals of the sulfur atom in the formation of
molecular orbitals, the bond order of the carbonyl C=O bond is calcu-
lated to be close to that of a carbon-carbon bond of benzene (Given et
al., 1965). These findings suggest that the thioxanthenone molecule is
best described by the resonance structures shown in Figure 2. This de-
localization of electrons leads to a charge distribution with permanent
electric dipole moment, the vector of which is located along the C9-S10
axis. In addition, the possibility that a conjugated double bond
system forms over the three rings lends credibility to a planar three-
ring structure. Although this possibility was doubted lately (Aizen-

1

2

Figure 1. The structural formula of thioxanthenone (10-thioxanthene-9-one).

4
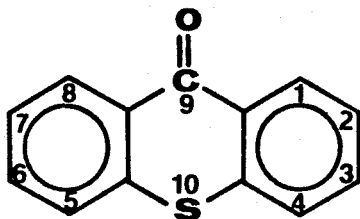
Figure 2. Resonance structures for thioxanthenone.
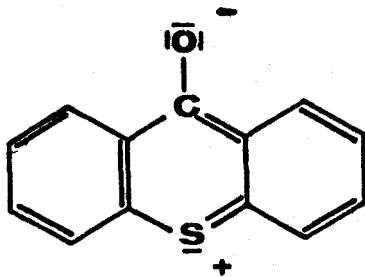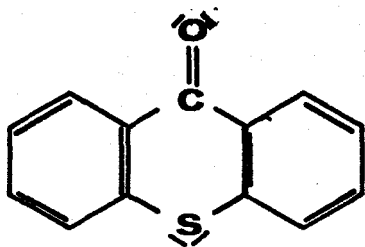
shtat et al., 1972), no good evidence exists to suggest that the thio-
xanthenone ring is not planar.

The importance of the exocyclic oxygen atom in maintaining the
planar ring structure can be demonstrated by the comparison of the thio-
xanthenone and thioxanthene (Figure 3) system. Thioxanthene is also a
polar molecule, but based on the measurement of dipole moments it has
been concluded that the molecule is definitely not planar (Aroney et
al., 1969). In fact, the dihedral angle determined by the planes of the
two benzene rings is calculated to be 135 $^{\circ}$ in carbon tetracholride and
160 $^{\circ}$ in benzene. NMR measurements have provided evidence that the
molecule rapidly inverts between the two possible dihedral conformations
(Aizenshtat et al., 1972).

I.2. The Structure and Physicochemical Properties of Thioxanthenone
Derivatives

Miracil D (Kikuth et al., 1946) is the trade name (Bayer) for
1-(4-ethyl-1,4-diazahexyl)-4-methyl-10-thioxanthene-9-one (Figure 4).
It is also marketed under the trade names Nilodin (Burroughs Wellcome)
and Lucanthone (Calbiochem). This crystalline yellow solid has a mole-
cular weight of 376.7 daltons (as monohydrochloride) and is soluble in
water up to 1-2 % (Blair, 1958; Hawking and Ross, 1948). Salts
decrease its solubility (Lea et al., 1972). Its melting point varies
between 195 and 197 $^{\circ}$C according to different authors (Blanz and
French, 1963; Mauss, 1948; Sharp, 1951). Infrared spectroscopy studies
suggest that in the solid phase the distal nitrogen atom in Miracil D
monohydrochloride is protonated (Zilversmit, 1970).

In aquaeous solution both nitrogen atoms of Miracil D partici-

Figure 3.   The structural formula of 10-thioxanthene.
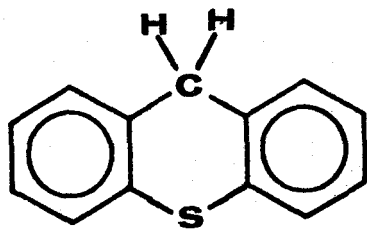
Figure 4. The structural formula of Miracil D (1-(4-ethyl-1,4-di-
azahexyl)-4-methyl-10-thioxanthene-9-one).
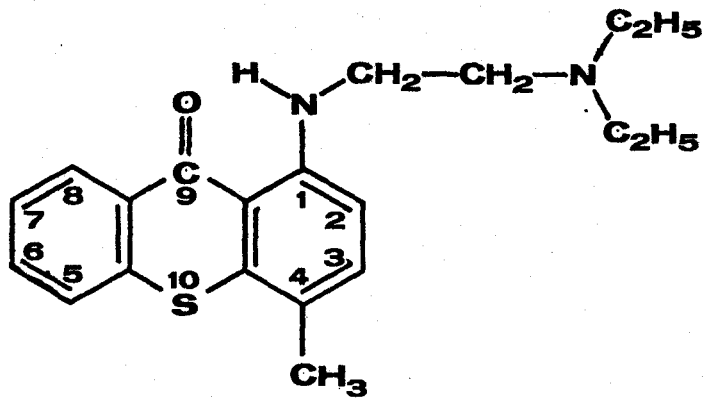
pate in acid-base equilibria. The pK_a of the proximal nitrogen atom was determined spectrophotometrically and found to be -0.20 (Zilversmit, 1970). Since the free base is not soluble in water, the pK_a of the distal nitrogen atom was determined from titration curves in ethanol-water mixtures (Munro, 1961). Extrapolation to pure water gave a pK_a of 7.4.

On the basis of electronic and vibrational spectral studies, Zilversmit found that the hydrogen atom on the proximal nitrogen atom forms an intramolecular hydrogen bond with the carbonyl oxygen of Miracil D, and the trigonal proximal nitrogen atom is coplanar with the heterocyclic ring system (Zilversmit, 1971).

The tendency of Miracil D to form aggregates in aquaeous solutions was noted in the work of Scholtan (Scholtan, 1959). In this study, sedimentation and diffusion coefficient measurements were combined to assess the degree of aggregation. However, the conditions used for these studies were not carefully defined and the validity of the quantitative findings is open to some question.

Methyl substitution on the proximal nitrogen atom of Miracil D leads to a conformational change in the molecular structure. The structure of methyl-Miracil D (Figure 5a) does not permit the formation of an intramolecular hydrogen bond. The steric interference between the methyl group and the oxygen atom of the carbonyl group necessitates a rotation of the amine side chain on the C1-proximal nitrogen atom bond axis to permit these substituents to achieve their Van der Waals separation (Zilversmit, 1970). As a result of this rotation, the conjugation of the lone electron pair of the proximal nitrogen atom to

Figure 5a. The structural formula of methyl-Miracil D (1-(4-ethyl-

1-methyl-1,4-diazahexyl)-4-methyl-10-thioxanthene-9-one).
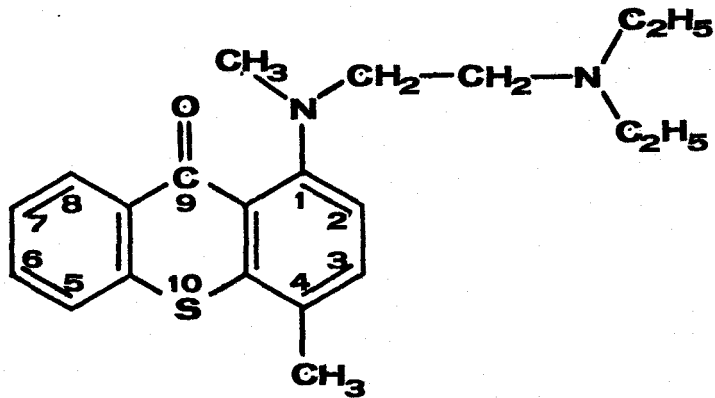
the aromatic ring system is reduced, and the electron density of the nitrogen atom is increased. The pK_a of the proximal nitrogen atom is 3.41 contrasted with a corresponding value of -0.20 for Miracil D.

MDMT (1-(4-methyl-1,4-diazapentyl)-4-methyl-10-thioxanthene) (Figure 5b), although not a thioxanthenone, will also be considered in this investigation. The MDMT molecule contains the 10-thioxanthene ring structure (Figure 3), and, therefore, the MDMT molecule is not planar but rather the molecule rapidly inverts between the two possible dihedral conformations (see section I.1). The purpose of this selection is to examine the effect of ring puckering on the intercalation process (see section I.6.2) and on the inhibiton of DNA dependent RNA synthesis.

I.3. Schistosomicidal Activity of Thioxanthenones

Schistosomes (Class Trematoda, Genus Schistosoma) are parasites which pass through a number of stages in their development. Several species of animals serve as hosts. In the disease schistosomiasis (also called bilharziasis), schistosomes penetrate the blood vessels of the urinary bladder, intestines, liver, and spleen of their hosts. Certain snails, in which the schistosomes spend one of their life cycles, act as intermediate hosts in the transmission of the disease. A particular segment of human populations, mostly in tropical countries, is infected by the species S. mansoni (South America), S. haematobium (Egypt), and S. japonicum (Philippines).

The discovery of the family of Miracils emerged from the world-wide need for the treatment of schistosomiasis. Miracil D proved to be the most potent member of the family against S. mansoni infections in

Figure 5b. The structural formula of MDMT (1-(4-methyl-1,4-diaza-
pentyl)-4-methyl-10-thioxanthene).
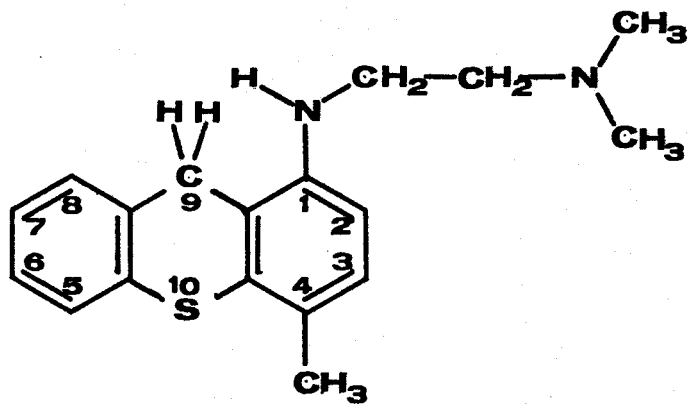
mice and monkies as judged from the decrease of egg secretion in feces
(Kikuth et al., 1946). Autopsy revealed that upon treating with the
drug, the mature schistosomes lose their motility, decrease in size,
and become fragile (Kikuth and Gönnert, 1948). The chief points of
drug attack are the sex- and yolk-cells. Clinical trials were also
succesful in humans (Blair, 1958). Investigations on the structure-ac-
tivity relationship of thioxanthenones showed that activity depends on
the genus of the host, even when the same strain of the parasite is
used for infection (Gönnert, 1961). However, an absolute requirement
for the 4-methyl group of Miracil D is present.

The host-dependent structure-activity relationship engendered
metabolic studies of Miracil D in different species to examine the
possibility that the drug was converted to an active agent in vivo.
In mammalian organisms, there are three major metabolic pathways for
Miracil D: hydroxylation of the 4-methyl group, desethylation of the
terminal side chain nitrogen, and sulfoxidation (Rosi et al., 1967).
The first of these appears crucial for the in vivo activation of
Miracil D, since the hydroxylated derivative, Hycanthone (Figure 6), is
significantly more active than the parent compound. This clarifies
the absolute requirement for the 4-methyl group mentioned earlier.

Recently it was found that Hycanthone is an inhibitor of acetyl-
choline receptors of the nervous system in S. mansoni (Hillman and
Gibler, 1975).

I.4. Carcinostatic Activity of Thioxanthenones

In early experiments, Miracil D was found effective in retarding
the growth of the Walker rat carcinoma, less effective against a benzo-

18

Figure 6. The structural formula of Hycanthone (1-(4-ethyl-1,4-di-azahexyl)-4-hydroxymethyl-10-thioxanthene-9-one).
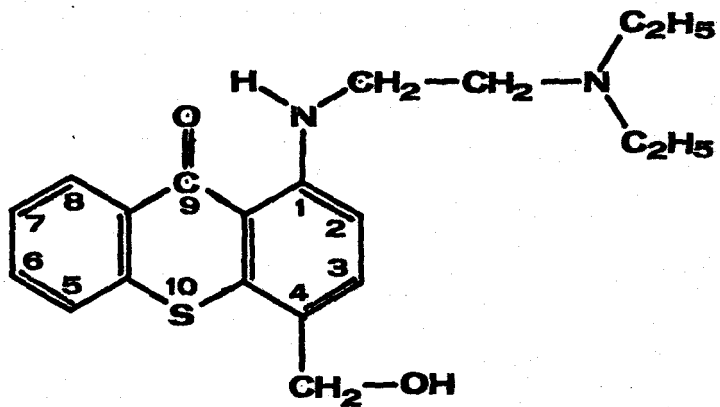
pyrene induced rat sarcoma, and entirely inactive against the solid form of the Ehrlich carcinoma in mice (Hackman et al., 1949).

In a subsequent more extensive study, Miracil D was found to exhibit a wide spectrum of carcinostatic activity against a variety of transplantable mouse tumors at non-toxic dosage levels (Hirschberg et al., 1959). Sarcoma 180 and lymphoid leukemia L1210 ascites respond most readily, followed by Adenocarcinoma 755 and E0771. Glioma 26 and the Ehrlich ascites carcinoma show a marginal response at best. Seventeen other thioxanthenones have been compared to Miracil D in terms of cytotoxicity in tissue cultures of human and mouse brain tumors, maximum tolerated dosage levels in the mouse, and carcinostatic activity against a variety of mouse tumors. None of the analogues approaches the pronounced activity of Miracil D in vivo. In tissue culture, however, many of the thioxanthenones are more active than the parent compound. No correlation was found between in vivo and in vitro carcinostatic activity, and schistosomicidal activity.

Studies, such as the above, were later extended to forty-four thioxanthenone derivatives (Blanz and French, 1963). As a result of these investigations, the following generalities, regarding the structures of the more effective antitumor derivatives, were formulated for leukemia L1210, Adenocarcinoma 755, and Sarcoma 180:

(a) the carbon chain between the nitrogen atoms of the side chain of the thioxanthenone molecule must be two carbon atoms in length,

(b) the terminal alkyl group(s) must be small,

(c) the ring attached nitrogen atom must bear one hydrogen atom,

(d) there must be an unsubstituted sulfur atom in position 10,

(e) there must be a carbonyl group in position 9, and

(f) there must be a compact, fairly chemically stable substituent in position 4.

These structural characteristics lead to the speculation that the metal chelating ability _via_ the carbonyl group and the dialkylaminoethyl- amino chain may be essential for carcinostatic activity.

Subsequently it was established that the carcinostatic activity of Miracil D against leukemia L1210 in mice was completely abolished by the simultaneous administration of nontoxic doses of SKF 525-A (β-di- ethylaminoethyl diphenylpropylacetate hydrochloride) (Hirschberg _et al._, 1964). Since SKF 525-A inhibits microsomal enzyme systems which catalyze a variety of metabolic transformations of drugs, this obser- vation suggests that Miracil D is converted _in vivo_ to an active me- tabolite before exhibiting its carcinostatic activity. In search of the carcinostatic metabolite of Miracil D, Hirschberg and his coworkers investigated the products formed in mammalian metabolism of Miracil D (Hirschberg _et al._, 1968). None of the metabolites, including Hycan- thone, proved superior to Miracil D. No correlation was found between the schistosomicidal and the carcinostatic activities of these drugs.

Miracil D has been found to cause a concentration dependent in- hibition of DNA and RNA synthesis in leukemia L1210 ascite cells of mice (Wilson _et al._, 1972). The drug inhibits DNA synthesis to a greater extent than RNA synthesis in contrast to analogous findings in bacteria. Methyl-Miracil D was much less effective while Hycanthone behaved similarly to Miracil D (Wilson _et al._, 1975).

I.5. Bacteriostatic Activity of Thioxanthenones

Miracil D inhibits the growth of B. subtilis (Weinstein et al., 1955), E. coli (Weinstein et al., 1967), S. typhimurium (Hartman et al., 1973), and the slime mold D. discoideum (Hirschberg et al., 1968). At the same time, Miracil D causes complete inhibition of total cellular RNA synthesis and partial inhibition of DNA and protein syntheses, and blocks the induction of β-galactosidase in E. coli (Weinstein et al., 1967). In B. subtilis, the growth inhibition is accompanied by the complete inhibition of RNA synthesis and the partial inhibition of protein synthesis (Weinstein et al.,1955). DNA synthesis is not inhibited in the first 20 minutes of an exponentially growing culture. However, after 20 minutes DNA synthesis is also inhibited (Haidle et al., 1970). From transformation experiments using donor DNA from cells grown in the presence of Miracil D, it was concluded that in B. subtilis the drug permits the DNA molecules in the process of replication to complete the process, but prevents the reinitiation of chromosome replication. Although protein synthesis, using natural or synthetic m-RNA, is not inhibited by the drug in subcellular systems (Weinstein et al., 1967), the prevention of reinitiation of chromosome replication is ascribed to the rapid inhibition of RNA synthesis and the subsequent inhibition of protein synthesis (Weinstein and Hirschberg, 1971).

The possibility that Miracil D affects the utilization of RNA precursors in vivo was excluded by investigating the inhibition of DNA dependent RNA polymerase of E. coli in vitro (Weinstein et al.,1967). It was found indeed that the drug inhibits RNA polymerase in vitro.

In addition, supplementation of the system with excess DNA reversed the inhibition, whereas supplementation with excess enzyme did not, indicating that the target of drug action is the DNA and not the enzyme.

Methyl-Miracil D also inhibits the growth of B. subtilis, but to a much lesser degree than Miracil D (Hirschberg et al., 1968). In contrast with the parent compound, methyl-Miracil D is reported not to inhibit RNA synthesis in vitro.

I.6. The Interaction of Thioxanthenones with Nucleic Acids

I.6.1. Physicochemical Evidence for the Interaction of Thioxanthenones with Nucleic Acids

Direct evidence for the interaction between Miracil D and nucleic acids has been obtained from the spectrophotometric studies of Weinstein and his coworkers (Weinstein et al., 1965). Miracil D in 0.33 mM phosphate buffer, pH 6.8 exhibits absorption maxima at 330 and 442 nm. Upon addition of calf thymus DNA, the maxima shift to longer wavelengths and the absorbances decrease at the maxima. At a DNA concentration of 50 μg/ml, the maxima are shifted to 337 and 450 nm, respectively. Qualitatively similar changes are produced by synthetic single stranded ribonucleic acids. However, some quantitative differences are noted among nucleic acids when compared with respect to their ability to induce a shift in the absorption maximum of Miracil D from 330 to 337 nm. At high polymer concentrations the order of relative effectiveness is: DNA > poly A > poly U > poly C. At lower polymer concentrations poly A appeared to be the most effective in this respect.

Miracil D also has been found to stabilize native calf thymus DNA from heat denaturation (Weinstein et al., 1965). For example, in a

buffer of low ionic strength and at a Miracil D concentration of 4 µg/ml, the melting temperature of DNA increases from 56 to 79 °C. Methyl-Miracil D is much less effective in this respect (Hirschberg et al., 1968). High ionic strength and addition of the tetramine spermine seem to abolish the stabilizing effect.

Miracil D and Hycanthone cause an increase in the intrinsic viscosity of native calf thymus DNA. Methyl-Miracil D did not increase the intrinsic viscosity of DNA under similar conditions (Carchman et al., 1969). The addition of spermine , as well as magnesium and sodium ions reverses the effect of Miracil D and Hycanthone on DNA viscosity. The significance of these data might be in some doubt in view of the fact that the measurements were not carried out at constant drug-DNA binding ratios.

I.6.2. The Intercalation of Thioxanthenones with Nucleic Acids

In 1961 Lerman proposed a model for the interaction of acridines with DNA (Lerman, 1961). According to this model, the acridine molecules, which possess planar heterocyclic ring systems, intercalate between adjacent base pairs in DNA. The intercalation is accompanied by an unwinding of the double helix, which, however, leaves the hydrogen bonded base pairing intact. This model is consistent with the X-ray diffraction patterns of DNA-proflavine fibers, as well as the increase in the intrinsic viscosity, and the decrease in the sedimentation coefficient of DNA in the presence of acridines.

On the basis of the experimental findings presented in the preceding section, it was proposed that Miracil D intercalates forming a complex, in which the thioxanthenone ring system is located between ad-

jacent DNA base pairs (Weinstein and Hirschberg, 1971). In this complex, the positively charged distal nitrogen atom of the side chain interacts with the negatively charged phosphate residues of the DNA backbone.

In the intercalated Miracil D-DNA complex, the Miracil D molecules should be oriented parallel to the base pairs and perpendicularly to the long axis of DNA. Indeed, flow dichroism studies have suggested that the Miracil D chromophore is oriented perpendicularly to the long axis of DNA, i.e. it is coplanar with the base pairs (private communications to Weinstein and Hirschberg, 1971). This observation serves as additional evidence that Miracil D interacts with DNA by intercalation.

The intercalation model for Miracil D has been further supported, though indirectly, by the sedimentation experiments of Waring (Waring, 1970). The replicative form (RF I) of bacteriophage ΦX 174 DNA consists of a covalently closed circular double helix. In addition to the Watson-Crick type helical turns of the strands, the double helix of the RF I form is folded into supercoils or superhelical structures. Because of topological pecularities, characteristic of circularity, this kind of DNA molecule displays large changes in supercoiling in response to intercalation induced local unwinding of the helix. Specifically, during the first phase of drug binding to superhelical DNA, the number of right-handed supercoils, originally present in DNA, decreases. At a certain level of binding, all supercoils are removed. As further drug binding takes place, left-handed supercoils begin to appear. Since the supercoiled DNA molecules, no matter whether they are left- or right-handed, are more compact than the DNA molecules with-

out supercoils, they sediment more rapidly. Therefore, the loss or re-appearance of supercoiling can be observed by monitoring changes in the sedimentation coefficient.

The hydroxylated derivative of Miracil D, Hycanthone, exhibits this characteristic property of intercalating drugs (such as ethidium bromide, propidium iodide, proflavin, etc.) on the sedimentation coefficient of the closed circular duplex. The intercalation of one Hycanthone molecule causes an unwinding of 16.4 $^\circ$ (corrected value) in the angle of the helix*. Lately four indazole analogues of Miracil D and Hycanthone were found to intercalate with DNA of bacteriophage PM2 (Waring, 1973). Because of the relative insolubility of these analogues, however, their binding to DNA has not been quantitated, and, therefore, the author reports only lower limits of the unwinding angles between 10.4 and 16.2 $^\circ$ (corrected values, see footnote). These lower limits are compatible with an unwinding angle of 16.4 $^\circ$ obtained for Hycanthone (see above).

The double helical oligoribonucleic acid poly A·poly U also binds Miracil D through an intercalation process as concluded from NMR studies of such complexes (Heller et al., 1974). This conclusion was deduced from the shift and broadening of resonance of the 4-methyl group of the drug. Similar but weaker effects were observed with the single stranded oligoribonucleic acid poly A. No effect was discerni-

*Unwinding angles were initially calculated relative to an assumed unwinding angle of 12 $^\circ$ for ethidium bromide (Waring, 1970). However, since this value was more recently modified to 29 $^\circ$ (Tsai et al., 1975), previously reported unwinding angles must be multiplied by a factor of 29/12=2.42 to obtain the corrected values.

ble with the single stranded oligoribonucleic acid poly U.

Based on these observations, a structure for the Miracil D-poly A·poly U complex was suggested, in which carbons 1, 2, 3, and 4 of the thioxanthenone ring are located between the adenine bases, and the diethylaminoethylamino side chain portion extends from the major groove of the helix (Figure 7). This orientation allows a complete intercalation of the thioxanthenone ring system between the stacked base pairs, and allows the distal nitrogen atom of the side chain to reach near the phosphate oxygen atoms of the polymer, making electrostatic interaction between these groups possible.

I.6.3. The Effect of the Intercalation between Thioxanthenones and Nucleic Acids on RNA Synthesis

In the enzymatic synthesis of RNA catalyzed by DNA dependent RNA polymerase (enzyme), the enzyme directs the synthesis of RNA from mononucleoside triphosphates according to genetic information encoded in the template. The synthesis may be visualized as consisting of a number of steps. The commonly accepted steps are (Chamberlin, 1974): (1) Template (i.e. DNA) binding, in which the enzyme (i.e. RNA polymerase) attaches to the DNA template, locates a specific site at which chain initiation can occur, and assumes an active conformation. (2) RNA chain initiation, in which the enzyme catalyzes the coupling of ATP or GTP with a second ribonucleoside triphosphate (substrate). Inorganic pyrophosphate is eliminated and a dinucleoside tetraphosphate is produced. This moiety remains tightly bound to the enzyme-template complex. (3) RNA chain elongation, in which successive nucleoside monophosphate residues are added from the substrate nucleoside tri-

Figure 7. The structure of the Miracil D-poly A·poly U complex. The Miracil D molecule is intercalated between two adjacent base pairs (Heller et al., 1974).
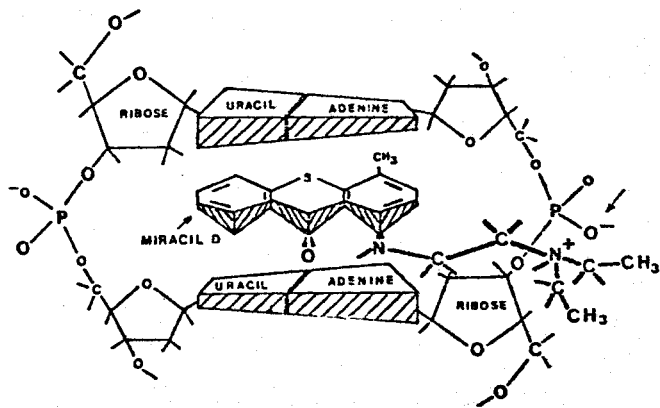
phosphates to the 3'-OH terminus of initial dinucleoside tetra-

phosphate leading to elongation of the nascent RNA chain. (4) RNA

chain termination and enzyme release, in which the newly formed RNA

chain and enzyme are released from the template.

As a result of the formation of complexes between thioxanthe-

nones and nucleic acids, the template activity of nucleic acids in RNA

synthesis is affected. The DNA dependent RNA polymerase of E. coli

using calf thymus DNA as template is inhibited by Miracil D (Weinstein

et al., 1967). This inhibition can be ascribed exclusively to the

interaction of Miracil D with the template DNA since supplementation of

the system with excess DNA reverses the inhibition, whereas supple-

mentation with excess enzyme does not, indicating that the target of

drug action is the template and not the enzyme. Methyl-Miracil D

produces no apparent inhibition in the same system under similar con-

ditions (Hirschberg et al., 1968c).

Wilson and his coworkers investigated the effectiveness of

Miracil D as inhibitor of RNA synthesis using synthetic single and

double stranded ribo- and deoxyribonucleic acids (Wilson et al.,

1972b). In general, inhibition was most pronounced for polynucleotides

containing deoxyribose and adenine. Specifically, for double stranded

polydeoxyribonucleotides the following order of relative inhibition was

observed: calf thymus DNA < poly dG·poly dC < poly dA·poly dT <

poly d(A-T). The authors concluded that Miracil D has a great affinity

for adenine residues.

I.7. Circular Dichroism of Drug-DNA Complexes

I.7.1. Circular Dichroism Definitions

One manifestation of optical activity is that optically active compounds or complexes absorb the left and right circularly polarized lights to different extent. This manifestation is termed circular dichroism. If Beer's law is obeyed for these two kinds of lights, we have

$$A_L = E_L \cdot c \cdot 1 \quad \text{and}$$
$$A_R = E_R \cdot c \cdot 1 \; ,$$

where A_L, A_R and E_L, E_R are the absorbances and molar extinction coefficients, respectively, c is the molar concentration of the substance exhibiting circular dichroism, and 1 is the path length in cm. The subscripts L and R refer to the left and right circularly polarized lights, respectively. From these equations, we obtain

$$A_L - A_R = (E_L - E_R) \cdot c \cdot 1 \; .$$

The quantity $A_L - A_R$ is called differential absorbance and $E_L - E_R$ is called differential molar extinction coefficient, expressed in units of absorbance and liter$\cdot$Mole$^{-1}\cdot$cm^{-1}, respectively. In general, the differential molar extinction coefficient $E_L - E_R$ is used to express the circular dichroism properties of these optically active substances.

As a consequence of the difference in extinction coefficients for the left and right circularly polarized lights, substances exhibiting circular dichroism polarize the plane polarized light elliptically, that is, if a plane polarized light beam passes through

these substances, the emerging light becomes elliptically polarized. The major axis of the ellipse is also rotated with respect to the plane of the incident plane polarized light, resulting in optical rotation. The ellipticity Θ (the ratio of the minor to the major axis of the ellipse) of the emerging elliptically polarized light can be expressed, if Beer's law is obeyed, as

$$\Theta = [\Theta] \cdot c \cdot l ,$$

where Θ is the ellipticity in degrees, c is the molar concentration of the substance, and $[\Theta]$ is the molar ellipticity in $deg \cdot lit \cdot Mole^{-1} \cdot cm^{-1}$.

The molar ellipticity $[\Theta]$ and the differential molar extinction coefficient $E_L - E_R$ are related according to the equation

$$[\Theta] = 33 \cdot (E_L - E_R) .$$

Clearly then, in addition to the differential molar extinction coefficient, the molar ellipticity can be used to quantitate the circular dichroism properties of optically active substances.

I.7.2. Optical Activity of Drug-DNA Complexes

Many drug and dye molecules that are themselves optically inactive, become active when bound to DNA. Typical examples are ethidium bromide (Aktipis and Martz, 1970), proflavine, acridine orange (Blake amd Peacocke, 1966), and the aminoacridines (Dalgleish et al., 1969). All these molecules are derivatives of planar heterocyclic ring systems, and are known to interact with DNA by intercalation. For the characterization of the complexes formed, the concept of the binding

ratio is a useful parameter. The binding ratio r is defined as

$$r = \frac{c_b}{[P]} \, ,$$

where c_b is the concentration of drug or dye bound to the nucleic acid, and $[P]$ is the nucleic acid concentration expressed as nucleic acid phosphorous (Scatchard, 1949). This quantity is proportional to the degree of saturation of nucleic acids by the ligand. If the ligand exhibits no preference for binding sites of a particular composition, then the distribution of bound molecules on a linear polymer nucleic acid can be considered as random. Therefore, in this case, the binding ratio r would be inversely proportional to the average physical distance between bound molecules.

In the circular dichroism spectra of aminoacridine-DNA and ethidium bromide-DNA complexes, two kinds of circular dichroism bands have been described: (1) those, the differential molar extinction coefficients of which are relatively independent of the binding ratio r, and (2) those, the differential molar extinction coefficients of which steeply increase with increasing binding ratios. In the first instance, the induced circular dichroism appears to be the result of direct interactions between the symmetric intercalated molecule and the asymmetric binding site of DNA (Jackson and Mason, 1971). The value of $E_L - E_R$ for an isolated intercalated molecule (which in practice is the value of $E_L - E_R$ at very low r values) is not affected by the presence of molecules bound to the neighbouring sites. In the second case, the induced circular dichroism is the result of an interaction between mole-

cules intercalated at neighbouring binding sites (Jackson and Mason, 1971). In this case, the differential molar extinction coefficients are zero or nearly zero at an r of 0 and increase rapidly with increasing binding ratios up to saturation (Dalgleish et al., 1969; Aktipis and Kindelis, 1973). Either type or both types of bands appear in the circular dichroism spectra of these compounds when bound to DNA.

I.8. The Scope of This Investigation

As mentioned earlier in this chapter, a number of attempts have been made to correlate the schistosomicidal, the carcinostatic and the bacteriostatic activities of thioxanthenones. However, there does not seem to be a unique mechanism responsible for all these activities. The biochemical basis of the schistosomicidal and carcinostatic activities remains elusive.

The bacteriostatic activity of thioxanthenones, however, appears to be related to the inhibition of cellular RNA synthesis. Especially in the case of two well-investigated thioxanthenones, Miracil D and methyl-Miracil D, a good correlation can be obtained between bacteriostatic activity and the effectiveness of these compounds as inhibitors of RNA synthesis. A puzzling aspect among the results of previous studies has been the reported almost complete ineffectiveness of methyl-Miracil D in inhibiting RNA synthesis compared to Miracil D. Therefore, this investigation was undertaken to determine whether the observed differences in the inhibition of RNA synthesis by Miracil D and methyl-Miracil D could be related to the physicochemical properties of the complexes formed between these drugs and DNA, and whether the

lack of inhibitory effectiveness of methyl-Miracil D could be explained on the basis of the physicochemical properties of this drug.

In this investigation, the drug-DNA complexes are examined by means of absorption spectroscopy, circular dichroism, and melting profiles. The results of binding studies between DNA and the thio-xanthenones are used to interpret the relationship between the physicochemical properties of drug-DNA complexes and the inhibitory effectiveness of these drugs. Circular dichroism measurements are utilized to investigate the structural features of drug-DNA complexes with special regard to long range changes in DNA conformation leading to exclusion in binding. Melting profiles of these complexes are studied in order to establish the relative effectiveness of Miracil D and its methyl derivative, when bound to DNA, in stabilizing DNA against heat denaturation, and to obtain insight into the mechanism of inhibiton of RNA chain elongation by these drugs.

The inhibition of both initiation and elongation of RNA synthesis by these drugs is also investigated. Miracil D is found to inhibit both initiation and elongation of RNA synthesis. Finally, it is established that Miracil D and its methyl derivative, when bound to DNA, are equally effective inhibitors of RNA synthesis.

CHAPTER II

MATERIALS AND METHODS

II.1. Materials

Calf thymus deoxyribonucleic acid as a white fibrous material was purchased from Worthington Biochemical Corporation (Freehold, New Jersey 07728) and Sigma Chemical Company (Saint Louis, Missouri 63178).

Bacteriophage T2 (ATCC No. 11303 B_2; Host: E. coli B, ATCC No. 11303) as a suspension in 0.05 $\underline{M}$ Tris buffer, pH 7.6, containing 0.1 $\underline{M}$ NaCl and 1 m$\underline{M}$ EDTA, was obtained from Miles Laboratories, Inc. (Elkhart, Indiana 46514). The suspension (Control No. 21-6-790) had a titer of 5×10^{12} plaque forming units per ml and an absorbance of 43 per ml at 260 nm.

DNA dependent RNA polymerase (Nucleosidetriphosphate: RNA nucleotidyltransferase; E.C. No. 2.7.7.6) from E. coli, strain K-12 was purchased from Sigma as a solution in 50 % glycerol and 50 % 0.01 $\underline{M}$ Tris buffer, pH 7.9, containing 0.01 $\underline{M}$ MgCl$_2$, 0.1 $\underline{M}$ KCl, 0.1 m$\underline{M}$ dithiothreitol, and 0.1 m$\underline{M}$ EDTA. The enzyme solution (Lots No. 33C-2510 and 94C-0284-2) had specific activities of 382 and 565 units/mg, and protein concentrations of 2.10 and 1.77 mg/ml, respectively. One unit of enzyme will incorporate 1 nMole of labeled ATP into an acid insoluble product in 10 minutes at pH 7.9 and 37 ^{o}C, using calf thymus DNA as template (Burgess, 1969).

Miracil D (1-(4-ethyl-1,4-diazahexyl)-4-methyl-10-thioxanthene-9-one) as a yellow crystalline solid was purchased from Calbiochem

(La Jolla, California 92037) under the trade name Lucanthone, as hydro-chloride, with a molecular weight of 376.7 daltons (Lot No. 802205).

Methyl-Miracil D (1-(4-ethyl-1-methyl-1,4-diazahexyl)-4-methyl-10-thioxanthene-9-one) and MDMT (1-(4-methyl-1,4-diazapentyl)-4-methyl-10-thioxanthene) as crystalline solids were generous gifts from Dr. Edward Elslager of Park, Davies & Company (Ann Arbor, Michigan 48106) and Dr. Frederic A. French of Mount Zion Hospital and Medical Center (San Francisco, California 94115), respectively. Methyl-Miracil D was supplied as dihydrochloride monohydrate with a molecular weight of 445.45 daltons and MDMT as the free base with a molecular weight of 298.44 daltons.

Sodium salts of the four nucleoside triphosphates ATP, CTP, GTP, and UTP as white crystalline solids were purchased from Sigma and P-L Biochemicals, Inc. (Milwaukee, Wisconsin 53205). The preparations were at least 97 % pure according to the manufacturer's specifications.

5-[^{3}H]-uridine-5'-triphosphate, tetrasodium salt (specific activity: 19 Ci/mMole) in ethanol-water (1:1) mixture was obtained from Schwarz/Mann (Orangeburg, New York 10962).

γ-[^{32}P]-adenosine-5'-triphosphate, ammonium salt (specific activity: 15.8 Ci/mMole) as freeze-dried solid was purchased from Amersham/Searle Corporation (Arlington Heights, Illinois 60005).

All common chemicals used were of analytical grade.

II.2. Instruments

The following instruments were used in these studies:

Cary Model 15 Recording Spectrophotometer (Varian, Cary Instruments Division, Monrovia, California 91016)

Jasco Model ORD/UV-5 Optical Rotatory Dispersion Recorder
(Japan Spectroscopic Company, Ltd., Tokyo, Japan) equipped with CD
attachement and modified (SS-10 modification) to a maximum sensi-
tivity of 0.002 degrees of ellipticity per cm

Beckman Model LS-250 Liquid Scintillation System (Beckman
Instruments, Inc., Fullerton, California 92634)

Beckman T_M Analyzer (Beckman Instruments, Inc., Fullerton,
California 92634)

Beckman Temperature Bridge (Beckman Instruments, Inc., Fullerton,
California 92634)

Moseley Model 7035B X-Y Recorder (Hewlett Packard Corporation,
Palo Alto, California 94304)

International Model PR-2 Portable Refrigerated Centrifuge
(International Equipment Company, Needham Heights, Massachusetts 02194)

Beckman/Spinco Model L Ultracentrifuge (Beckman Instruments,Inc.
Spinco Division, Palo Alto, California 94304)

Corning Model 12-B Research pH Meter (Corning Scientific
Instruments, Medfield, Massachusetts 02052)

Lauda/Brinkman Model K-2/R Refrigerated Circulator (Brinkman
Instruments, Inc., Westbury, New York 11590)

II.3. Purification of Miracil D

Miracil D (0.4 g) was dissolved in 50 ml distilled water at
50 $^{\circ}$C. The solution was titrated with 50 % sodium hydroxide solution
until no further precipitation was observed (about pH 11). The pre-
cipitate was collected on a sintered glass filter and redissolved in
absolute ethanol at 50 $^{\circ}$C. Concentrated hydrochloric acid (10 ml) was

added and the Miracil D was crystallized at 4 $^{\circ}$C. The crystals were dried over Drierite dessicant (anhydrous CaSO$_4$) and stored in a dark bottle at 4 $^{\circ}$C.

Thin layer chromatography was performed in the following solvent systems (Zilversmit, 1970): butanol/acetic acid (9:1), chloroform/methanol (9:1), ethyl acetate/n-heptane (6:4), and ethanol/ammonium hydroxide (9:1). No contaminants could be detected in the purified preparation. The melting point was 195 $^{\circ}$C, in agreement with Mauss (Mauss, 1948).

II.4. Preparation of Deoxyribonucleic Acid from Bacteriophage T2

Deoxyribonucleic acid from bacteriophage T2 was prepared by the method of Bautz and Dunn (Bautz and Dunn, 1971).

Commercial bacteriophage suspension (5 ml) was dialyzed versus 2 liters of 0.1 M sodium phosphate buffer, pH 7.2 for 5 hours. The dialyzate was transferred into a 10 ml test tube and 0.55 ml of freshly prepared 10 % sodium dodecyl sulfate solution was added. The mixture was then placed into a water bath and the temperature was raised to 65 $^{\circ}$C. The mixture after three minutes at this temperature became quite viscous. After chilling on ice, 1 ml of 2 M KCl solution was added in small portions with gentle swirling. A white precipitate of potassium dodecyl sulfate and protein appeared. The mixture was then poured into a polyallomer centrifuge tube and centrifuged at 27,000 g and 4 $^{\circ}$C for fifteen minutes in the Beckman/Spinco Model L ultracentrifuge using the swinging bucket rotor SW 36 (at 16,000 rpm). The supernatant containing the T2 DNA was decanted into a conical stoppered glass centrifuge tube and the pellet was discarded. 6.5 ml

of freshly distilled phenol (collected between 176 and 178 ^{o}C) containing 0.08 % of 8-hydroxy-quinoline and saturated with 0.1 $\underline{M}$ sodium phosphate buffer, pH 7.2 was added to the supernatant and the mixture was rocked for 30 minutes at room temperature with a frequency of about 40 cycles/minute. After centrifugation in the International Model PR-2 Portable Refrigerated Centrifuge using head No. 296 at 2,000 rpm and 4 ^{o}C, the top aquaeous phase was transferred into a polyallomer centrifuge tube and was further centrifuged at 27,000 g for 30 minutes as described above. The supernatant was decanted and dialyzed against 1 liter of 0.01 $\underline{M}$ Tris-HCl buffer, pH 7.3, containing 0.01 $\underline{M}$ KCl and 0.5 m$\underline{M}$ EDTA. The dialyzis was performed at 4 ^{o}C for four days with daily changes of the buffer. The resulting T2 DNA solution was stored at 4 ^{o}C.

'   This DNA preparation had a melting temperature of 86 ^{o}C and 46 % hyperchromicity at 260 nm in 0.08 $\underline{M}$ Tris-HCl buffer, pH 7.0, containing 0.4 $\underline{M}$ KCl and 0.02 $\underline{M}$ MgCl$_2$. The A_{260}/A_{280} ratio was 1.75, indicating low protein contamination (Thomas and Abelson, 1966).

        T2 DNA concentrations were determined spectrophotometrically using an extinction coefficient of 6500 at 260 nm (Mahler et al., 1964) and a mean residue weight of 357 daltons (Rubinstein et al., 1961).

II.5.   Preparation of Stock and Working Solutions

        Calf thymus DNA was dissolved (3-4 mg/ml) in 0.01 $\underline{M}$ sodium chloride solution with slow stirring at 4 ^{o}C for 48 hours. The solution was then dialyzed twice, each time against 40 volumes of 0.01 $\underline{M}$ sodium chloride solution for 24 hours at 4 ^{o}C. The resulting DNA stock solution was stored at 4 ^{o}C.

Before each experiment, a working DNA solution was prepared by diluting the DNA stock solution with the appropriate buffer. The concentration of DNA was determined spectrophotometrically using a molar extinction coefficient of 6600 liter/cm/Mole of DNA phosphorous (Mahler et al., 1964) or a specific extinction coefficient of 20 liter/cm/g of DNA (Nakamoto et al., 1964).

Working solutions of Miracil D, methyl-Miracil D, and MDMT were prepared by dissolving these compounds in buffer. For this purpose, the purified Miracil D preparation (see section II.3) was used, while both methyl-Miracil D and MDMT were used as supplied (see section II.1). Drug concentrations were determined spectrophotometrically using the following estimated molar extinction coefficients in liter$\cdot$Mole$^{-1}\cdot$cm^{-1}:

Miracil D	8040 at 330 nm
Methyl-Miracil D	3600 at 425 nm
MDMT	3900 at 302 nm

These molar extinction coefficients in buffer were calculated on the basis of the weighed amounts (about 10 mg) and the molecular weights of the compounds specified by the suppliers (see section II.1).

Unlabeled nucleoside triphosphate solutions were prepared simply by dissolving the salts in deionized water (total volume not more than 1 ml). The solutions (pH 4) were titrated with 50 % sodium hydroxide solution to pH 7.0 using 1 µl chromatographic applicators.

Radioactively labeled nucleoside triphosphate solutions were prepared by dissolving the solid commercial preparations in unlabeled nucleoside triphosphate solutions. Whenever these preparations were in

liquid form, they were placed in an ice bath and dried under a stream of nitrogen.

II.6. Preparation of Drug–DNA Complexes

Drug–DNA complexes were prepared from working solutions (see section II.5) of the drugs and DNA. Since the drug solutions have a tendency to be retained on the inner surfaces of glass pipettes used for transfer, a specific procedure was used for the preparation of the complexes to insure greater accuracy. Since in the binding studies and circular dichroism measurements the drug concentration was maintained constant at 2×10^{-5} $\underline{M}$ and the DNA concentration was varied as appropriate, typically, 5 g of drug solution was weighed into a 25 ml volumetric flask followed by the addition of the required volume of DNA working solution, and filled up with buffer to volume.

II.7. Dimerization Studies

Solutions for these studies were prepared from working solution of Miracil D by weighing a given amount and diluting it with buffer to the required final volume. The concentration c_t of the drug in these solutions and the path length 1 of the spectrophotometric cells were selected so that the product $c_t \cdot 1$ was identical for each sample. This method permits isosbestic points to be located by visual inspection of the resulting spectra.

Absorption spectra of drug solutions in the near ultraviolet wavelength region were recorded at room temperature. Because of the tendency of the drug to be absorbed to the surfaces of the glassware, spectra were recorded immediately following the preparation of the solutions. Scanning rates were about 1.6 Å/sec, the slowest possible

in order to insure the most accurate recorder pen response. Both rectangular and cylindrical fused silica cells of different pathlengths were used.

For the determination of the dimerization constant, the method of Lamm and Neville (Lamm and Neville, 1965) was utilized. This method is based on the following principle. In a solution containing the monomeric and dimeric forms of a compound, the laws of mass conservation and mass action can be stated as

$$c_t = c_m + 2 \cdot c_d$$

and

$$K_d = \frac{c_d}{c_m^2} \ ,$$

where c's are the molar concentrations, the subscripts m and d refer to monomer and dimer, respectively, and K_d is the dimerization constant. From the law of mass action, the dimer concentration c_d can be expressed as $c_d = K_d \cdot c_m^2$. Substitution for c_d in the law of mass conservation yields the relationship $2 \cdot K_d \cdot c_m^2 + c_m - c_t = 0$, which is quadratic in the monomer drug concentration c_m . Using the general solution formula of quadratic equations gives

$$c_m = \frac{\sqrt{1 + 8 \cdot K_d \cdot c_t} - 1}{4 \cdot K_d} \ .$$

Defining α as the fraction of drug present as monomer by $\alpha = c_m / c_t$, α can be expressed as a function of c_t and K_d:

$$\alpha = \frac{\sqrt{1+8 \cdot K_d \cdot c_t} - 1}{4 \cdot K_d \cdot c_t} \quad . \tag{1}$$

If the monomer and the dimer are the only two absorbing species, the absorbance A of the solution can be expressed as the sum of contributions from the monomer and dimer:

$$A = E_m \cdot c_m \cdot 1 + E_d \cdot c_d \cdot 1 \quad ,$$

where E_m and E_d are the molar extinction coefficients of the monomer and dimer, respectively. By defining the apparent molar extinction coefficient E_{app} of a solution as $E_{app} = A/(c_t \cdot 1)$, it follows that

$$E_{app} = (E_m - E_d/2) \cdot \alpha + E_d/2 \quad . \tag{2}$$

This indicates that the apparent molar extinction coefficient is a linear function of α, and the slope and the intercept of the E_{app} versus α line are determined by the molar extinction coefficients of the monomer and dimer.

The linear property of equation (2) was used in the determination of the dimerization constant. First, arbitrary values were assigned to K_d and the fraction α of drug present as monomer was calculated according to equation (1) for each sample and each K_d. Using these α values and the corresponding apparent extinction coefficients, which were obtained experimentally, the best straight line fit to equation (2) was calculated by the method of non-weighted least-squares. The procedure was repeated with different values of K_d until a minimum was reached in the root-mean-square deviation between the

experimentally obtained apparent molar extinction coefficients and the computed best straight line values. The K_d is the dimerization constant of the drug most compatible with the experimental results.

For the K_d value that gives the minimal root-mean-square deviation, the slope and the intercept of the best fitting straight line can be used to determine the monomer and dimer molar extinction coefficients.

II.8. Binding Studies

The binding of thioxanthenones to nucleic acids was investigated by the spectrophotometric method of Peacocke and Skerrett (Peacocke and Skerrett, 1956). The method utilizes, as a binding parameter, the change in the absorption spectrum of the ligand as it binds to the nucleic acids.

The absorption spectra of drug-nucleic acid complexes were recorded in the visible and near ultraviolet wavelength regions. A buffered solution of DNA with a concentration equal to that present in each drug-DNA complex was employed as reference. For these measurements, fused silica cells of 5 and 10 cm pathlengths were used. The procedures described for the dimerization studies (see section II.7) were used for recording the spectra.

II.8.1. The Analysis of the Spectra of Drug-Nucleic Acid Complexes

The method of Peacocke and Skerrett was also used for the analysis of the spectra. A brief description of this method is presented below.

For a mixture of free and bound ligands in the presence of nucleic acids, Beer's law and the law of mass conservation can be

stated as

$$A=(E_f \cdot c_f + E_b \cdot c_b) \cdot 1$$

and

$$c_t = c_f + c_b \ ,$$

where A, E's, c's and 1 are the absorbance, the molar extinction coefficients, the molar concentrations, and the pathlength, respectively. The subscripts t, f, and b refer to the total, free, and bound ligands, respectively. It is assumed that both the free and bound ligands themselves obey Beer's law and that the DNA does not absorb light at the wavelength selected for the study. Any deviation from the principle of additivity is considered as evidence for the presence of more than one kind of species of free or bound ligands.

The absorbance of the mixture of free and bound ligands can be expressed from these equations as

$$A=[E_f \cdot c_t - (E_f - E_b) \cdot c_b] \cdot 1 \ .$$

If a wavelength can be found for which $E_f = E_b$, then $A = E_f \cdot c_t \cdot 1$, which means that the absorbance of the mixture is independent of its composition. This wavelength is called the isosbestic wavelength.

In practice, a series of solutions are prepared with identical ligand concentrations and varying nucleic acid concentrations. If an isosbestic wavelength is present then the spectra of all complexes cross through a single point (isosbestic point) at the isosbestic wavelength. The existence of an isosbestic point is a good indication of the presence of only two kinds of absorbing species. Obviously, the

lack of an isosbestic point does not preclude the possibility that only two kinds of absorbing species are present.

For the absorbance A_f of the solution which does not contain bound ligand, we have

$$A_f = E_f \cdot c_t \cdot l ,$$

and for the absorbance A_b of the solution which does not contain free ligand, we have

$$A_b = E_b \cdot c_t \cdot l .$$

By combining these relationships, the concentration of bound ligand can be calculated according to the equation

$$c_b = \frac{A_f - A}{A_f - A_b} \cdot c_t .$$

To improve the accuracy of the determination of c_b, a wavelength is selected for the measurements which maximizes the value of $A_f - A_b$.

II.8.2. The Determination of the Absorption of Bound Drug

In general, the value of A_b is not available experimentally. For its determination, the method of Crothers (Crothers, 1974) was used with some modifications. According to this method, at extremely high nucleic acid concentrations [P], the double reciprocal relationship

$$\frac{1}{A_f - A} = \frac{1}{A_f - A_b} + \frac{1}{K_{app} \cdot B_{app} \cdot (A_f - A_b)} \cdot \frac{1}{[P]} ,$$

where K_{app} and B_{app} are the apparent binding constant and the apparent number of binding sites, respectively, can be used to obtain the value of the absorption A_b of bound drug. This is possible because the plot of the reciprocal differential absorbance $1/(A_f-A)$ versus the reciprocal nucleic acid concentration $1/[P]$ should yield a straight line with an intercept of $1/(A_f-A_b)$. Since at low nucleic acid concentrations deviations from linearity are known to occur (Hayman, 1962), a polynomial rather than linear extrapolation was used to obtain the value of the intercept. The calculations were performed using the computer program POLFIT available from the Public Library of the Computer Center at Loyola University of Chicago.

II.8.3. Scatchard Plots and Their Interpretation

For the presentation of the results of binding studies, the method of Scatchard was chosen (Scatchard, 1949). Plots of r/c_f versus r were prepared, where the binding ratio r is defined by

$$r = \frac{c_b}{[P]} . \qquad (3)$$

The values of r/c_f and r were calculated directly from absorbance measurements using the equations

$$\frac{r}{c_f} = \frac{A_f-A}{A-A_b} \cdot \frac{1}{[P]}$$

and

$$r = \frac{A_f-A}{A_f-A_b} \cdot \frac{c_t}{[P]} .$$

The binding of thioxanthenones to nucleic acids was interpreted on the basis of the exclusion model for binding (McGhee and von Hippel, 1974). According to this model, if the binding of ligands to nearest neighbour sites of nucleic acids is not allowed, then the binding isotherm may be described by the equation

$$\frac{r}{c_f} = K \cdot \frac{(1-4 \cdot r)^2}{2 \cdot (1-2 \cdot r)} \quad , \tag{4}$$

where K is the intrinsic association constant between the ligand and the nucleic acid.

The intercepts of the isotherm with the r and r/c_f axes must be located at r=0.25 and r/c_f=K/2, respectively, and the isotherm must always fall below the line determined by these intercepts. The curvature of the isotherm is most pronounced in the region of 0.125 < r < 0.25.

The fitting of the exclusion model to the experimental data was performed using the computer program described in Appendix B. In this procedure, arbitrary values were given to K and the theoretical binding isotherms were calculated. The K which produced an isotherm which fit the experimental points within experimental error was assumed to be the true intrinsic association constant. A maximum error of 0.003 in absorbance and an error of 1.5 % in nucleic acid concentration was assumed throughout all calculations.

II.9. Circular Dichroism Measurements

Circular dichroism measurements were carried out on the Jasco Model ORD/UV-5 Optical Rotatory Dispersion Recorder. The instrument

was calibrated with an 0.1 % aquaeous solution of d-10-camphorsulfonic

acid (supplied by Durrum Instruments Corporation, Palo Alto, California

94303). This standard solution placed in a 1 cm spectrophotometric

cell gives an ellipticity of +0.313 degrees at 290 nm, corresponding to

a pen deflection of 15.65 cm on the 0.02 degrees/cm scale of the

spectropolarimeter.

The circular dichroism spectra of drug-DNA complexes were re-

corded in 5 and 10 cm cylindrical fused silica cells at room temper-

ature. The absorbance of the samples was always maintained below 2.0

in order to avoid artifacts in optical activity.

The results of circular dichroism measurements are reported

either as differential molar extinction coefficients E_L-E_R or differ-

ential absorbance A_L-A_R. They were calculated using equations

$$A_L-A_R = \frac{\Theta}{33}$$

and

$$E_L-E_R = \frac{\Theta}{33 \cdot c \cdot l} \quad , \qquad (5)$$

where the ellipticity Θ (in degrees) was read directly from the chart

paper, l is the pathlength in cm, and c is the molar concentration of

species responsible for the circular dichroism. Therefore, the values

of A_L-A_R and E_L-E_R were obtained in units of absorbance and liter·

$Mole^{-1} \cdot cm^{-1}$, respectively.

II.10. Measurements at Elevated Temperatures

II.10.1. Definitions, Terminology, and Formulas Used in Hyper-

chromicity Measurements

Hyperchromicity h is defined (Mahler et al., 1964) by the e-

quation

$$h = \frac{A_t}{A_{t_o}} - 1 \; ,$$

where A_t and A_{t_o} are the absorbances of a hyperchromic substance at a

given wavelength, temperature t, and reference temperature t_o. There-

fore, hyperchromicity measurements are carried out by the measurement

of absorbance as a function of temperature. The instrumentation used

for these studies is described in the next section.

A typical set of hyperchromicity versus temperature plots (also

referred to as melting curves or melting profiles) of nucleic acids and

drug-nucleic acid complexes are shown in Figure 8. It can be seen that

the hyperchromicity increases, reaching a maximum plateau, with in-

creasing temperature. If the maximum hyperchromicity value reached is

denoted by $\bar{h}$, the melting temperature T_m is defined as the temperature

at which 50 % of the maximum hyperchromicity is attained (Mahler et

al., 1964), that is

$$h(T_m) = 0.5 \cdot \bar{h} \; .$$

This classical definition is readily applicable for melting curves

representing a single cooperative transition restricted to a relatively

narrow temperature range (Figure 8, curve a). For cases where the

52

Figure 8. Typical dependence of hyperchromicity h on the temperature of nucleic acids and drug-nucleic acid complexes (see text for details).
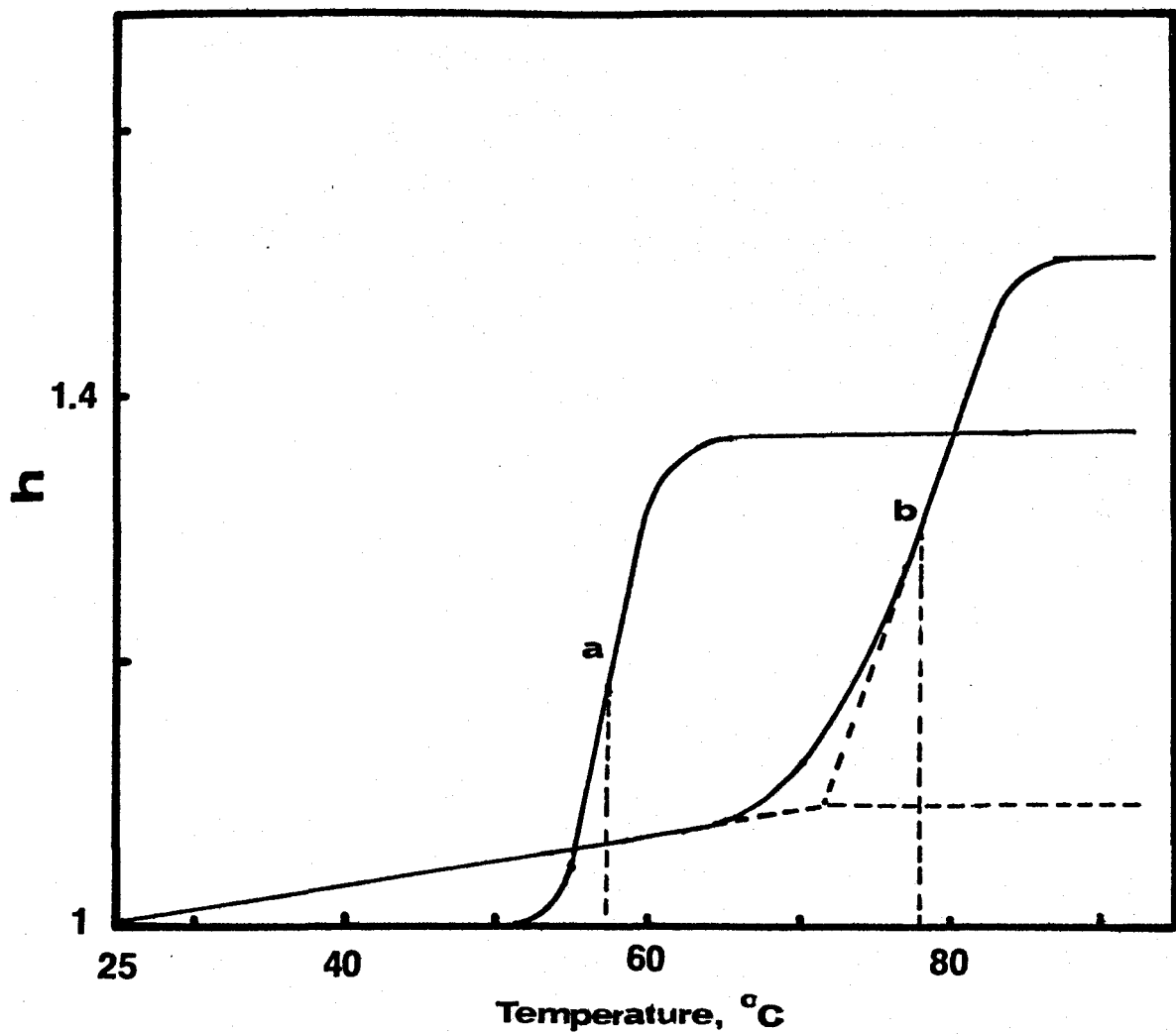
transition is more complex and it takes place in a relatively wide

temperature range, a modified melting temperature T_m' is defined (Gersch

and Jordan, 1965). According to this new definition, T_m' is the temper-

ature at which 50 % of the maximum hyperchromicity is attained from

the onset of the rapid increase to the maximum of hyperchromicity. The

intercept of the extrapolated linear segments of the melting curves

determines the onset of the rapid increase (Figure 8, curve b). In

the present investigation both the classical and modified definitions

for melting temperatures are used. Reference to the appropriate

melting curve indicates which definition is applicable in each instance.

In the presentation of the present experimental results, the normalized

hyperchromicity h_n will be used, which is defined by the equation

$$h_n = \frac{h}{\bar{h}} \; .$$

Since melting temperatures are invariant to this linear transformation,

they can be determined directly from the normalized hyperchromicity

versus temperature plots.

In the present studies, the reference temperature is 25 ^{o}C, and

the maximum hyperchromicity is obtained at 98 ^{o}C, i.e.

$$\bar{h} = h(98) = \frac{A_{98}}{A_{25}} - 1 \; ,$$

so the normalized hyperchromicity h_n at temperature t was calculated

using the equation

$$h_n = \frac{A_t - A_{25}}{A_{98} - A_{25}} . \qquad (6a)$$

Measurements of absorbance as a function of temperature were also carried out at wavelengths where the nucleic acids do not absorb light (i.e. 440 nm). The changes of absorbance at these wavelengths are the result of drug dissociation from the drug-nucleic acid complexes. For the quantitative treatment of drug release from the complexes, the normalized absorbance change ΔA_n is used, which is calculated using the equation

$$\Delta A_n = \frac{A_t - A_{25}}{A_{98} - A_{25}} . \qquad (6b)$$

For the normalized absorbance change ΔA_n <u>versus</u> temperature profiles, the concept of dissociation transition temperature of drug-DNA complexes, corresponding to the melting temperature T_m of melting profiles, can be introduced. The dissociation transition temperature of drug-DNA complexes is the temperature at which 50 % of the maximum normalized absorbance change is attained. At this temperature, 50 % of the drug bound at the reference temperature (i.e. at 25 $^{\circ}$C) is released from the complex.

II.10.2. Instrumentation

The dependence of absorbance and circular dichroism on temperature was studied by the simultaneous recording of absorbance or circular dichroism and temperature of drug-DNA complexes.

Solutions were placed in a special heated cell holder assembly

(a modified part of the Beckman T_M Analyzer), which can be fitted within the sample compartments of the Cary Model 15 Recording Spectrophotometer or the Jasco Model ORD/UV-5 Spectropolarimeter. The temperature of the cell holder assembly can be linearly increased at a programmed rate by means of the Beckman T_M Analyzer. The rate used was $3~^oC$/minute. The sample temperature was measured, using the Beckman Temperature Bridge, which monitors the temperature of distilled water in a cell adjacent to the sample cell within the cell holder assembly. The Analyzer produces an electrical signal (between 0 and 10 mV), proportional to the temperature of the sample. Potentiometers installed on the pen drive shafts of the spectrophotometer and spectropolarimeter produce resistances (between 0 and 10 kΩ), proportional to the absorbance or the circular dichroism of the sample under examination. The potentiometers are connected through a custom-made calibration box to the Y-axis input of the Moseley Model 7035B X-Y Recorder (Martz and Aktipis, 1971). The calibration box serves two purposes. One is to transform the resistances of the potentiometers to electrical signals and the other to provide for expansion and baseline adjustments of the electrical signal. The signal from the Beckman Temperature Bridge is directly applied to the X-axis input of the recorder. With this instrument assembly it is possible to obtain directly the absorbance or circular dichroism as the function of temperature.

II.10.3. Determination of the Dependence of Association Constants on Temperature

The dependence of the intrinsic association constant K for the binding between drug and nucleic acid on the temperature can be de-

termined by combining the results of binding studies at room temperature with the results of absorbance measurements at 440 nm as the function of temperature. Since the increase of absorbance at 440 nm is the result of drug release from the drug-DNA complexes, therefore, $\Delta A_n(t)$ denotes the fraction of the drug which is bound at 25 $^{\circ}$C, but which is released at temperature t, i.e.

$$\Delta A_n(t) = \frac{c_b(25) - c_b(t)}{c_b(25)} \quad ,$$

from which

$$c_b(t) = c_b(25) \cdot [1 - \Delta A_n(t)] \quad . \qquad (7)$$

Dividing by the nucleic acid concentration [P] and using the definition of the binding ratio r, we obtain

$$r(t) = r(25) \cdot [1 - \Delta A_n(t)] \quad . \qquad (8)$$

In this formulation it is assumed that both the free and bound drug extinction coefficients are independent of temperature or that if these coefficients depend on it, their dependence is small and such that equation (8) is still obeyed. From equations (3) and (4), the intrinsic association constant K can be expressed as

$$K = \frac{2 \cdot r \cdot (1 - 2 \cdot r)}{(1 - 4 \cdot r)^2 \cdot (c_t - r \cdot [P])} \quad . \qquad (9)$$

From the known values of the normalized absorbance changes at temperature t and of the intrinsic association constant K at room temperature, the intrinsic association constant K at temperature t can

be calculated using equations (8) and (9). The results of these calculations are reported as $\log_{10}K$ versus $1/T$ (van't Hoff plots), where T is the absolute temperature. The resulting slope is equal to $-\Delta H^O/(2.303 \cdot R)$, where ΔH^O and R are the standard enthalpy change and the gas constant, respectively. The standard enthalpy change ΔH^O can be calculated from the slope of the van't Hoff plots. The standard free energy change ΔG^O and the standard entropy change ΔS^O can be calculated using the equations

$$\Delta G^O = -R \cdot T \cdot \ln K$$

and

$$\Delta G^O = \Delta H^O - T \cdot \Delta S^O$$

(Klotz and Rosenberg, 1972).

II.10.4. Measurements of the Circular Dichroism of Drug-DNA Complexes at Elevated Temperatures

Investigations of the dependence of circular dichroism on the temperature were performed with instrumentation similar to that used in hyperchromicity measurements except that the spectrophotometer was replaced by the spectropolarimeter (see section II.10.2). The dependence of the differential molar extinction coefficient on the temperature was calculated in the following way. From equations (3) and (7) (see sections II.8.3 and II.10.3, respectively), the bound drug concentration $c_b(t)$ at temperature t can be expressed as

$$c_b(t) = r(25) \cdot [P] \cdot [1 - \Delta A_n(t)] \ ,$$

where $r(25)$ is the binding ratio at 25 ^{O}C, [P] is the nucleic acid

concentration, and $\Delta A_n(t)$ is the normalized absorbance change at temperature t. Using the equation for $\Delta A_n(t)$ (equation (6b), section II.10.1), we have

$$c_b(t) = r(25) \cdot [P] \cdot \{1 - \frac{A_t - A_{25}}{A_{98} - A_{25}}\} \; .$$

Substitution of this expression into equation (5) (see section II.9) gives

$$(E_L - E_R)_t = \frac{\Theta_t}{33 \cdot 1 \cdot r(25) \cdot [P] \cdot \{1 - (A_t - A_{25})/(A_{98} - A_{25})\}} \; .$$

The differential molar extinction coefficient $(E_L - E_R)_t$ at temperature t was calculated according to this equation, where the ellipticity Θ_t at temperature t was directly read from the recorder chart paper (see section II.10.2), the path length 1 was 1 cm in each instance, and the absorbances A_{25}, A_{98}, and A_t at 440 nm (see section II.10.3 as well) were directly read from the recorder chart paper (see section II.10.2).

II.11. RNA Polymerase Assays

DNA dependent RNA polymerase activity was determined by the method of Richardson (Richardson, 1973) with minor modifications. In this method the enzymatic activity is determined by measuring the incorporation of radioactively labeled nucleoside triphosphates into ribonucleic acid insoluble in 5 % trichloracetic acid.

Assay mixtures were prepared with Hamilton syringes in 10x75 mm disposable glass test tubes. The test tubes and all glassware were preheated at 180 $^\circ$C for at least 48 hours before use in order to in-

activate any possible nuclease contamination (Sreevalsan, 1973). Disposable plastic gloves were worn in the course of this work to prevent any contamination by skin nucleases.

The three major components of an assay mixture, i.e.: DNA dependent RNA polymerase (the enzyme), DNA (the template) with or without inhibitor, and the four nucleoside triphosphates NTP (the substrates) were dissolved in 0.1 ml of buffered solution with the following composition:

0.04 $\underline{M}$ Tris-HCl, pH 7.0 at 25 ^{o}C

0.2 $\underline{M}$ KCl

0.01 $\underline{M}$ MgCl$_2$

0.1 m$\underline{M}$ EDTA

0.1 m$\underline{M}$ dithiothreitol

0.4 m$\underline{M}$ K$_2$HPO$_4$

0.4 mg/ml bovine serum albumin

A solution with the same composition but in which the concentrations of the components are 2.5 times higher will be referred to as buffer A.

In these experiments, the template solution with or without inhibitor was prepared in a total volume of 45 μl in an ice bath from deionized water, DNA stock solution (see section II.5) and an unbuffered solution of the inhibitor. The latter solution was titrated to pH 5.0 before use, in order to prevent the precipitation of DNA by the inhibitors. After the addition of 37 μl ice-cold buffer A to the template solution, the enzyme was added in 3 μl of an ice-cold solution consisting of commercial enzyme solution, deionized water, and 3 μl of buffer A. The mixture was transferred to a 37 ^{o}C water bath and was

incubated for 6 minutes. The reaction was then initiated by the rapid addition (using Hamilton syringe) of 10 μl of a solution consisting of ATP, CTP, GTP, and 8-[^{3}H]-UTP (specific activity: 4.99 counts/minute/ pMole of UTP) at a concentration of 5mM each (i.e. ten times the final concentration) in deionized water, pH 7.0. The reaction was allowed to proceed for 8 minutes at 37 ^{o}C, and it was terminated by the addition of 1 ml of freshly prepared ice-cold 5 % trichloracetic acid solution containing 0.05 M sodium pyrophosphate.

After thorough vortexing and standing in ice for at least 20 minutes, but not longer than 90 minutes, the insoluble material was collected by filtration through Whatman GF/C filter disks (2.4 cm in diameter). The precipitate on the disks was rinsed with 20 ml of ice-cold 5 % trichloracetic acid solution containing 0.05 M sodium pyro-phosphate. The precipitate was further washed with 30 ml of ice-cold 95 % ethanol and then dried under vacuum overnight.

The radioactivity retained on the disks was counted after addition of 10 ml of 0.4 % 2,5-diphenyloxazol solution in toluene.

The radioactivity absorbed and retained by the filter disks themselves and the radioactivity trapped within the precipitated components of the assay mixtures was determined from the residual radio-activity of blanks which did not contain any enzyme.

The specific activities of nucleoside triphosphate solutions were determined from measurements carried out using 10 μl aliquots of these solutions. These aliquots were placed on filter disks, dried under vacuum overnight, and then counted as described above.

Experiments, in which the template concentration or the reaction

time were varied, were performed in the absence of inhibitors. The same experimental procedure described above was used with the exception that in the case of experiments in which the reaction time was varied, 0.1 ml aliquots were removed at different times from a master assay mixture (1.2 ml) and dispensed into 1 ml of ice-cold 5 % trichloracetic acid solution containing 0.05 $\underline{M}$ sodium pyrophosphate. The mixture was filtered and dried as described above.

Experiments designed to measure the inhibition of ribonucleic acid chain initiation were conducted as described above except that a nucleoside triphosphate solution consisting of γ-[^{32}P]-ATP, CTP, GTP, and 8-[^{3}H]-UTP (specific activities: 2200 cpm/pMole of ATP and 27 cpm/pMole of UTP, respectively) at a concentration of 2.5 $\underline{mM}$ for each nucleoside triphosphate (ten times the final concentration) in deionized water, pH 7.0 was used. In these experiments 7 minutes preincubation and 7 minutes incubation were employed.

Special procedures for terminating the reaction and for washing were used for the experiments involving ^{32}P incorporation, so as to reduce the high background due to unincorporated radioactivity, which were noted. Reactions were terminated by the addition of 0.5 ml ice-cold 0.1 $\underline{M}$ sodium pyrophosphate solution containing 20 $\underline{mM}$ ATP and 2 $\underline{mM}$ UTP and 0.5 ml of ice-cold 10 % trichloracetic acid solution containing 1 $\underline{M}$ KCl. The insoluble material collected on the filter disks was soaked in 50 ml of ice-cold 5 % trichloracetic acid solution containing 1 $\underline{M}$ KCl and 0.01 $\underline{M}$ sodium pyrophosphate for 1 hour, and further soaked in 40 ml of ice-cold 95 % ethanol for 20 minutes. The filter disks were dried as before and placed in 10 ml of 0.4 % 2,5-diphenyloxazole

solution in toluene for counting the radioactivity.

Simultaneous counting of ^{3}H and ^{32}P activities were performed in the Beckman Model LS-250 Liquid Scintillation System using the ^{3}H below ^{14}C and ^{32}P above ^{3}H Isosets at a gain setting of 310. Under these counting conditions less than 2 % activity spill-over between ^{3}H and ^{32}P could be detected.

EXPERIMENTAL RESULTS

III.1. Dimerization Studies

The ultraviolet spectra of Miracil D in 0.01 $\underline{M}$ sodium acetate buffer, pH 5.0 over a 50-fold concentration range are shown in Figure 9. In dilute solutions, the absorption maximum is at 330 nm with a shoulder around 350 nm. As the concentration is increased, the shoulder becomes more pronounced and the absorption peak decreases in intensity and shifts to longer wavelengths. As it can be seen in Figure 9, Miracil D does not obey Beer's law. The existence of isosbestic points at 303.5 and 352 nm indicates that two spectral species are present over the concentration range of 10^{-3} to 2×10^{-5} $\underline{M}$.

For the determination of the dimerization constant K_d, the method of Lamm and Neville (Lamm and Neville, 1965) was used (see section II.7). In the calculations, absorbances of Miracil D solutions in the range between 315 and 350 nm at 2.5 nm intervals (a total of 15 wavelengths) were used. The root-mean-square (RMS) deviation in absorbance units as the function of the dimerization constant K_d is shown in Figure 10. The minimum value of the RMS deviation is at $K_d = 406$ $\underline{M}^{-1}$ and this value is assumed to be the dimerization constant of Miracil D in 0.01 $\underline{M}$ sodium acetate buffer, pH 5.0. At its minimum, the RMS deviation is only 0.002 which is within the limits of the error specifications of the spectrophotometer used.

According to equation (2) (see section II.7), the apparent ex-

Figure 9. The absorption spectrum of Miracil D in 0.01 $\underline{M}$ sodium acetate buffer, pH 5.0 at room temperature. Miracil D concentrations: (a) 2×10^{-5} $\underline{M}$ in 5 cm cell, (b) 5×10^{-4} $\underline{M}$ in 0.2 cm cell, and (c) 10^{-3} $\underline{M}$ in 0.1 cm cell.
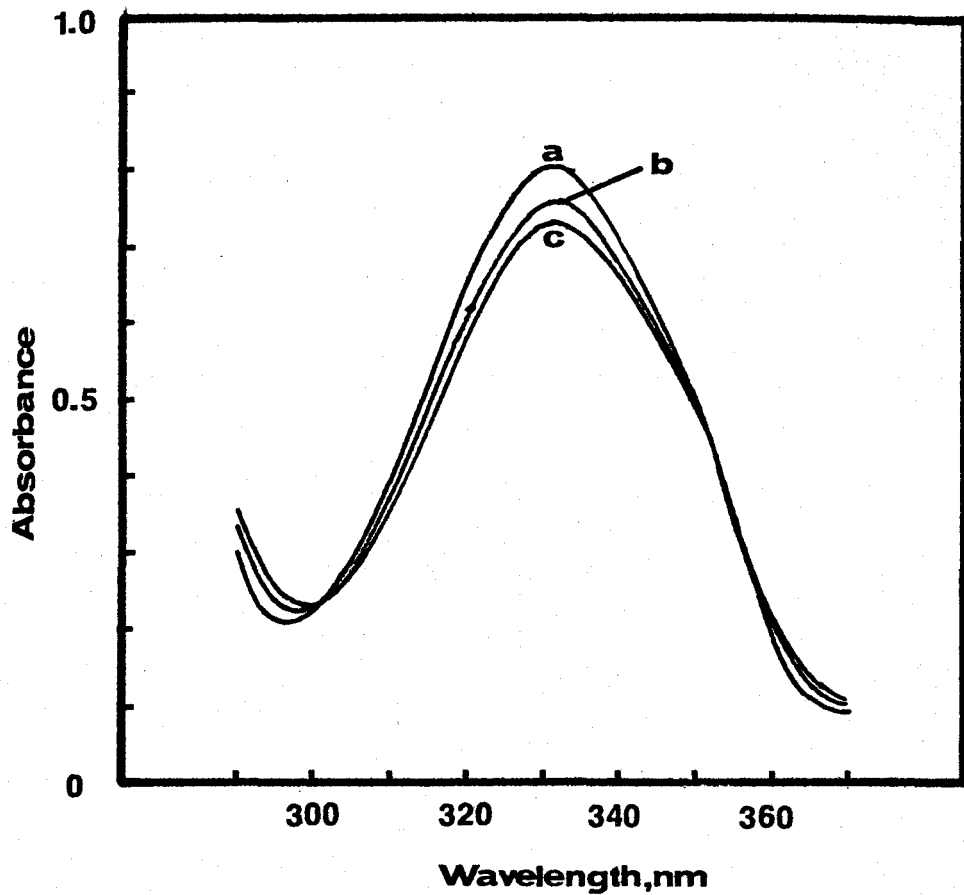
Figure 10. The dependence of the root-mean-square (RMS) deviation (in units of absorbance) on the dimerization constant K_d of Miracil D at room temperature. A minimum is observed at $K = 406$ $\underline{M}^{-1}$.
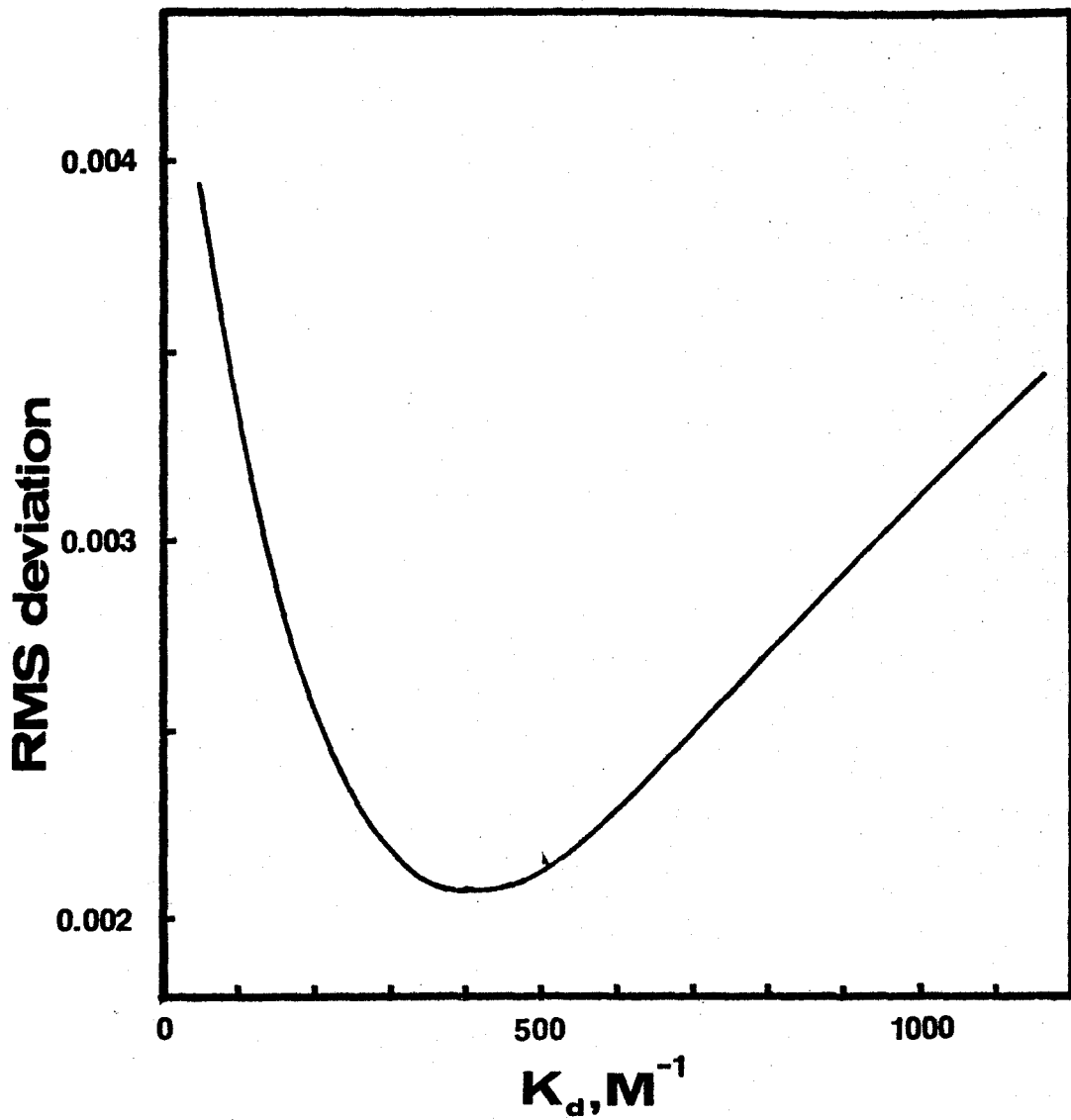
tinction coefficient E_{app} is a linear function of the fraction α of

drug present as monomer. To illustrate the precision of the fit with

$K_d=406$ $\underline{M}^{-1}$, the apparent extinction coefficient E_{app} of Miracil D so-

lutions as a function of α at 315, 320, 325, and 330 nm is presented in

Figure 11. The straight lines calculated on the basis of equation (2)

and a K_d value of 406 $\underline{M}^{-1}$, are the best fitting lines to the experi-

mentally obtained apparent extinction coefficients.

The dimerization of Miracil D was also investigated in 0.2 $\underline{M}$

sodium acetate buffer, pH 5.0 at room temperature. A value for the

dimerization constant K_d of 410 $\underline{M}^{-1}$ was obtained, indicating that the

dimerization is practically independent of ionic strength in the ionic

strength range studied.

Since the pK_a's for Miracil D are -0.20 and 7.4, in aquaeous

solutions at pH 5.0 the drug is present as a positively charged ion

with a single charge localized on the distal nitrogen atom. Therefore,

the present dimerization studies describe an equilibrium between the

singly charged monomeric and doubly charged dimeric forms of the drug.

III.2. Binding Studies

III.2.1. The Binding of Miracil D to Calf Thymus DNA at 0.01 and

0.2 M Salt Concentrations

The binding of Miracil D to calf thymus DNA was investigated in

0.01 $\underline{M}$ sodium acetate buffer, pH 5.0 at room temperature. In these

measurements, the concentration of Miracil D was maintained constant

at 2×10^{-5} $\underline{M}$, while the DNA concentration was varied. The absorption

spectra of Miracil D-DNA complexes are shown in Figure 12.

Free Miracil D exhibits an absorption maximum at 330 nm with

Figure 11. The dependence of the apparent extinction coefficient E_{app} on the fraction α of Miracil D present as monomer at various wavelengths as indicated in the figure. The straight lines are calculated with $K_d = 406 \, \underline{M}^{-1}$.

72
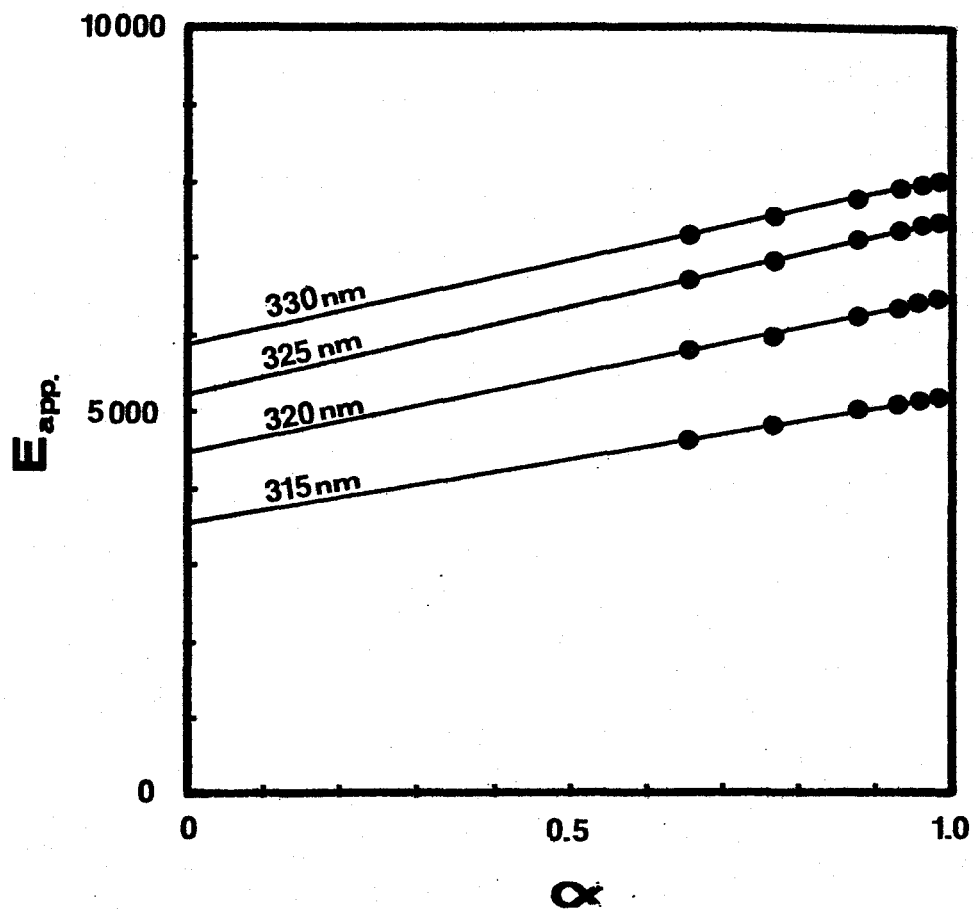
Figure 12. The absorption spectra of Miracil D-DNA complexes in 0.01 $\underline{M}$ sodium acetate buffer, pH 5.0 at room temperature obtained in 5 cm cells. Miracil D concentration: 2×10^{-5} $\underline{M}$, DNA concentrations: (a) 0, (b) 8.4×10^{-6} $\underline{M}$, (c) 5×10^{-5} $\underline{M}$, and (d) 3.4×10^{-4} $\underline{M}$.
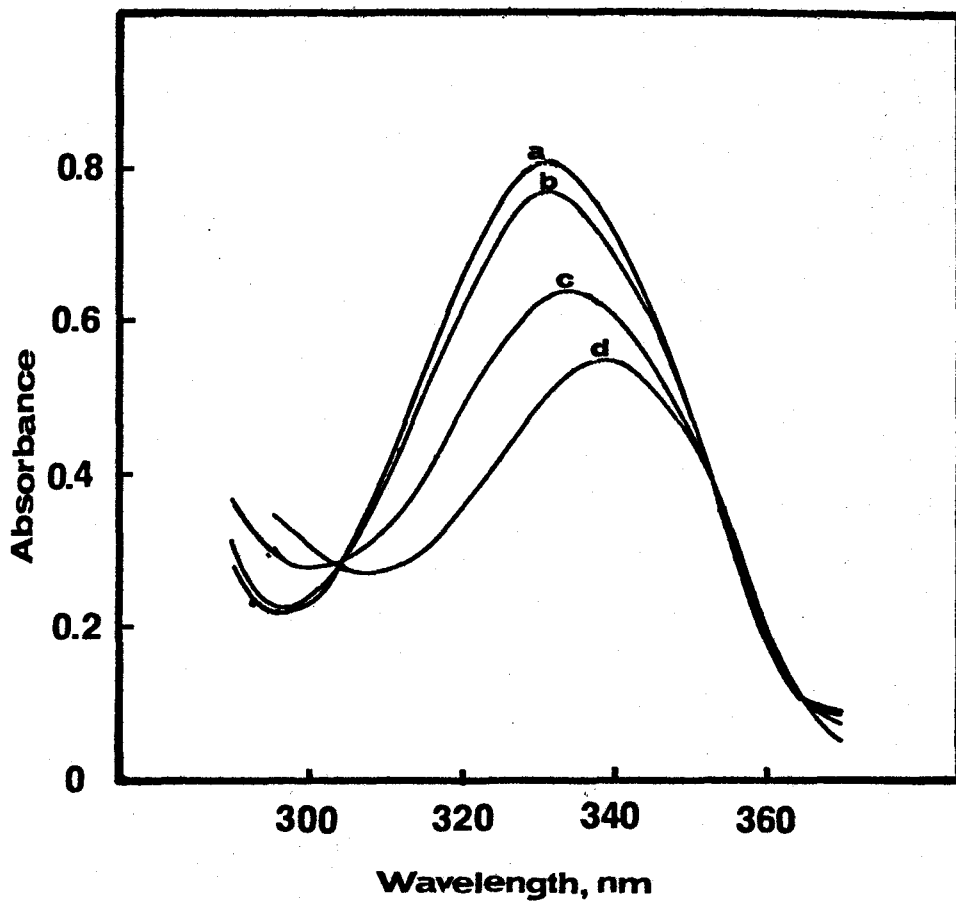
a slight shoulder centered around 352 nm. Upon addition of DNA, the intensity of the maximum decreases, the maximum shifts to longer wavelengths, and the shoulder becomes a little more pronounced. At the highest DNA concentration (3.4×10^{-4} $\underline{M}$), the maximum shifts to 337 nm. Qualitatively similar spectral changes were observed for the interaction of other intercalating drugs, such as ethidium bromide (Waring, 1965), proflavine (Dourlent and Helene, 1971), and acriflavine (Tubbs et al., 1964) with nucleic acids. The existence of three isosbestic points at 304, 352, and 364 nm indicates that only two spectral species are present. The largest changes of absorbance were obtained at 325 nm and, therefore, absorbances at this wavelength were used in calculating the binding parameters.

Since the value of the absorbance of the bound drug, A_b, is not generally obtainable experimentally, it was determined from the plot of the reciprocal differential absorbance $1/(A_f-A)$ _versus_ the reciprocal nucleic acid concentration $1/[P]$ (see section II.8.2), which is presented in Figure 13. As it can be seen, the plot is not linear in the experimentally available nucleic acid concentration region, and, therefore, a standard polynomial curve fitting procedure was used to obtain the intercept of the best fitting polynomial (solid line) with the ordinate.

The Scatchard plot of the binding of Miracil D to calf thymus DNA in 0.01 $\underline{M}$ sodium acetate buffer, pH 5.0 at room temperature is shown in Figure 14. The experimental points are shown together with the calculated theoretical isotherm obtained using an intrinsic association constant of 1.2×10^6 $\underline{M}^{-1}$. The isotherm describes the binding of

Figure 13. A plot of reciprocal differential absorbance $1/(A_f-A)$ <u>versus</u> reciprocal DNA concentration $1/[P]$ for determining the absorbance A_b of bound drug (see text for details).
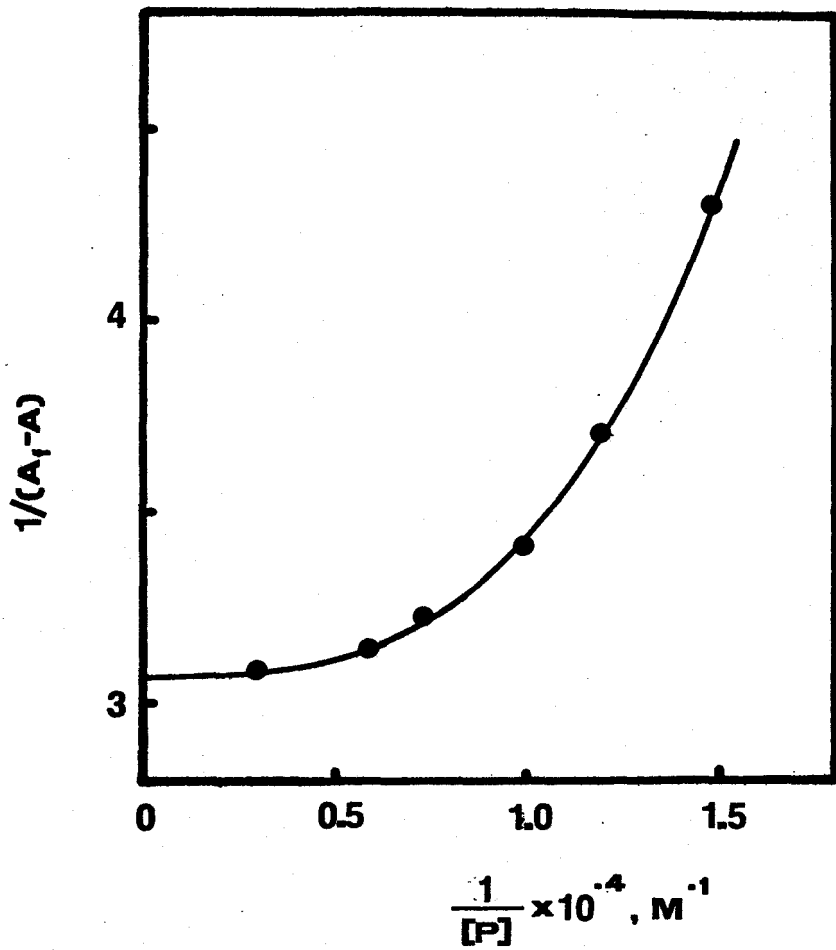
Figure 14. The Scatchard plot of the binding of Miracil D to calf thymus DNA in 0.01 $\underline{M}$ sodium acetate buffer, pH 5.0 at room temperature. The experimentally obtained points are shown together with the calculated isotherm (solid line) for an intrinsic association constant of $1.2 \times 10^6 \ \underline{M}^{-1}$.
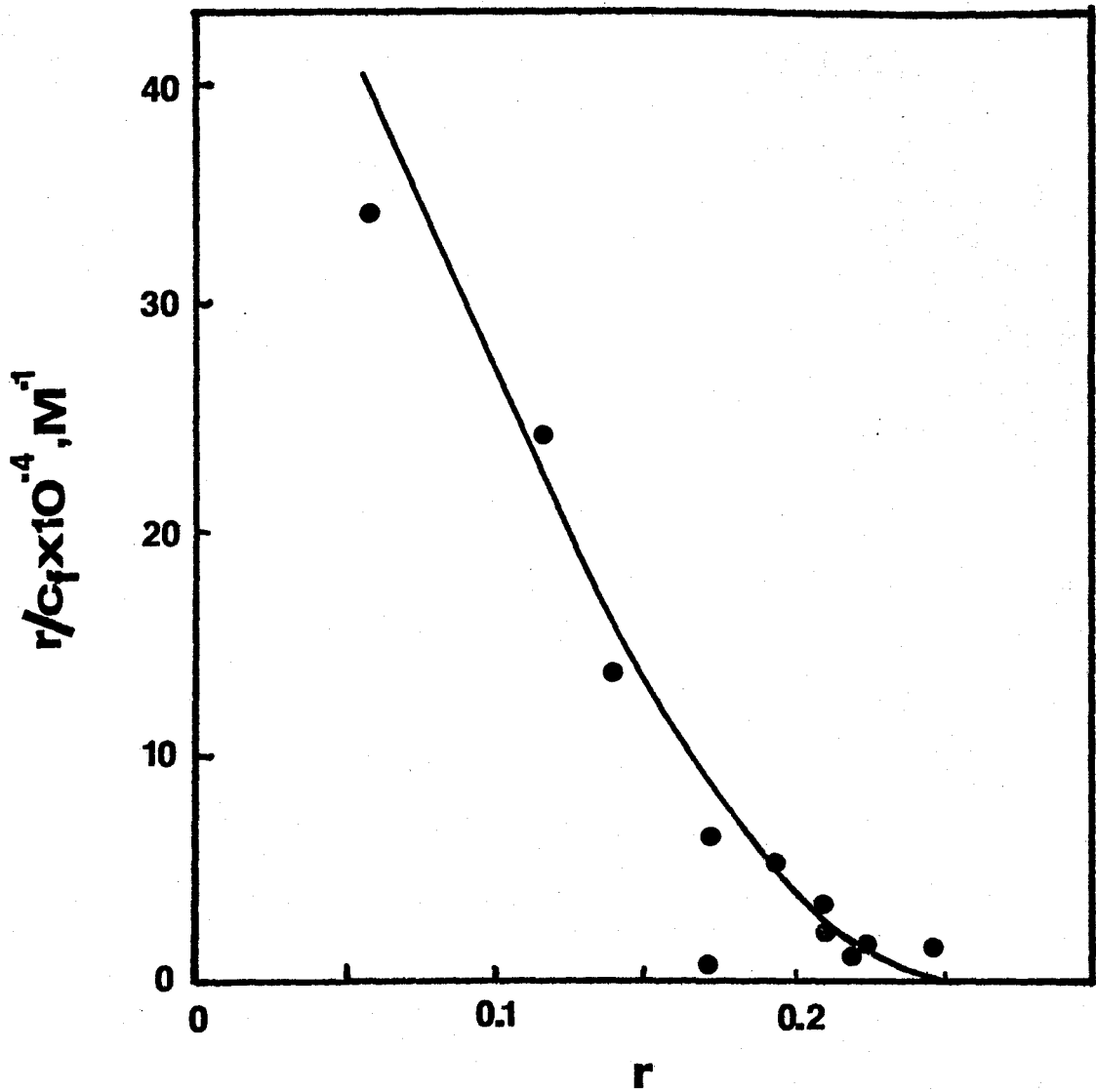
Miracil D to calf thymus DNA on the basis of the exclusion model. In this model, it is assumed that the binding of one Miracil D molecule to DNA prevents the binding of other Miracil D molecules to the nearest neighbour binding sites. The validity of this assumption will be discussed in section IV.2. The calculations were performed as outlined in section II.7.

The binding of Miracil D to calf thymus DNA was also investigated in 0.2 $\underline{M}$ sodium acetate buffer, pH 5.0 under identical experimental conditions. For this case, the Scatchard plot and the calculated theoretical isotherm determined by an intrinsic association constant of $4.5 \times 10^4 \underline{M}^{-1}$ are shown in Figure 15.

At Miracil D concentrations of $2 \times 10^{-5} \underline{M}$ more than 98 % of the drug is present as a monomer with a single positive charge (K_d's of 406 $\underline{M}^{-1}$ in 0.01 $\underline{M}$ sodium acetate buffer, pH 5.0 and 410 $\underline{M}^{-1}$ in 0.2 $\underline{M}$ sodium acetate buffer, pH 5.0 were used for these calculations; see section III.1). Therefore, the spectral changes observed in the binding studies are the result of an equilibrium between the singly charged monomeric form of Miracil D and the intercalated form of the drug.

It should be noted that increasing ionic strength decreases the extent of binding. A 27-fold decrease in the intrinsic association constant was observed going from 0.01 $\underline{M}$ to 0.2 $\underline{M}$ sodium acetate buffer, pH 5.0. This finding is in agreement with the general trend exhibited in the binding of other intercalators to nucleic acids (Aktipis and Kindelis, 1973; Blake and Pecocke, 1968; Waring, 1965).

Figure 15. The Scatchard plot of the binding of Miracil D to calf

thymus DNA in 0.2 $\underline{M}$ sodium acetate buffer, pH 5.0 at room temperature.

The experimentally obtained points are shown together with the calcu-

lated isotherm (solid line) for an intrinsic association constant of

$4.5 \times 10^4 \ \underline{M}^{-1}$.
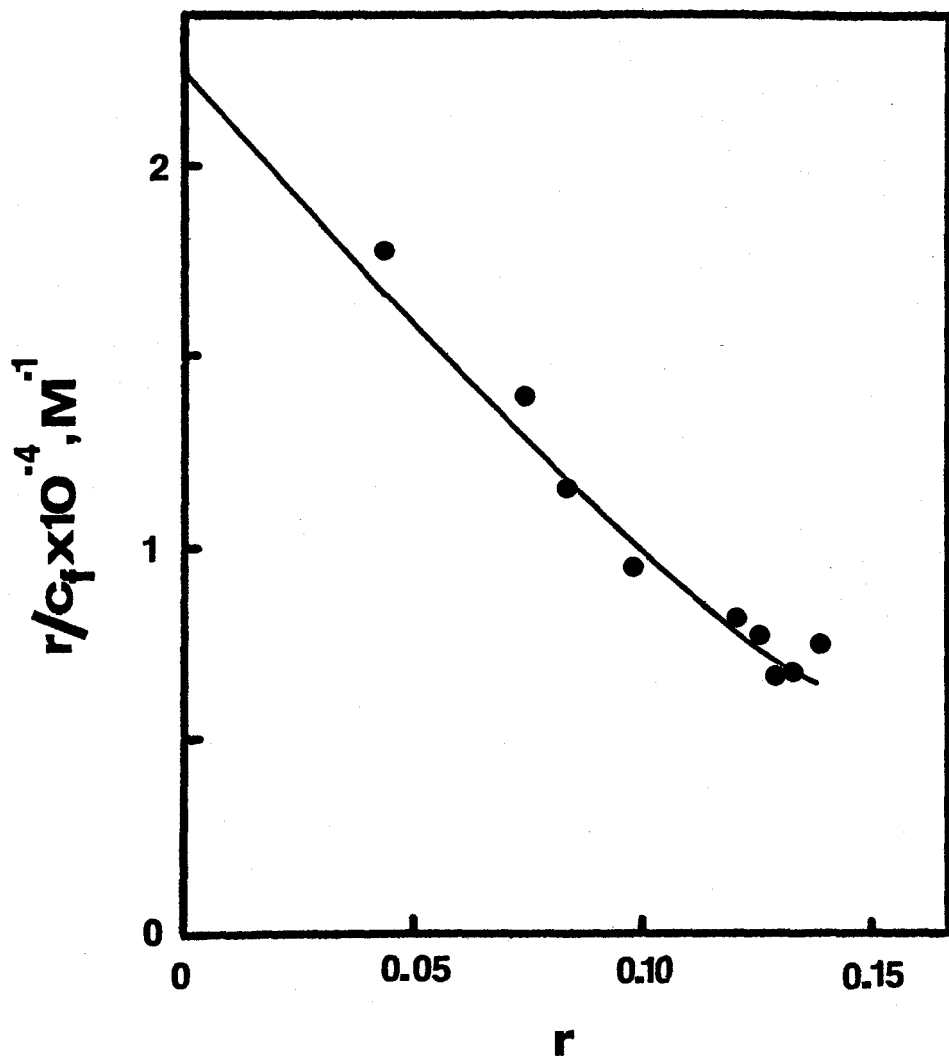
III.2.2. The Binding of Miracil D to Calf Thymus DNA under RNA
Polymerase Assay Conditions

The binding of Miracil D to calf thymus DNA was also investi-
gated under the experimental conditions used for DNA dependent RNA
polymerase assays. These studies were carried out at 37 ^{o}C and in
the same buffer as the RNA polymerase assays (see section II.11) with
the exception that bovine serum albumin and dithiothreitol were o-
mitted. Preliminary experiments showed that this omission had no
effect on the extent of binding.

The Scatchard plot and the calculated theoretical isotherm de-
termined, using an intrinsic association constant of $1.35 \times 10^{4} \underline{M}^{-1}$, are
shown in Figure 16. Comparison of the intrinsic association constants
under these conditions and in 0.01 $\underline{M}$ sodium acetate buffer, pH 5.0 (see
section III.2.1) indicates an 88-fold decrease in the value of the
constant. This decrease is the result of the concerted effect of
changes in both the ionic strength and the temperature to adjust for
the conditions under which these measurements were carried out.

III.2.3. The Dependence of the Binding of Miracil D to Calf Thymus
DNA on Temperature

The effect of temperature changes on the binding of Miracil D
to calf thymus DNA were obtained from the measurements of absorbance of
Miracil D-calf thymus DNA complexes at 440 nm as the function of
temperature according to the method outlined in section II.10.1. The
intrinsic association constants were calculated as outlined in section
II.10.3.

The plot of $\log_{10} K$ versus the reciprocal absolute temperature

Figure 16. The Scatchard plot of the binding of Miracil D to calf thymus DNA under RNA polymerase assay conditions at 37 ^{o}C (see section II.11). The experimentally obtained points are shown together with the calculated isotherm (solid line) for an intrinsic association constant of 1.35×10^4 $\underline{M}^{-1}$.
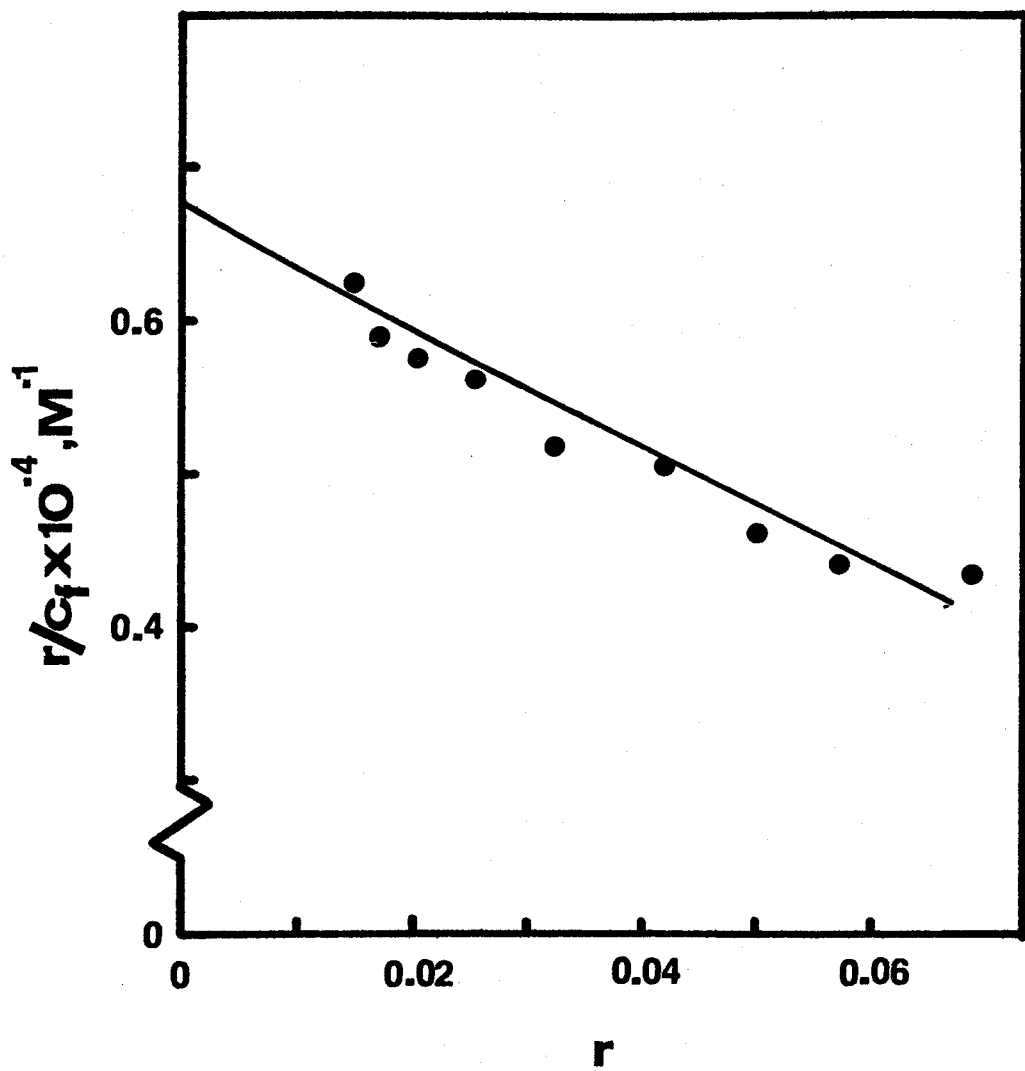
1/T for the binding of Miracil D to calf thymus DNA in 0.01 $\underline{M}$ sodium acetate buffer, pH 5.0 is shown in Figure 17. A linear relationship was obtained in the temperature range of 25 to 60 $^{\circ}$C. From the slope (=2.35) of the plot and from the intrinsic association constant at 25 $^{\circ}$C (1.2×10^6 $\underline{M}^{-1}$; see section III.2.1), the following thermodynamic quantities were calculated: $\Delta G^{\circ} = -8.2$ Kcal/Mole, $\Delta H^{\circ} = -10.7$ Kcal/Mole, and $\Delta S^{\circ} = -8.2$ cal/Mole/K. These values are correct of course only to the extent that the activty coefficients can be assumed to be at unity.

Since the absolute value of ΔH° is greater than that of $T \cdot \Delta S^{\circ}$ ($10700 > 298 \cdot 8.2$), and both ΔH° and $T \cdot \Delta S^{\circ}$ have the same sign, it appears that the unfavourable entropy change, which accompanies the binding process, is overcompensated by the attending enthalpy change. Therefore, the binding process is enthalpy-driven.

For a comparison of the thermodynamic quantities presented above with those characteristic of other intercalators, the binding of ethidium bromide to DNA in 1 $\underline{M}$ NaCl may be considered. Using the exclusion model, Bresloff and Crothers found that $\Delta H^{\circ} = -7.8$ Kcal/Mole and $\Delta S^{\circ} = -7.72$ cal/Mole/K (Bresloff and Crothers, 1975). This binding process is also enthalpy-driven.

III.2.4. The Binding of Methyl-Miracil D to Calf Thymus DNA at 0.01 M Salt Concentration

The binding of methyl-Miracil D to calf thymus DNA was investigated in 0.01 $\underline{M}$ sodium acetate buffer, pH 5.0 at room temperature. The absorption spectra of methyl-Miracil D-DNA complexes in the visible spectral region (Figure 18) were obtained at constant drug concentration (2×10^{-5} $\underline{M}$) as the DNA concentration was varied.

Figure 17. The van't Hoff plot of Miracil D-DNA binding in 0.01 $\underline{M}$ sodium acetate buffer, pH 5.0.

88
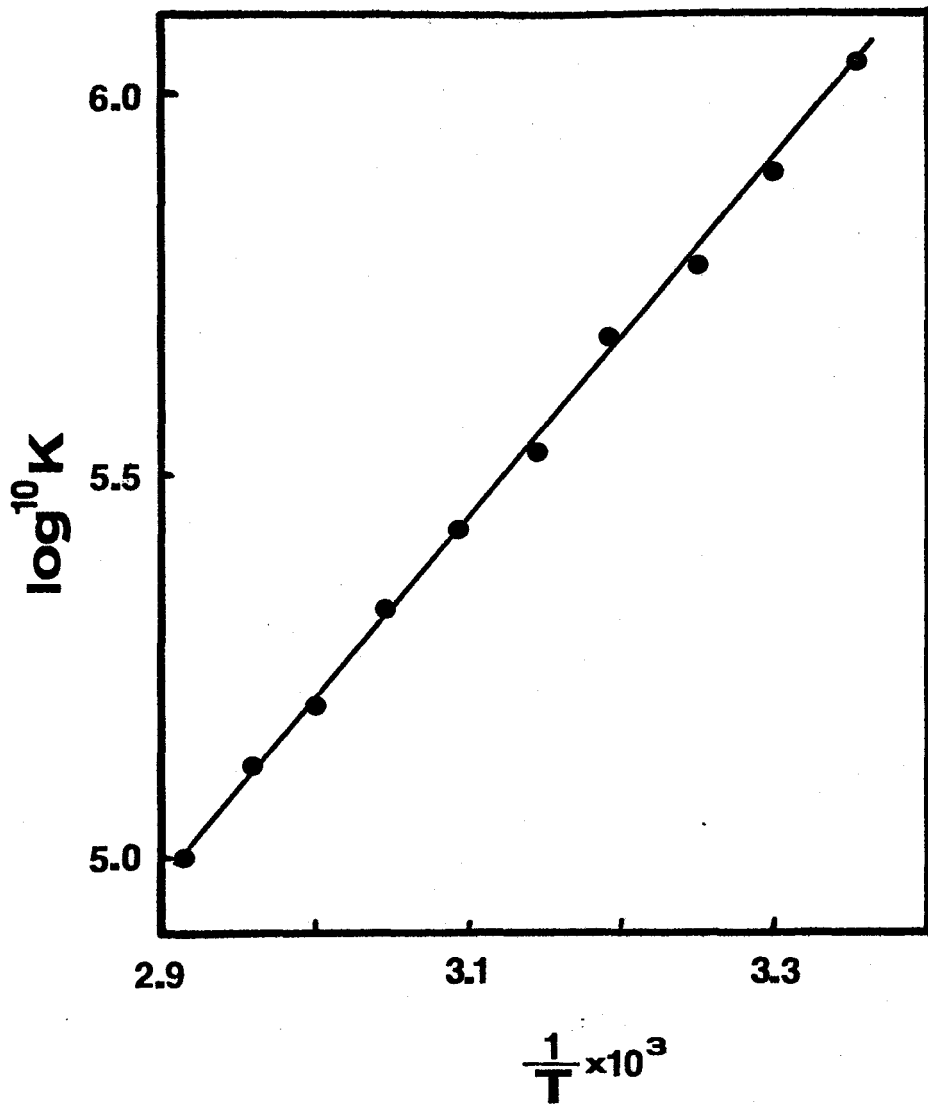
Figure 18. The absorption spectra of methyl-Miracil D-DNA complexes in 0.01 $\underline{M}$ sodium acetate buffer, pH 5.0 at room temperature obtained in 10 cm cells. Methyl-Miracil D concentration: 2×10^{-5} $\underline{M}$, DNA concentrations: (a) 0, (b) 5×10^{-5} $\underline{M}$, (c) 1.2×10^{-4} $\underline{M}$, and (d) 6.2×10^{-4} $\underline{M}$.
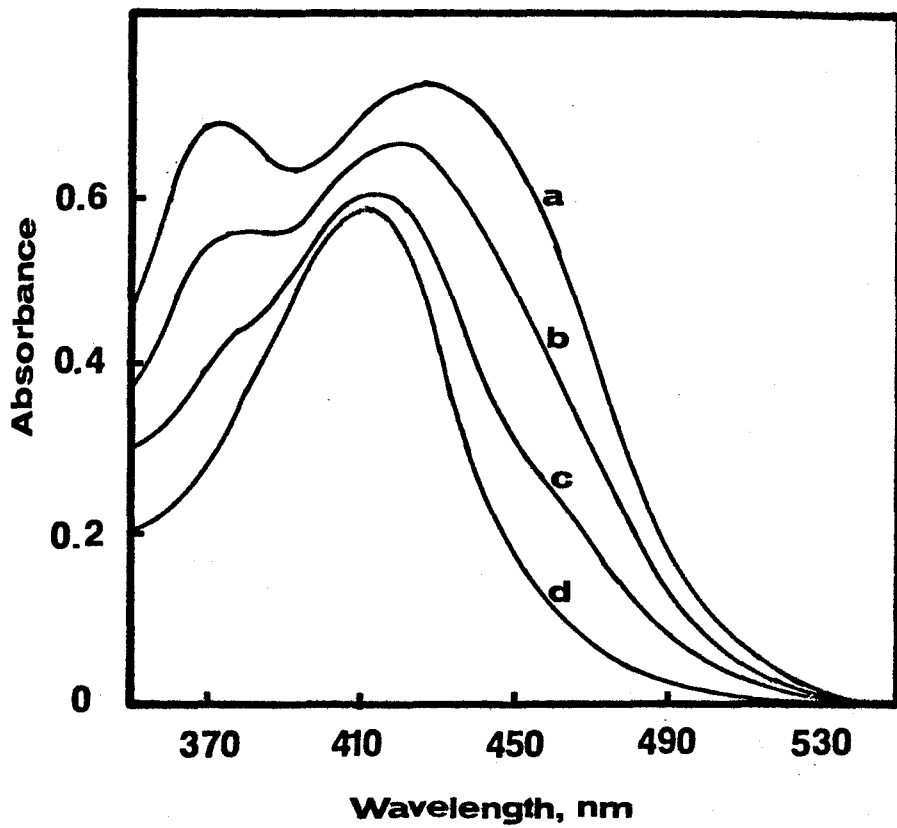
Free methyl-Miracil D exhibits two absorption maxima at 374 and 425 nm. Upon addition of DNA, the intensity of both maxima decreases, and the two bands appear to merge into a single band centered around 410 nm. The largest changes in absorbance were obtained at 370 and 450 nm. The absorbances at these wavelengths were, therefore, used in calculating the intrinsic association constant for the system.

Although no isosbestic point is observed, the absorption spectra were evaluated with the assumption that only two spectral species are present in these solutions. If there were a DNA concentration range in which the spectra of complexes exhibited an isosbestic point while in another DNA concentration range no isosbestic point could be observed, this would be a clear indication of the presence of more than two spectral species. This is not the case; therefore, the assumption about the presence of only two spectral species is compatible with the spectra of methyl-Miracil D-DNA complexes (Figure 18). This reasoning is obviously supportive but not conclusive.

However, the assumption that only two absorbing species are present is further supported by the finding that the intrinsic association constants determined from the spectral changes at 370 and 450 nm are in good agreement with one another as it is apparent from examining the values listed below.

The Scatchard plot of the binding of methyl-Miracil D to calf thymus DNA in 0.01 $\underline{M}$ sodium acetate buffer, pH 5.0 is shown in Figure 19. The experimental points obtained at 370 nm are shown together with the calculated theoretical isotherm determined, using an intrinsic association constant of 1.7×10^5 $\underline{M}^{-1}$. This constant corresponds to a ΔG^o

Figure 19. The Scatchard plot of the binding of methyl-Miracil D to calf thymus DNA in 0.01 $\underline{M}$ sodium acetate buffer, pH 5.0 at room temperature. The experimentally obtained points are shown together with the calculated isotherm (solid line) for an intrinsic association constant of 1.7×10^5 $\underline{M}^{-1}$.
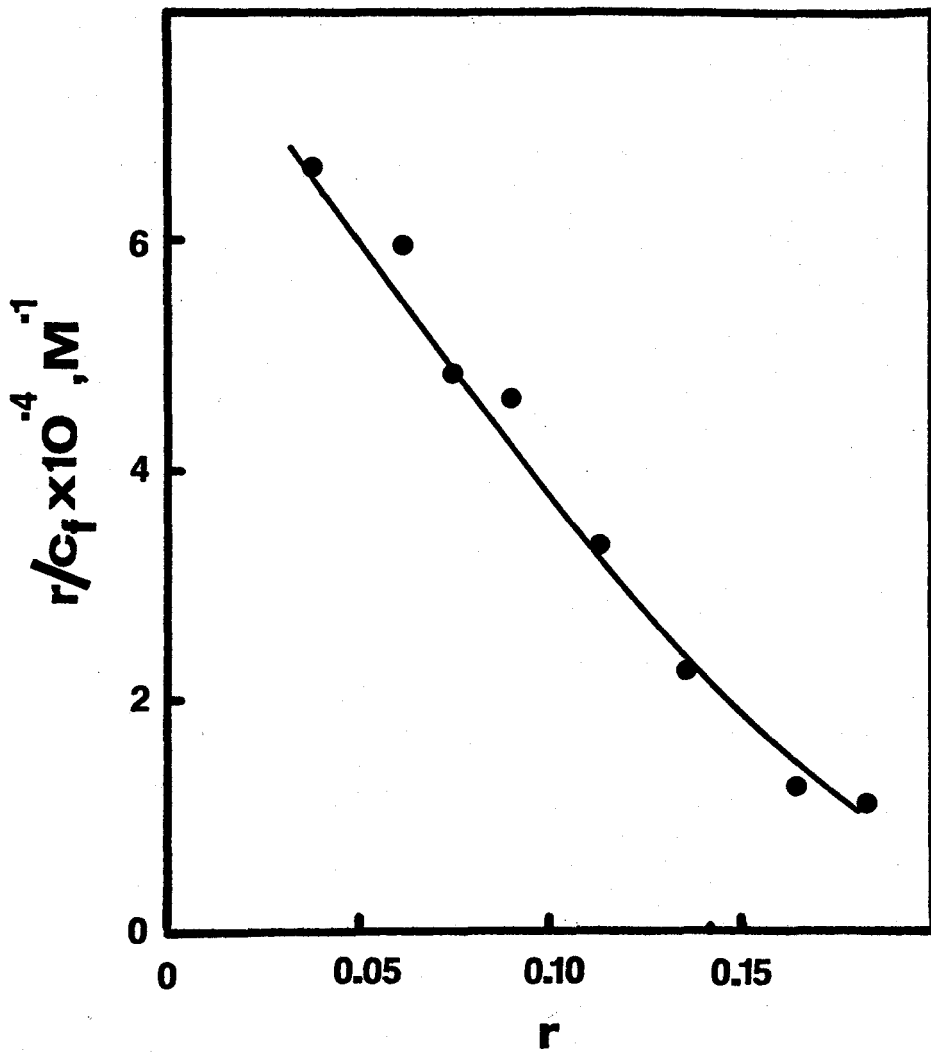
value of -7.1 Kcal/Mole ($=-R \cdot T \cdot \ln(1.7 \times 10^5)$). The isotherm describes the binding of methyl-Miracil D to calf thymus DNA on the basis of the exclusion model, the applicability of which will be discussed in sections IV.2 and IV.3. The calculations were performed as outlined in section II.7. The same calculations were performed on the experimental data obtained at 450 nm and an intrinsic association constant of 1.5×10^5 $\underline{M}^{-1}$ was obtained in good agreement with a value of 1.7×10^5 $\underline{M}^{-1}$ obtained from data at 370 nm (see above).

It is reasonable to assume that the pK_a of the distal nitrogen atom of Miracil D is not much affected by the methyl substitution on the proximal nitrogen atom. Therefore, the pK_a of the distal nitrogen atom of methyl-Miracil D should not be much different than 7.4, the value noted for Miracil D. In addition, since the pK_a of the proximal nitrogen atom of methyl-Miracil D is 3.41, this drug, in analogy to Miracil D, should carry at pH 5.0 a positive charge on its distal nitrogen atom. Assuming that methyl-Miracil D has a dimerization constant comparable to that of Miracil D, at a concentration of 2×10^{-5} $\underline{M}$ more than 98 % of the drug should be present as singly charged mono-mer. Therefore, the spectral changes observed in the binding studies are the result of an equilibrium between the singly charged monomeric form of methyl-Miracil D and the intercalated form of the drug.

An examination of the binding of methyl-Miracil D to calf thymus DNA under the conditions of RNA polymerase assays was also attempted. However, extremely large DNA concentrations are required to observe small spectral changes in the spectrum of methyl-Miracil D under these conditions. Since a meaningful association constant cannot be ob-

tained by the spectrophotometric method used in these investigations, an estimation was performed to obtain the intrinsic association constant which is outlined in section III.5.3.

III.2.5. The Binding of MDMT to Calf Thymus DNA

The binding of MDMT to calf thymus DNA was investigated in 0.01 $\underline{M}$ sodium acetate buffer, pH 5.0 at room temperature. In the course of this investigation, difficulties were encountered in the evaluation of spectral data because of two reasons. First, absorbance changes occuring upon addition of DNA are small even at the highest possible nucleic acid concentrations. Second, the maximal spectral changes take place in the 300 to 315 nm region. In this region, considerable absorbances are exhibited by DNA especially at high DNA concentrations. The spectra obtained cross over one another without establishing a well-defined isosbestic point. Although this appears to be the result of limitations in the accuracy with which the DNA absorbances can be blanked out, the possibility that more than two absorbing species are present in these solutions cannot be ruled out.

In spite of the difficulties mentioned above, the intrinsic association constant K was estimated by giving arbitrary values to the absorbance A_b of DNA-bound MDMT. The best fitting theoretical isotherms were then calculated using the method described in section II.8.3. An intrinsic association constant K ranging between 5×10^3 and 5×10^4 $\underline{M}^{-1}$ was the most compatible with the spectral data as judged by the standard error of estimate. Therefore, it appears that the binding of MDMT to calf thymus DNA in 0.01 $\underline{M}$ sodium acetate buffer, pH 5.0 at room temperature is weaker than that of methyl-Miracil D under similar

conditions (see section III.2.4).

III.3. Circular Dichroism Measurements

III.3.1. The Miracil D-DNA Complex

The circular dichroism of Miracil D-calf thymus DNA complexes was investigated in 0.01 $\underline{M}$ sodium acetate buffer, pH 5.0 at room temperature. In these measurements, the concentration of Miracil D was maintained constant at 2×10^{-5} $\underline{M}$, while the DNA concentration was varied. The circular dichroism spectra of the complexes are shown in Figure 20.

Miracil D itself is optically inactive, but clearly optical activity is induced upon addition of DNA. The circular dichroism spectra in the 300 to 375 nm wavelength region are composed of two overlapping negative peaks with maxima near 337 and 347 nm. These maxima appear to correspond to the absorption maximum of the bound drug at 337 nm and to the shoulder noted near 352 nm (cf. Figure 12). The positive circular dichroism band centered near 447 nm appears to correspond to the absorption maximum of the bound drug at 450 nm.

The dependence of the differential molar extinction coefficient $E_L - E_R$ on the binding ratio r at 337, 347, and 447 nm is shown in Figures 21, 22, and 23. The concentration of Miracil D bound to DNA was calculated on the basis of an association constant of 1.2×10^6 $\underline{M}^{-1}$ (see section III.2.1). At all three wavelengths, the differential molar extinction coefficients decrease with increasing binding ratio. Since the circular dichroism bands with maxima near 337 and 347 nm partially overlap, $E_L - E_R$ values at these wavelengths are calculated with the understanding that they are overestimated.

The circular dichroism of Miracil D-calf thymus DNA complexes

Figure 20. The circular dichroism spectra of Miracil D–DNA complexes in 0.01 $\underline{M}$ sodium acetate buffer, pH 5.0 at room temperature in 10 cm cells. Miracil D concentration: 2×10^{-5} $\underline{M}$, DNA concentrations: (a) 0, (b) 3×10^{-5} $\underline{M}$, (c) 7.6×10^{-5} $\underline{M}$, and (d) 3×10^{-4} $\underline{M}$. Binding ratios: (b) 0.22, (c) 0.20, and (d) 0.065.

98

Figure 21. The dependence of the differential molar extinction coefficient $E_L - E_R$ of Miracil D-DNA complexes at 337 nm on the binding ratio r in 0.01 $\underline{M}$ sodium acetate buffer, pH 5.0 at room temperature.

Figure 22. The dependence of the differential molar extinction coefficient $E_L - E_R$ of Miracil D-DNA complexes at 347 nm on the binding ratio r in 0.01 $\underline{M}$ sodium acetate buffer, pH 5.0 at room temperature.

Figure 23. The dependence of the differential molar extinction coef-
ficient $E_L - E_R$ of Miracil D-DNA complexes at 447 nm on the binding ratio
r in 0.01 $\underline{M}$ sodium acetate buffer, pH 5.0 at room temperature.
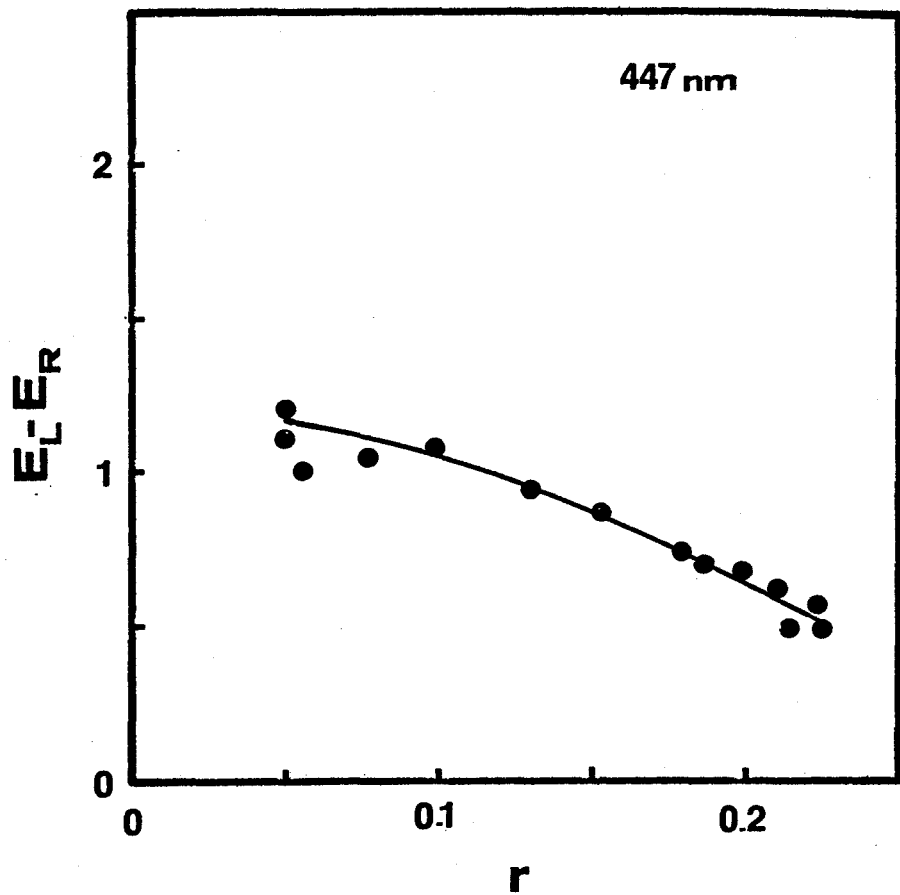
was also investigated in 0.2 $\underline{M}$ sodium acetate buffer, pH 5.0 at room temperature. Because of the lowered intrinsic association constant under these conditions relative to that in 0.01 $\underline{M}$ sodium acetate buffer, pH 5.0 (see section III.2.1), a range of binding ratios from 0.05 to 0.11 was studied. The spectra obtained under these conditions are similar to those in Figure 20 in their overall character and in the location of bands. The differential molar extinction coefficient $E_L - E_R$ at 337, 347, and 447 nm decreases with increasing binding ratios, and the numerical values of $E_L - E_R$ are essentially the same as those of Miracil D-calf thymus DNA complexes in 0.01 $\underline{M}$ sodium acetate buffer, pH 5.0 (Figures 21, 22, and 23).

III.3.2. The Methyl-Miracil D-DNA Complex

The circular dichroism of methyl-Miracil D-calf thymus DNA complexes was investigated in 0.01 $\underline{M}$ sodium acetate buffer, pH 5.0 at room temperature. In these measurements, the concentration of methyl-Miracil D was maintained constant at 2×10^{-5} $\underline{M}$, while the DNA concentration was varied. The circular dichroism spectra of the complexes are shown in Figure 24.

In analogy with Miracil D, methyl-Miracil D itself is optically inactive, but optical activity is induced upon association with DNA. The positive circular dichroism maximum at 405 nm appears to correspond to the absorption maximum of the bound drug at 410 nm (cf. Figure 18). The negative circular dichroism maximum at 335 nm and the shoulder at 353 nm correspond to the barely distinguishable shoulders at 335 and 353 nm on the long wavelength tail of the absorption spectrum of the bound drug.

105

Figure 24. The circular dichroism spectra of methyl-Miracil D-DNA complexes in 0.01 $\underline{M}$ sodium acetate buffer, pH 5.0 at room temperature in 10 cm cells. Methyl-Miracil D concentration: $2x10^{-5}$ $\underline{M}$, DNA concentrations: (a) 0, (b) $1x10^{-4}$ $\underline{M}$, (c) $4x10^{-4}$ $\underline{M}$. Binding ratios: (b) 0.14 and (c) 0.048.
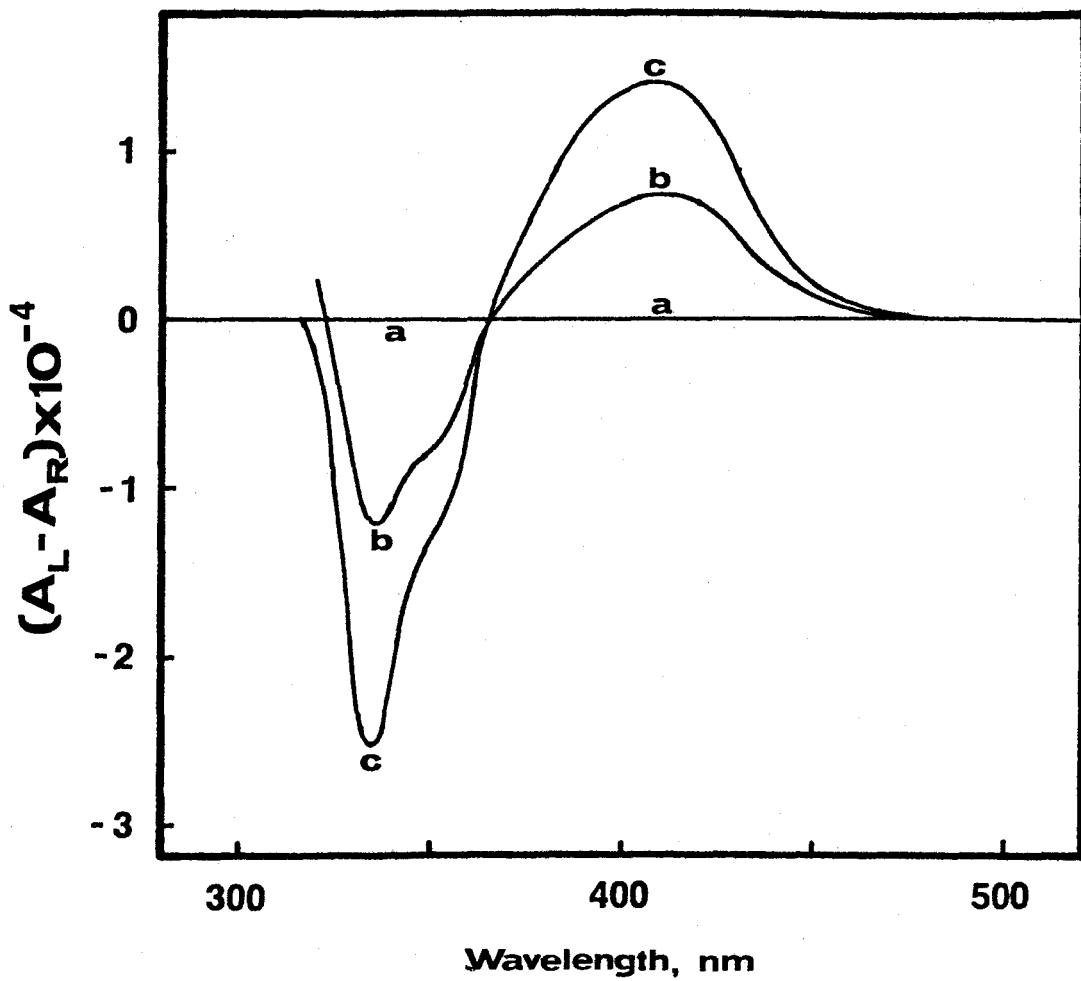
The dependence of the differential molar extinction coefficient $E_L - E_R$ on the binding ratio r at 335, 353, and 405 nm is shown in Figures 25, 26, and 27. The concentration of methyl-Miracil D bound to DNA was calculated on the basis of an association constant of 1.7×10^5 $\underline{M}^{-1}$ (see section III.2.4). In general, the differential molar extinction coefficients in this system are significantly lower than those characteristic of the Miracil D-DNA complexes, but their dependences on the binding ratio r are of similar character.

III.3.3. The MDMT-DNA Complex

The circular dichroism of MDMT-calf thymus DNA complexes was investigated in 0.01 $\underline{M}$ sodium acetate buffer, pH 5.0 at room temperature. As is the case with Miracil D and methyl-Miracil D, MDMT is optically inactive. At a drug concentration of 2×10^{-5} $\underline{M}$ and the highest practical nucleic acid concentration of 4×10^{-4} $\underline{M}$, no optical activity could be detected in the wavelength region between 300 and 600 nm. This finding suggests that either the complex formed is optically inactive or that it may be formed at such low concentrations that even if it were active, the circular dichroism would be below the sensitivity limits of the instrumentation.

III.4. Hyperchromicity and Circular Dichroism Measurements at Elevated Temperatures

III.4.1. Hyperchromicity of the Miracil D-DNA and Methyl-Miracil D-DNA Complexes

The effect of Miracil D and its methyl derivative on the stability of calf thymus DNA against heat denaturation was investigated in 0.01 $\underline{M}$ sodium acetate buffer, pH 5.0. The melting profiles at 260 nm

Figure 25. The dependence of the differential molar extinction coefficient $E_L - E_R$ of methyl-Miracil D-DNA complexes at 335 nm on the binding ratio r in 0.01 $\underline{M}$ sodium acetate buffer, pH 5.0 at room temperature.

110
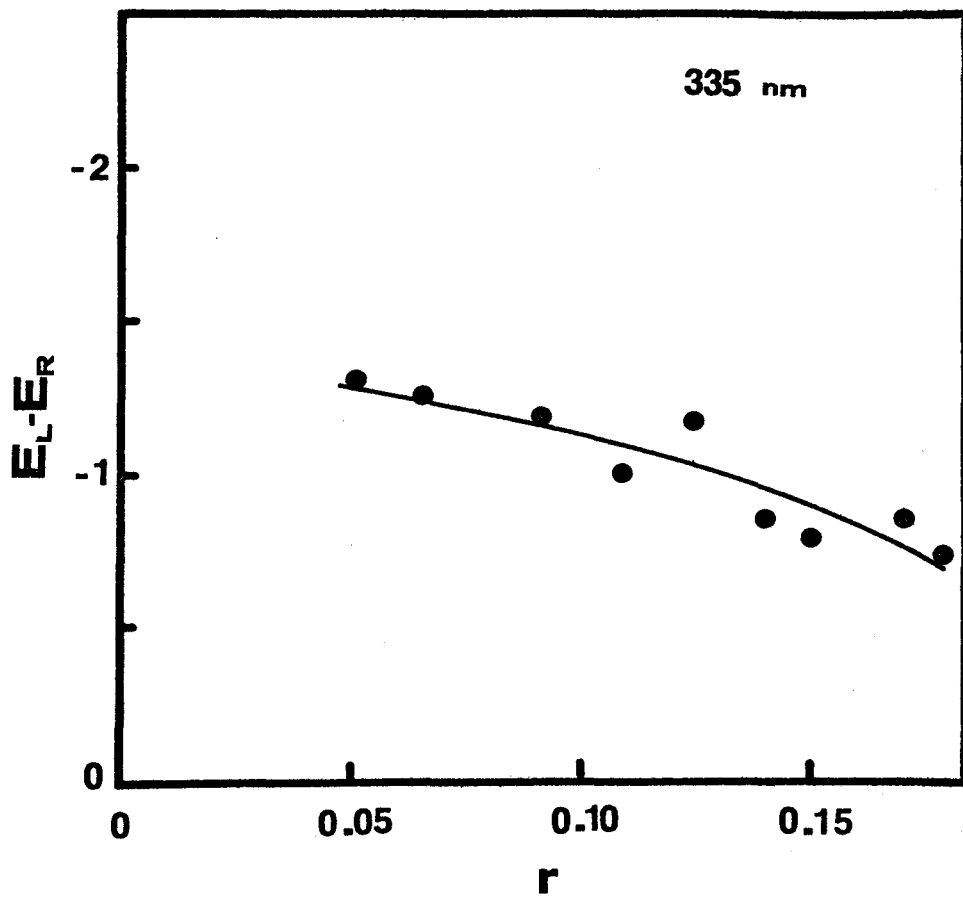
Figure 26. The dependence of the differential molar extinction coefficient E_L-E_R of methyl-Miracil D-DNA complexes at 353 nm on the binding ratio r in 0.01 $\underline{M}$ sodium acetate buffer, pH 5.0 at room temperature.
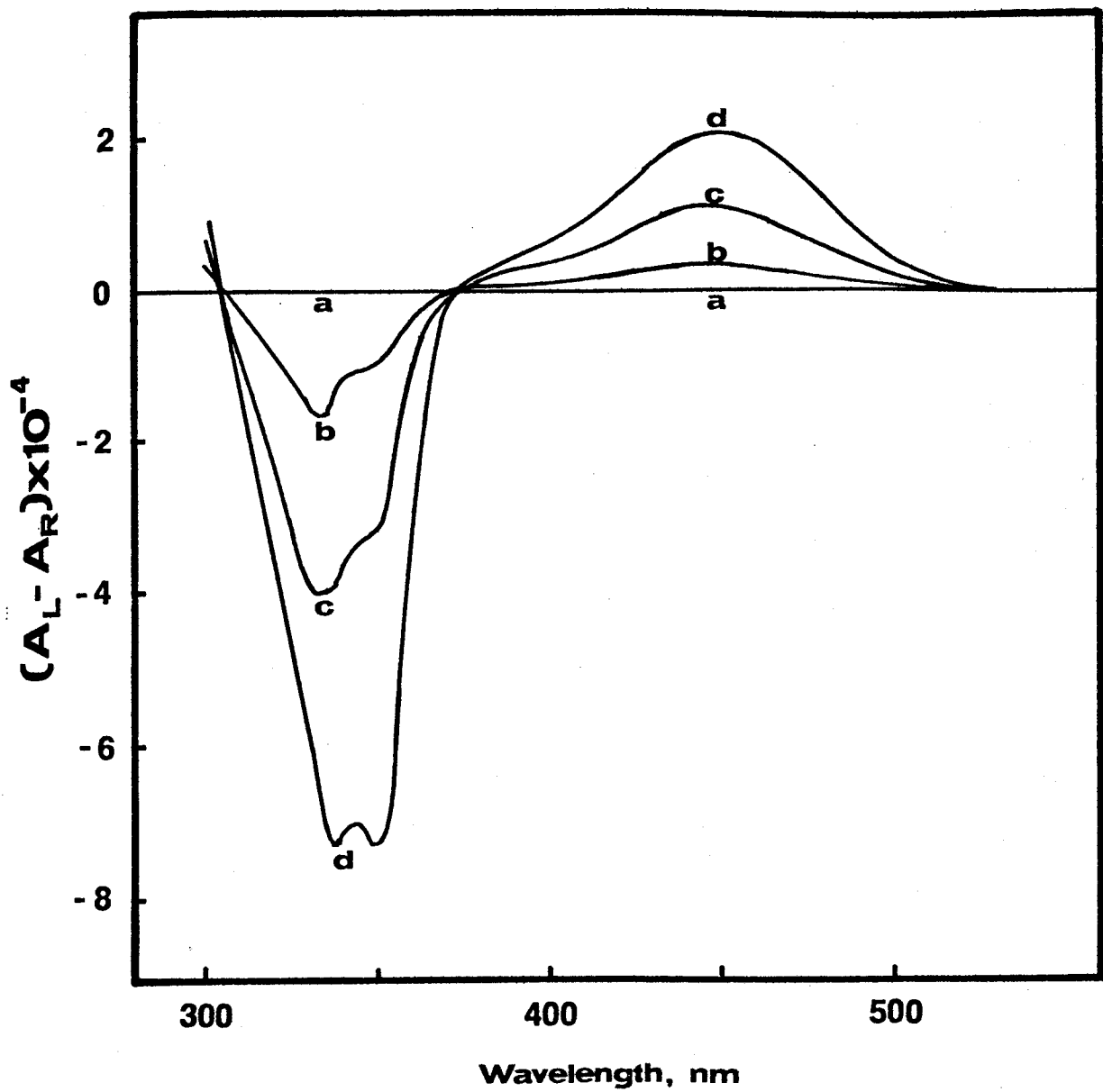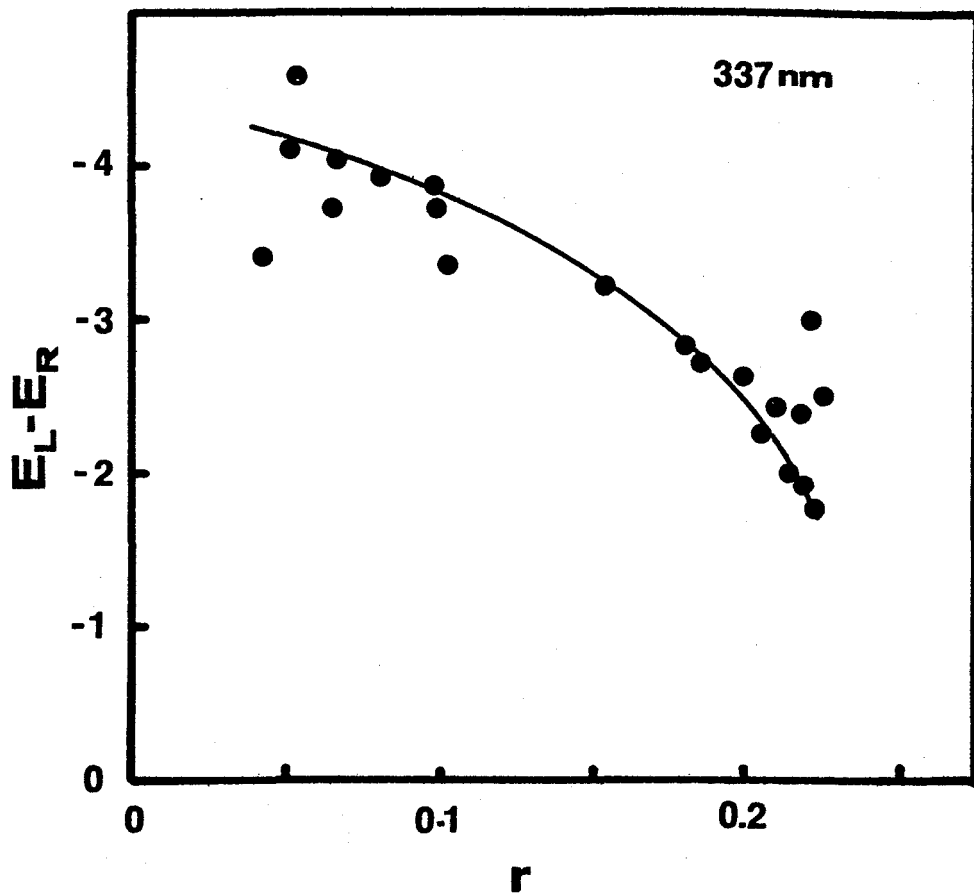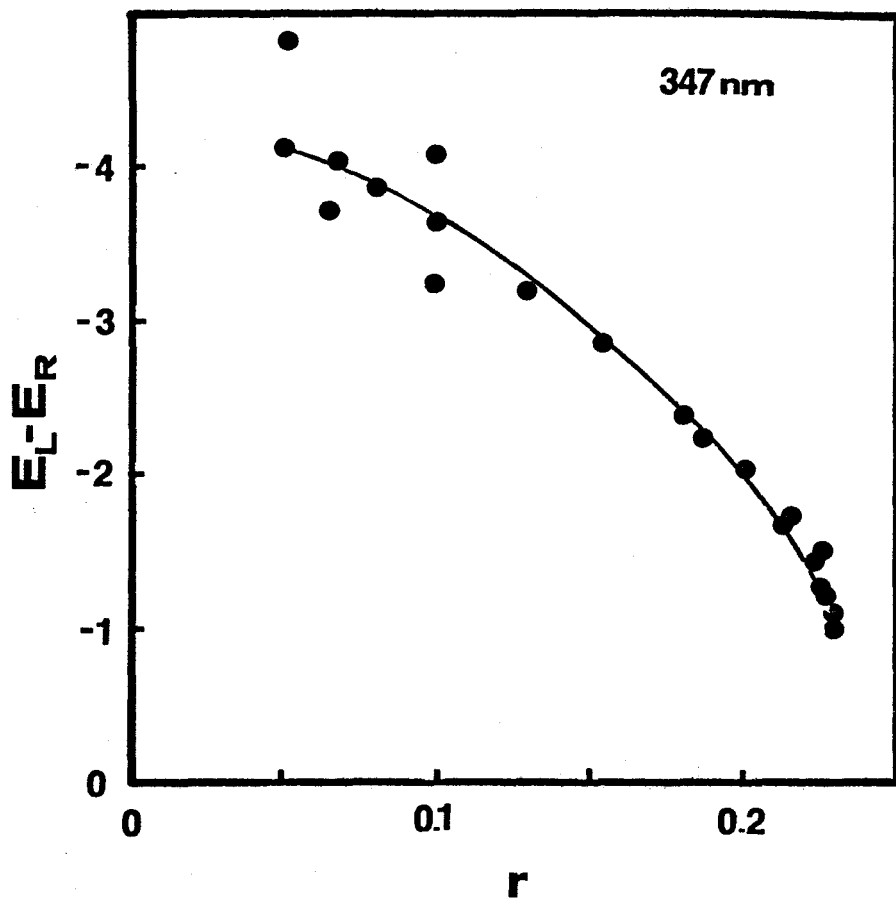
112
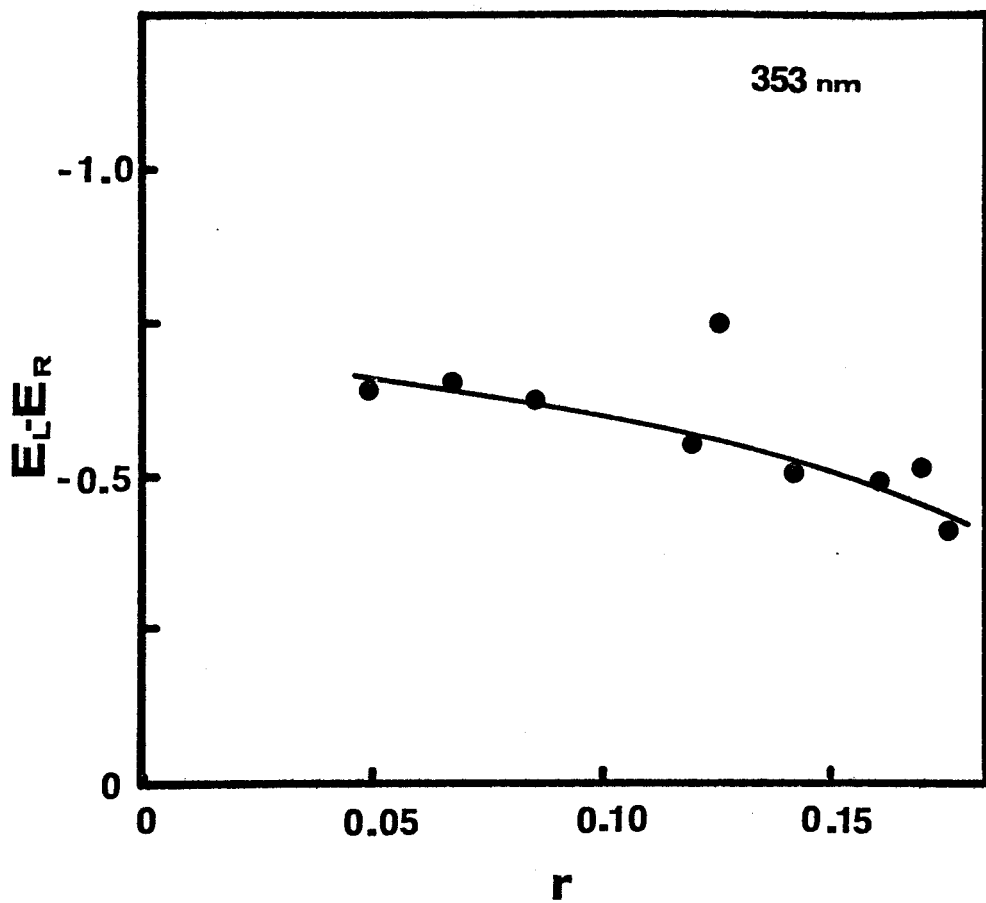
Figure 27. The dependence of the differential molar extinction coefficient E_L-E_R of methyl-Miracil D-DNA complexes at 405 nm on the binding ratio r in 0.01 $\underline{M}$ sodium acetate buffer, pH 5.0 at room temperature.
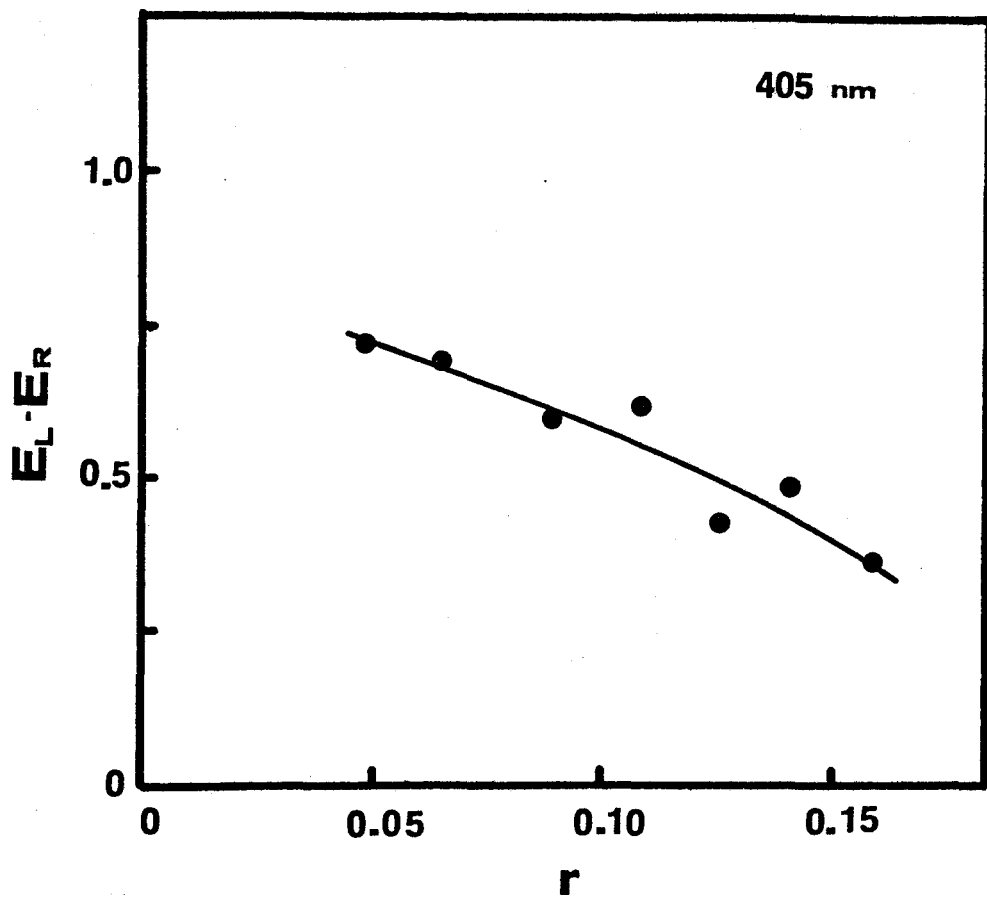
are presented in Figures 28 and 29. The melting temperatures at different drug concentrations are summarized in Table I. Both drugs increase the melting temperature of DNA, but Miracil D is more effective in this respect than its methyl derivative when the comparison is made on the basis of total drug concentrations present in these solutions. An interesting feature of these melting profiles is the slow increase in normalized hyperchromicity noted with increasing temperature _prior_ to DNA melting. Similar behaviour was observed in the case of aminoacridines, and the effect was assigned to the release of drug from the drug-DNA complex _prior_ to melting (Gersch and Jordan, 1965).

Both Miracil D and its methyl derivative are reported to increase the T_m of calf thymus DNA in 0.33 m$\underline{M}$ sodium phosphate buffer, pH 6.8, containing 3 m$\underline{M}$ NaCl and 0.1 m$\underline{M}$ EDTA (Hirschberg _et al._, 1968). At drug concentrations of 5×10^{-6} $\underline{M}$ and calf thymus DNA concentration of 5.8×10^{-5} $\underline{M}$, the increases in T_m are 13 and 3 ^{o}C, respectively (the ratio of total drug concentration to DNA concentration is about 0.086). For the comparison of these reported increases in the melting temperature with our results, complexes with drug concentration of 10^{-5} $\underline{M}$ and DNA concentrations of 1.66×10^{-4} $\underline{M}$ were selected (the ratio of total drug concentration to DNA concentration is 0.06). The purpose of this selection was to have the ratios of total drug concentrations to DNA concentrations for the reported complexes and our complexes as close as possible. In this case Miracil D and methyl-Miracil D cause 13.5 ^{o}C (=71-57.5, see Table I) and 6 ^{o}C (=63.5-57.5, see Table I) increase in the melting temperature, respectively. While the agreement between the reported values and our results is excellent for Miracil D, methyl-

Figure 28. The dependence of the normalized hyperchromicity h_n of calf thymus DNA (a) and Miracil D-calf thymus DNA complexes (b, c, and d) at 260 nm on the temperature in 0.01 $\underline{M}$ sodium acetate buffer, pH 5.0 and 1 cm cell. DNA concentration: 1.66×10^{-4} $\underline{M}$, Miracil D concentrations: (a) 0, (b) 1×10^{-5} $\underline{M}$, (c) 2×10^{-5} $\underline{M}$, and (d) 5×10^{-5} $\underline{M}$. Binding ratios: (b) 0.059, (c) 0.117, and (d) 0.219.
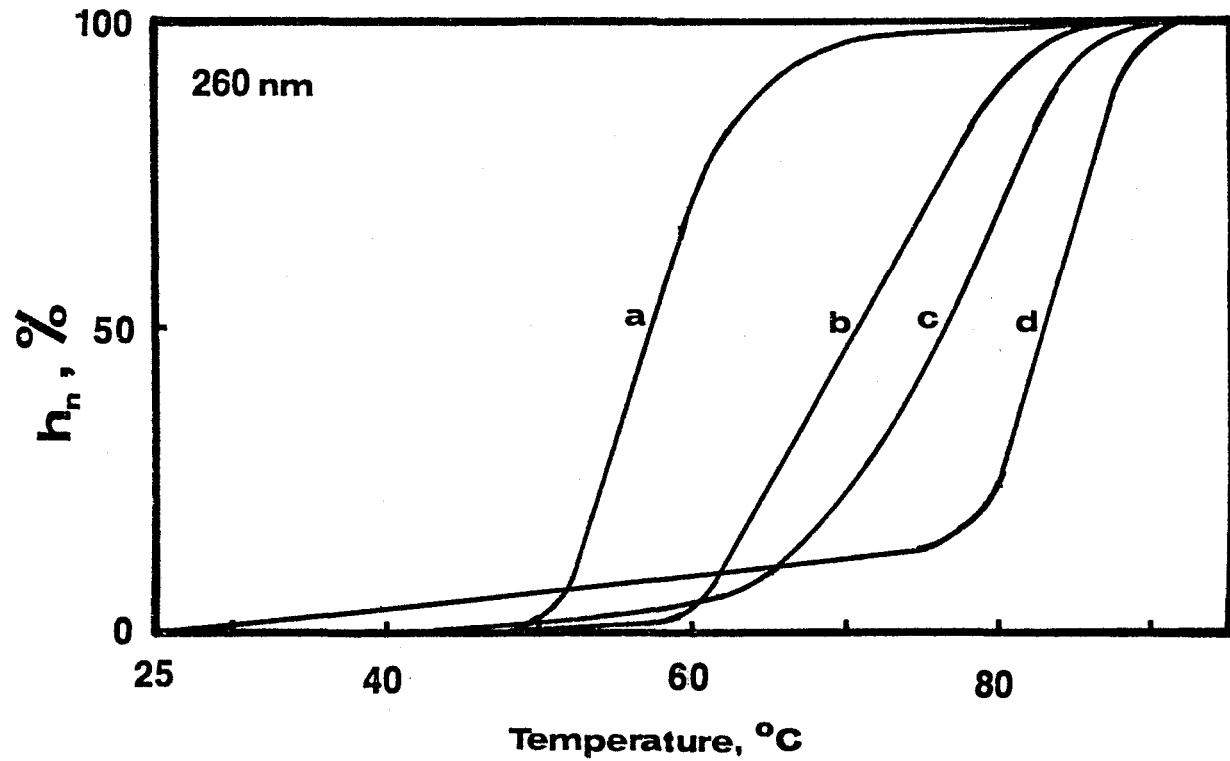
Figure 29. The dependence of the normalized hyperchromicity h_n of calf thymus DNA (a) and methyl-Miracil D-calf thymus DNA complexes (b and c) at 260 nm on the temperature in 0.01 $\underline{M}$ sodium acetate buffer, pH 5.0 and 1 cm cell. DNA concentration: 1.66×10^{-4} $\underline{M}$, methyl-Miracil D concentrations: (a) 0, (b) 1×10^{-5} $\underline{M}$, and (c) 5×10^{-5} $\underline{M}$. Binding ratios: (b) 0.051 and (c) 0.170.

260 nm

h_n, %

Temperature, °C

a   b   c
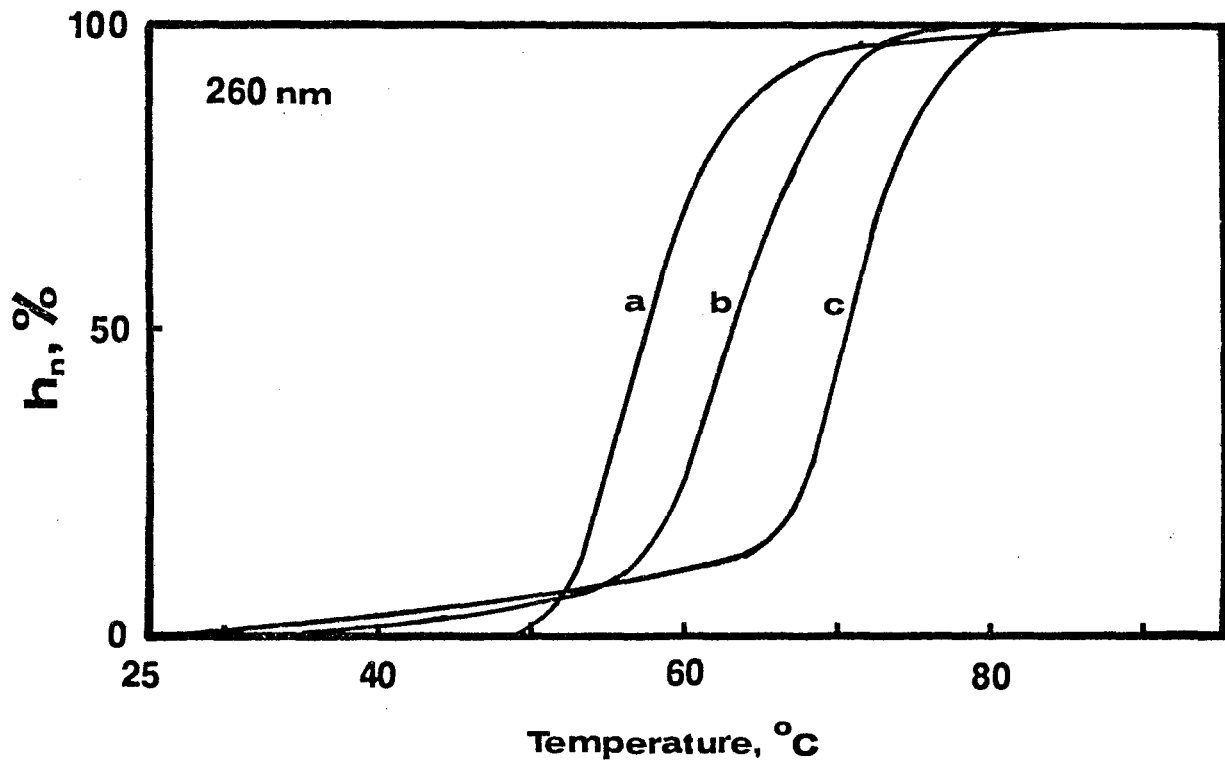
Table I

The effect of Miracil D and methyl–Miracil D on the thermal stability of calf thymus DNA (1.66×10^{-4} $\underline{M}$) in 0.01 $\underline{M}$ sodium acetate buffer, pH 5.0.

Drug	Profile obtained at	Concentration of added drug, $\underline{M}$			
		0	10^{-5}	2×10^{-5}	5×10^{-5}
Miracil D	260 nm*	57.5 °C	71 °C	77 °C	84 °C
Methyl–Miracil D	260 nm*	57.5 °C	63.5 °C	--	71.5 °C
Miracil D	440 nm**	57.5 °C	74 °C	78 °C	84 °C
Methyl–Miracil D	440 nm**	57.5 °C	63.5 °C	--	71.5 °C

* Melting temperature T_m

** Drug–DNA dissociation transition temperature

Miracil D proved more effective in our study than previously reported (Hirschberg et al., 1968c). This increased effectiveness is understandable in the view of the considerations presented in the following section (see section III.4.3).

Both Miracil D and methyl-Miracil D absorb light at 440 nm and the free drugs exhibit larger extinction coefficients at this wavelength than the DNA-bound drugs. DNA does not absorb light at 440 nm. Therefore, changes in the absorbance at this wavelength are proportional to the amount of drugs released from the drug-DNA complexes, and can be used to quantitate the extent of binding of drugs to DNA. A similar approach has been used to investigate the proflavine-DNA and acridine orange-DNA systems (Kleinwächter et al., 1969).

The dependence of the normalized absorbance change ΔA_n at 440 nm on the temperature is presented in Figures 30 and 31, and the drug-DNA dissociation transition temperatures are summarized in Table I. It can be seen from Table I that the melting temperatures and the drug-DNA dissociation transition temperatures do not coincide for Miracil D for both concentrations of 10^{-5} and 2×10^{-5} $\underline{M}$. This is a good indication that Miracil D is released from the complex in the later stages of DNA melting.

This observation is understandable in the view of the reintercalation model proposed by Lazurkin and his coworkers (Lazurkin et al., 1970). According to this model, the least stable regions of the double helix of the drug-DNA complex will dissociate first causing the release of drug molecules from this region. This produces a decrease in the effective DNA concentration so that the pool of free drug molecules in-

Figure 30. The dependence of the normalized absorbance change ΔA_n of Miracil D-calf thymus DNA complexes at 440 nm on the temperature in 0.01 $\underline{M}$ sodium acetate buffer, pH 5.0 and 1 cm cell. DNA concentration: 1.66×10^{-4} $\underline{M}$, Miracil D concentrations: (a) 1×10^{-5} $\underline{M}$, (b) 2×10^{-5} $\underline{M}$, and (c) 5×10^{-5} $\underline{M}$. Binding ratios: (a) 0.059, (b) 0.117, and (c) 0.219.
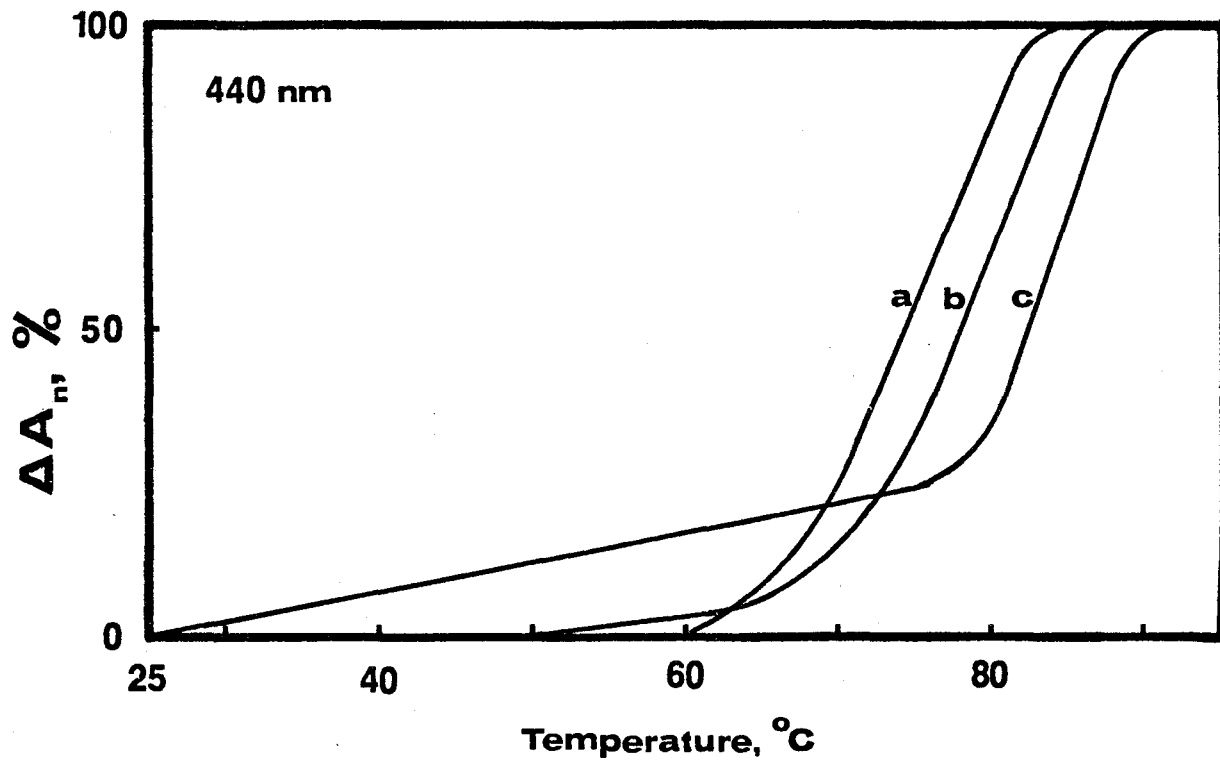
440 nm

Figure 31. The dependence of the normalized absorbance change ΔA_n of methyl-Miracil D-calf thymus DNA complexes at 440 nm on the temperature in 0.01 $\underline{M}$ sodium acetate buffer, pH 5.0 and 1 cm cell. DNA concentration: $1.66 \times 10^{-4} \underline{M}$, methyl-Miracil D concentrations: (a) $1 \times 10^{-5} \underline{M}$ and (b) $5 \times 10^{-5} \underline{M}$. Binding ratios: (a) 0.051 and (b) 0.17.
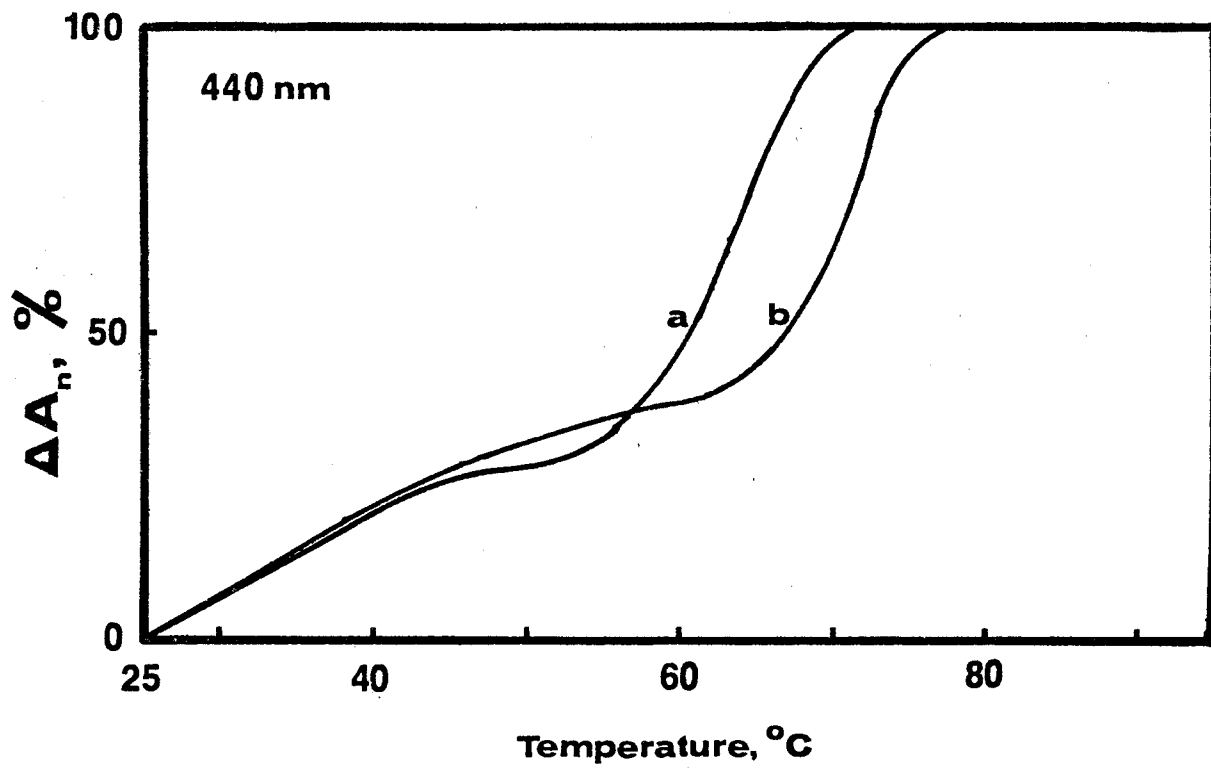
creases beyond the free drug concentration dictated by the law of mass action. Therefore, drug molecules bind to those intact regions of DNA molecule which are not saturated with drug molecules so as to reestablish the equilibrium. The overall effect is that the release of drug from the complex lags behind the process of the dissociation of the double helix, unless the DNA is completely saturated with the drug before the onset of melting. Similar conclusions have been drawn about the ethidium bromide-DNA complex (Aktipis et al., 1975).

The effect of ionic strength on the stabilization of calf thymus DNA against heat denaturation by Miracil D and methyl-Miracil D was investigated in 0.01 $\underline{M}$ sodium acetate buffer, pH 5.0, containing 0.075 $\underline{M}$ NaCl. The melting temperature of DNA under this condition is found to be 81 ^{o}C, contrasted with the value of 57.5 ^{o}C in the absence of sodium chloride (see Table I). This increase of T_m is the result of the decreased electrostatic repulsion between the phosphate groups of DNA in the presence of salts (Schildkraut and Lifson, 1965). At a total drug concentration of 10^{-5} $\underline{M}$ and DNA concentration of 1.66×10^{-4} $\underline{M}$, Miracil D increased the metling temperature of DNA by 2 ^{o}C, while methyl-Miracil D had no effect at all (the corresponding values in the absence of sodium chloride are 13.5 and 6 ^{o}C, respectively; see text above).

III.4.2. Circular Dichroism Measurements at Elevated Temperatures

Clearly as a result of drug reintercalation (see preceding section), the binding ratio r for the intact regions increases as the melting process is propagated. Since the differential molar extinction coefficient $E_L - E_R$ is dependent on the binding ratio, it was of interest

to investigate the dependence of E_L-E_R of Miracil D-DNA complexes as the temperature is increased.

III.4.2.1. Miracil D-DNA Complex at Low Binding Ratios

The dependence of the normalized absorbance change ΔA_n of the Miracil D-DNA complex on the temperature (Figure 32, curve a) suggests that no drug is released from the complex for temperatures lower than 55 °C. This is not surprising since under these conditions the DNA is far from being saturated (r=0.059 at 25 °C) and the intrinsic association constant remains within a fairly narrow range (1.2×10^6 $\underline{M}^{-1}$ at 25 °C, see section III.2.1, and 2.2×10^5 $\underline{M}^{-1}$ at 55 °C, obtained from the van't Hoff plot, see section III.2.3). However, over the same temperature range the differential molar extinction coefficient E_L-E_R decreases by about 20 % (Figure 32, curve b), apparently due to gradual conformational change in the complex. This probably results from a modification of the electronic and magnetic interactions which produce changes in the rotational strength. The rate of the change in E_L-E_R in this temperature range is -2.8×10^{-2} liter·Mole^{-1}·cm^{-1}·$^{\circ}$C^{-1}.

Above 55 °C, however, Miracil D is continuously released from the complex with increasing temperatures as suggested by the increases noted in the normalized absorbance change (Figure 32, curve a). The rate of the change in E_L-E_R in this temperature range is -7.8×10^{-2} liter·Mole^{-1}·cm^{-1}·$^{\circ}$C^{-1}, i.e. 2.8 times faster than below 55 °C. This increased rate appears to be the result of the gradual conformational changes noted below 55 °C (and continued at temperatures over 55 °C) and the reintercalation of Miracil D (see section III.4.1) which occurs during the course of the melting process. Assuming that the rate of

Figure 32. The dependence of (a) the normalized absorbance change ΔA_n at 440 nm, (b) the differential molar extinction coefficient $E_L - E_R$ at 347 nm, and (c) the differential molar extinction coefficient $E_L - E_R$ corrected for conformational changes at 347 nm (dashed line, see text for details) on the temperature of Miracil D-calf thymus DNA complex in 0.01 $\underline{M}$ sodium acetate buffer, pH 5.0 and 1 cm cell. DNA concentration: 8.4×10^{-4} $\underline{M}$ and Miracil D concentration: 5×10^{-5} $\underline{M}$. Under these conditions the binding ratio r is 0.059 at 25 $^{\circ}$C.
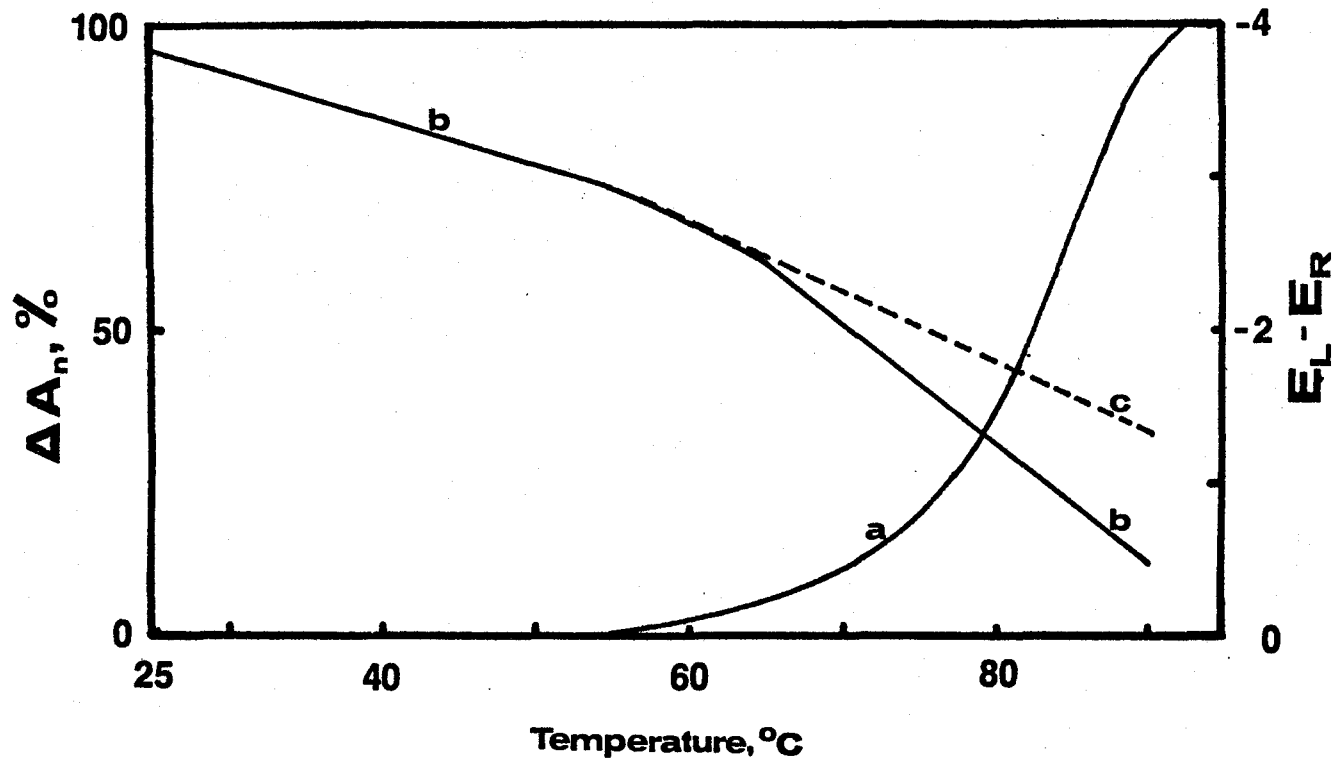
the change in E_L-E_R due to conformational change in the complex below 55 ^{O}C is maintained for temperatures above 55 ^{O}C, the experimentally observed differential molar extinction coefficient E_L-E_R can be adjusted so as to obtain E_L-E_R values, the changes of which may represent the reintercalation of Miracil D during melting. The corrected E_L-E_R curve is presented in Figure 32 (curve c, dashed line), which was constructed by drawing a tangent to curve b (Figure 32) at 55 ^{O}C with a slope of 5×10^{-2} liter·Mole^{-1}·cm^{-1}·^{O}C^{-1} ($=7.8 \times 10^{-2} - 2.8 \times 10^{-2}$).

Thus the corrected E_L-E_R curve may represent the change in circular dichroism due simply to reintercalation of Miracil D. At the onset of DNA melting (around 55 ^{O}C), the binding ratio of the complex is about 0.059 (no drug is released between 25 and 55 ^{O}C). Between 55 and 90 ^{O}C the corrected E_L-E_R values decrease by a factor of 2.5. A decrease in E_L-E_R values by the same factor of 2.5 is obtained if the binding ratio is increased from 0.059 to 0.23 using data on the dependence of the differential molar extinction coefficient on the binding ratio (Figure 22). A ratio of 0.23 is obtained by the end of the melting process, i.e. around 90 ^{O}C. Since at the point of saturation the binding ratio is 0.25, a binding ratio of 0.23 indicates that at the end of the melting process the DNA is almost completely saturated with Miracil D.

III.4.2.2. Miracil D-DNA Complex at High Binding Ratios

For a Miracil D-DNA complex in which the DNA is almost saturated by the drug at room temperature (i.e. r=0.22 at 25 ^{O}C), the release of drug occurs at lower temperatures so that both the release and the decrease of differential molar extinction coefficient E_L-E_R are initiated concurrently at 25 ^{O}C (Figure 33, curves a and b). The E_L-E_R is

linearly dependent on the temperature in the whole temperature range

studied, including the melting region (from 80 to 90 $^{\circ}$C, see Figure 33,

curve b) of DNA. The rate of change in E_L-E_R is -2.2×10^{-2} liter$\cdot$Mole$^{-1}\cdot$

cm$^{-1}\cdot^{\circ}$C^{-1}. The constancy of this rate throughout the whole temperature

range, including the melting region of DNA, suggests that the same

process takes place in the course of DNA melting as prior to DNA

melting (below 80 $^{\circ}$C). Furthermore, the similarity of this rate of

change in E_L-E_R to that of a Miracil D-DNA complex of low binding

ratios prior to melting (-2.8×10^{-2} liter$\cdot$Mole$^{-1}\cdot$cm$^{-1}\cdot^{\circ}$C^{-1}, see preceding

section) suggests that the conformational change which takes place in

the whole temperature range studied is not accompanied by reinterca-

lation and, therefore, is a change analogous to that which takes place

with Miracil D-DNA complex at low binding ratios and below 55 $^{\circ}$C. This

finding is in agreement with expectation, since the DNA is almost satu-

rated with the drug at room temperature, and consequently there are no

free binding sites for reintercalation.

The results presented here and the preceding section are quite

convincing in favour of the operation of the reintercalation process in

the Miracil D-DNA system. It should be also noted that in order for re-

intercalation to take place, the rate of the change of the intrinsic as-

sociation constant with temperature in the melting region must be

smaller than the rate of DNA denaturation. This requirement seems to be

fulfilled for Miracil D. However, inspection of the melting tempera-

tures (at 260 nm) and the corresponding drug-DNA dissociation transition

temperatures (at 440 nm) of methyl-Miracil D-DNA complexes (see Table I)

indicates that reintercalation does not take place (the temperatures at

Figure 33. The dependence of (a) the normalized absorbance change ΔA_n at 440 nm and (b) the differential molar extinction coefficient $E_L - E_R$ at 347 nm on the temperature of Miracil D-calf thymus DNA complex in 0.01 $\underline{M}$ sodium acetate buffer, pH 5.0 and 1 cm cell. DNA concentration: 1.68×10^{-4} $\underline{M}$ and Miracil D concentration: 5×10^{-5} $\underline{M}$. Under these conditions the binding ratio r is 0.22 at 25 ^{o}C.
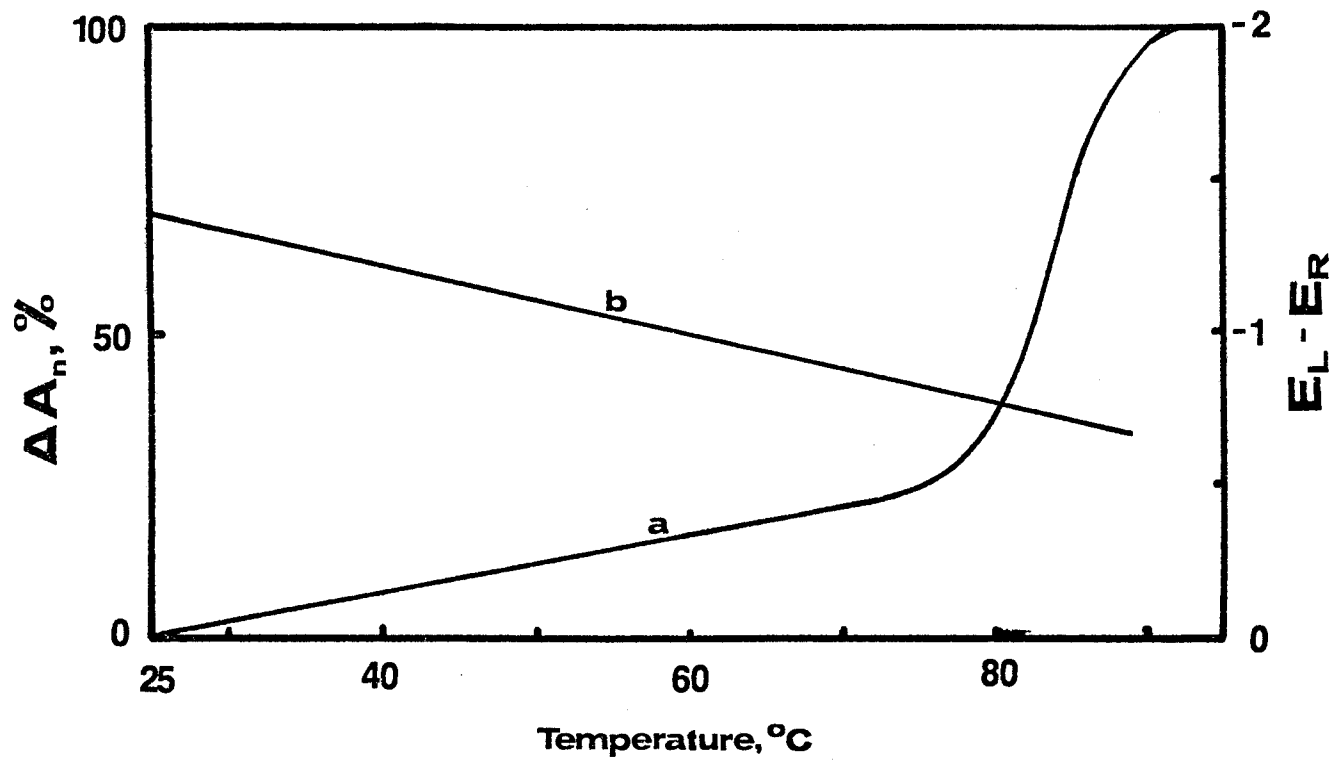
the two wavelengths are identical). It is possible, therefore, that

the above requirement is not satisfied in the case of methyl-Miracil D-

DNA system.

III.4.3. Stabilization of the DNA Helix by Miracil D and Methyl-Miracil D

Because of the dissociation of drugs from the drug-DNA complexes

at elevated temperatures, the binding ratios of these complexes are

clearly smaller at the onset of DNA melting than they are at 25 $^{\circ}$C. As

melting progresses, however, the binding ratio of the intact regions

increases rather than decreases due to reintercalation (see sections

III.4.1 and III.4.2). In order to compare each drug with respect to

its effectiveness in stabilizing the double helix, the state of the

complex at the melting temperature at 260 nm was chosen for the

standard state of the complex. At this temperature, 50 % of the binding

sites are assumed to be denatured, meaning that the effective nucleic

acid concentration at these temperatures is half of that at 25 $^{\circ}$C. The

binding ratios at these temperatures were obtained from the binding

ratios at 25 $^{\circ}$C and the observed normalized absorbance changes at 440

nm. The difference ΔT_m between the melting temperatures in the

presence and absence of drug measures the degree of stabilization

caused by each drug. The results of these calculations are summarized

in Table II, and the dependence of stabilization ΔT_m on the binding

ratio at the T_m of the drug-DNA complex is presented in Figure 34.

Surprisingly, a linear relationship is obtained, and the experi-

mental points for both Miracil D and methyl-Miracil D fall on the same

line. Consequently, the drugs, when bound to DNA, appear to stabilize

Table II

The extent of thermal stabilization (ΔT_m) of calf thymus DNA by Miracil D and methyl-Miracil D in 0.01 $\underline{M}$ sodium acetate buffer, pH 5.0 and the binding ratios of Miracil D-DNA and methyl-Miracil D-DNA complexes at the melting temperatures (at 260 nm).

	T_m of DNA (260 nm), °C	T_m of drug-DNA complex (260 nm), °C	Stabilization ΔT_m, °C	r (at 25 °C)	ΔA_n (at T_m of complex)	r (at T_m of complex)
	57.5	71	13.5	0.059	0.32	0.080
Miracil D	57.5	77	19.5	0.110	0.52	0.110
	57.5	84	26.5	0.220	0.64	0.160
Methyl-Miracil D	57.5	63.5	6	0.051	0.65	0.036
	57.5	71.5	14	0.170	0.74	0.088

The values of r at T_m of the drug-DNA complexes were calculated according to the equation

$$r(\text{at } T_m \text{ of complex}) = 2 \cdot r(\text{at } 25\ °C) \cdot [1 - \Delta A_n(\text{at } T_m \text{ of complex})] .$$

Figure 34. The effectiveness of Miracil D (●) and methyl-Miracil D (■) in stabilizing calf thymus DNA in 0.01 M sodium acetate buffer, pH 5.0 against heat denaturation. Binding ratios of drug-DNA complexes at the melting temperatures are indicated in the abscissa.
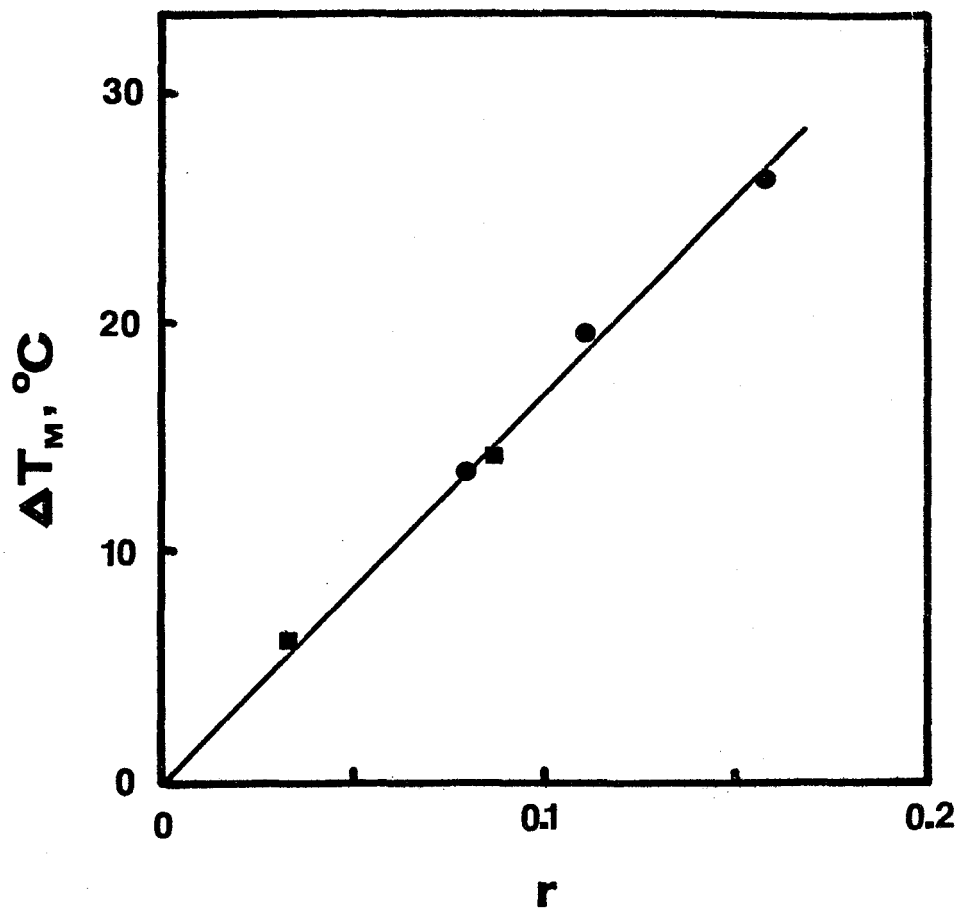
calf thymus DNA equally well. Therefore, previously reported data which indicate that Miracil D is much more effective in stabilizing calf thymus DNA against heat denaturation (Hirschberg et al., 1968c) than its methyl derivative are the result of the differences in the binding characteristics of these two compounds.

III.5. The Inhibition of RNA Synthesis by Thioxanthenones

III.5.1. The RNA Synthesis Assay at pH 7.0

Assays of RNA synthesis by DNA dependent RNA polymerase in the literature are generally carried out at pH 8.0, which is the pH optimum of the enzyme (Chamberlin and Berg, 1962). However, because of the very limited solubility of Miracil D at pH 8.0 and the difficulties in preparing soluble Miracil D-DNA complexes at this pH, the investigations on the inhibition of DNA dependent RNA polymerase by Miracil D, methyl-Miracil D as well as MDMT were carried out at pH 7.0. At this pH, the enzymic activity is 62 % of its maximum value (Chamberlin and Berg, 1962).

In order to establish the conditions for the reaction at pH 7.0, the synthesis of RNA as a function of reaction time was first investigated using calf thymus DNA as template (Figure 35). The reaction is linear with time for the first 8 minutes, and then it slows down appreciably. The time course of the reaction follows roughly first order kinetics, and the decrease in the rate of RNA synthesis cannot be accounted for simply by substrate depletion. The cessation of RNA synthesis after long reaction times is not peculiar to the pH conditions used for the assay, since similar kinetics have been observed under a variety of conditions (Hurwitz et al., 1962; Kozlov, 1971). A reaction time

Figure 35. The kinetics of RNA synthesis. Enzyme concentration: 7.9 units/ml and calf thymus DNA concentration: 30 µg/ml.
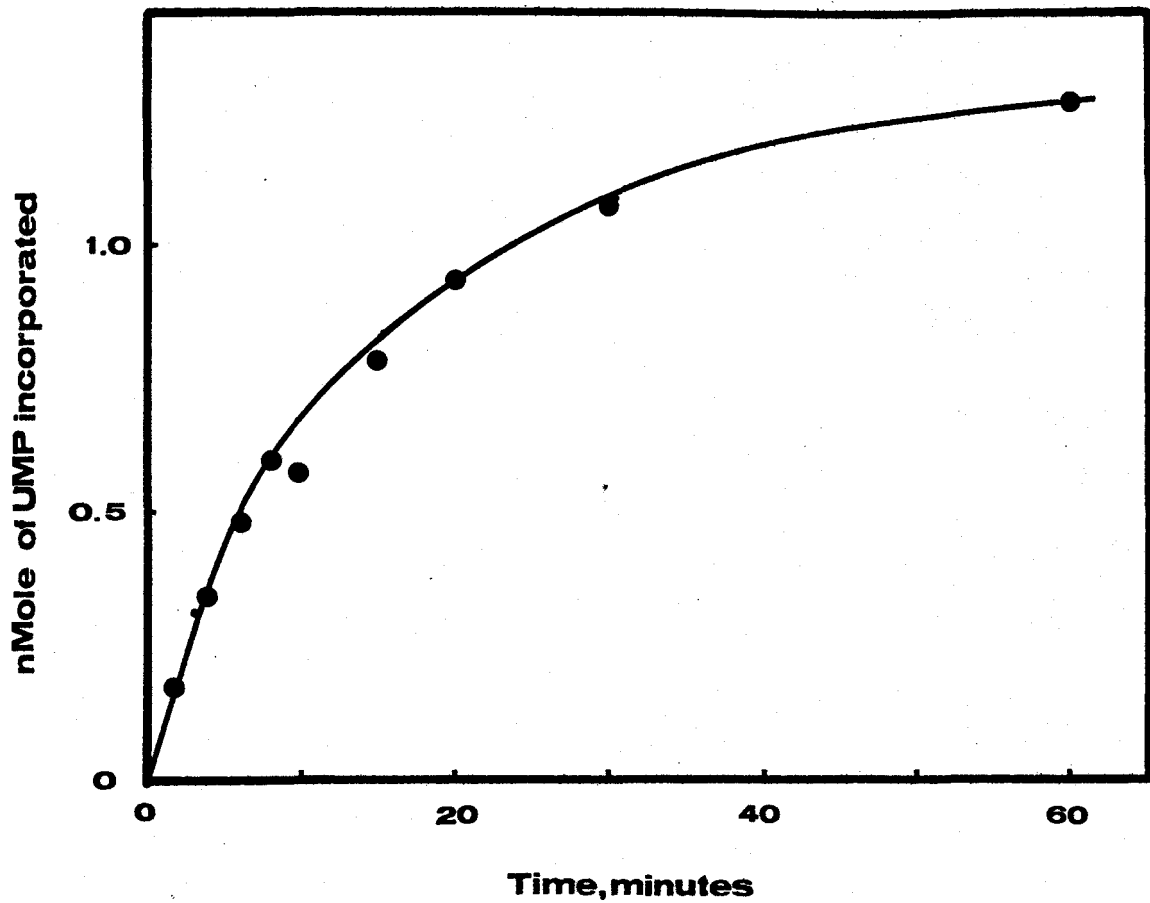
of 8 minutes was selected in all subsequent assays for which a calf
thymus DNA template was used. When using T2 bacteriophage DNA as
template, the rate of RNA synthesis was constant in the first 10
minutes of the synthesis.

The dependence of RNA synthesis on the concentration of calf
thymus DNA was also investigated, and the results are presented in
Figure 36. Although the plot resembles the usual Michaelis-Menten
hyperbolic relationship, the corresponding Lineweaver-Burk plot does
not yield a straight line. The concentration of calf thymus DNA, at
which half of the maximum incorporation is obtained, is about 10 µg/ml.
This value is in contrast to 4.8 µg/ml reported at pH 7.5 (Hurwitz et
al., 1962).

For the inhibition studies using calf thymus DNA as template, a
DNA concentration of 23 µg/ml was selected. This value represents a
compromise between two counteracting requirements: a template concen-
tration small enough to be rate limiting, but large enough to produce
significant incorporation of radioactive label.

III.5.2. The Inhibition of RNA Polymerase by Miracil D, Methyl-
Miracil D, and MDMT

The inhibition of DNA dependent RNA polymerase by Miracil D,
methyl-Miracil D, and MDMT was investigated under the experimental con-
ditions described in the preceding section. The experiments were per-
formed as outlined in section II.11, and the results are presented in
Figures 37 and 38.

It is apparent that all three drugs inhibit RNA synthesis.
Methyl-Miracil D and MDMT appear to be equally effective when compared

141

Figure 36. The dependence of RNA syntheis on the template (calf thymus DNA) concentration. Enzyme concentration: 7.6 units/ml.

143
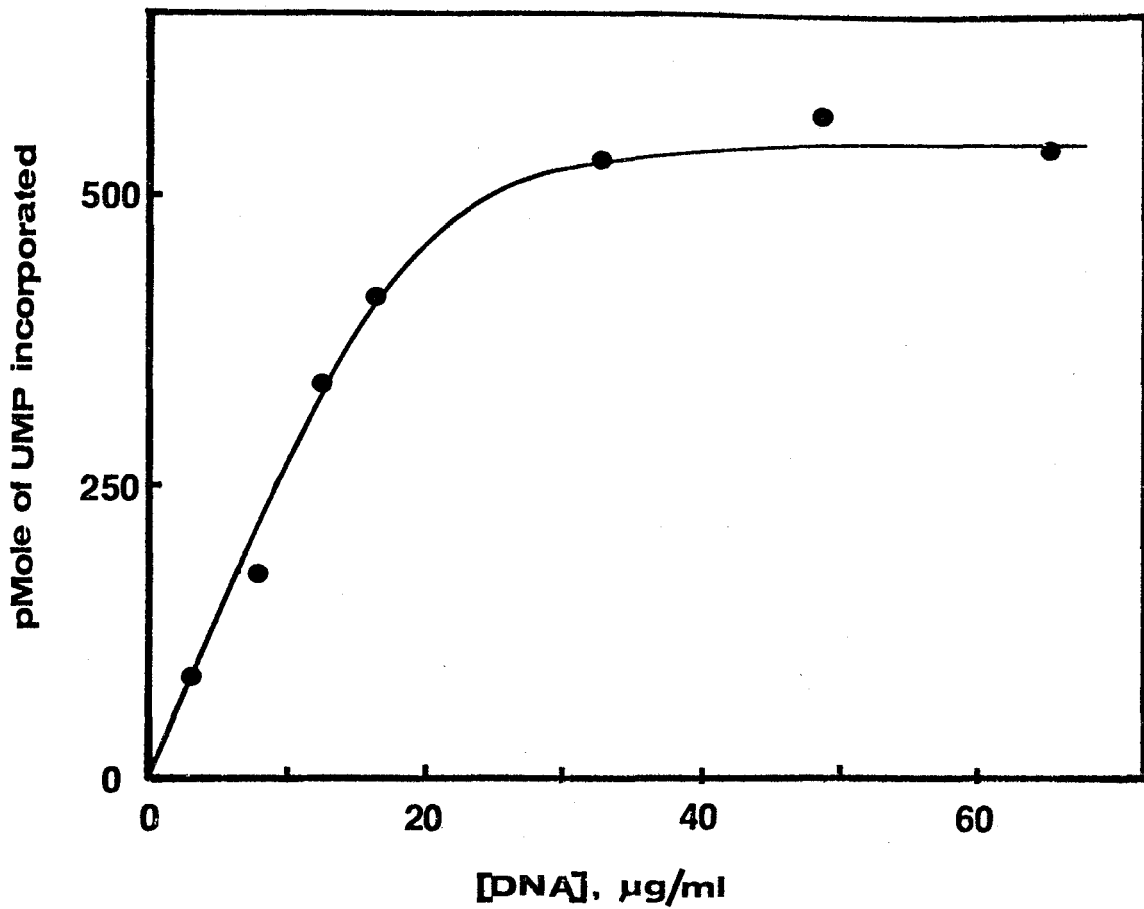
Figure 37. The inhibition of RNA synthesis by Miracil D. Enzyme concentration: 10 units/ml, calf thymus DNA concentration: 23 µg/ml, and nucleoside triphosphate concentration: 0.5 m$\underline{M}$ (each).
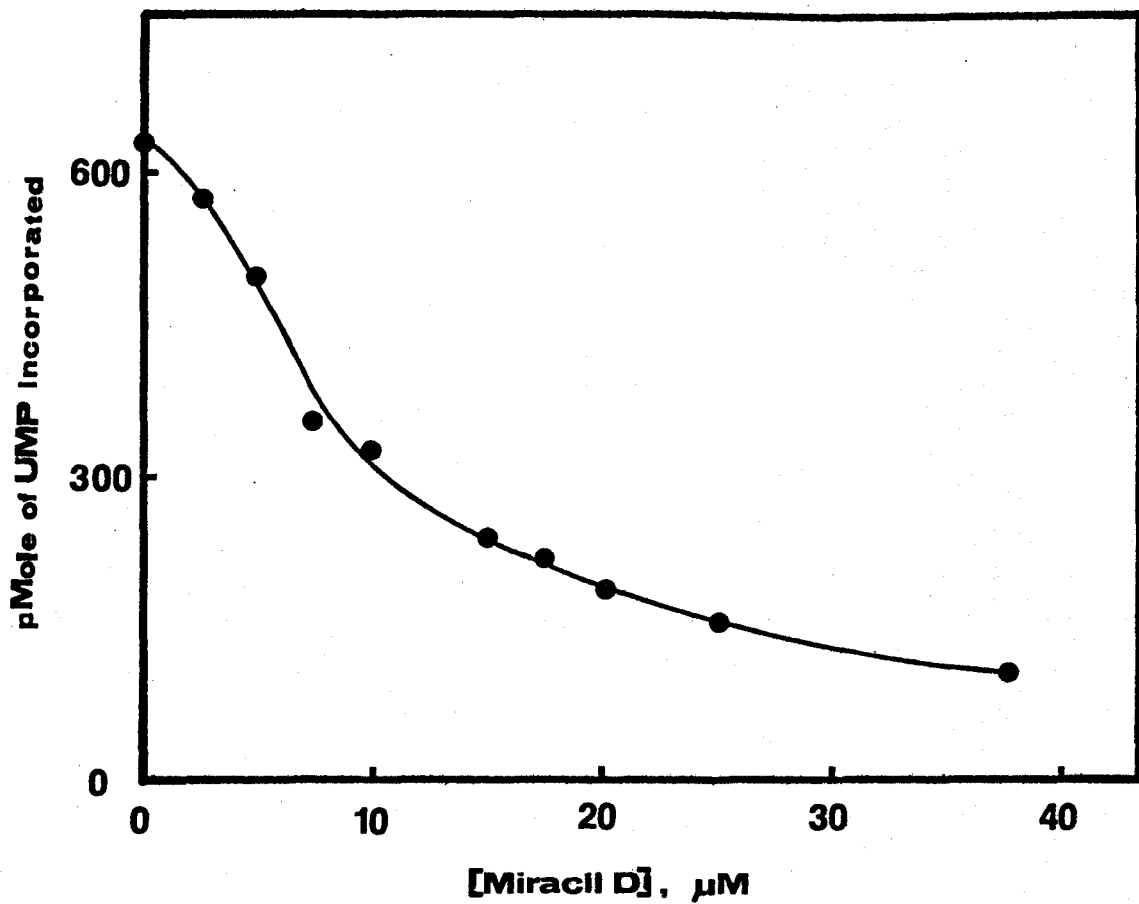
Figure 38. The inhibition of RNA synthesis by methyl-Miracil D (●) and MDMT (▲). Enzyme concentration: 10 units/ml, calf thymus DNA concentration: 23 μg/ml, and nucleoside triphosphate concentration: 0.5 mM (each).
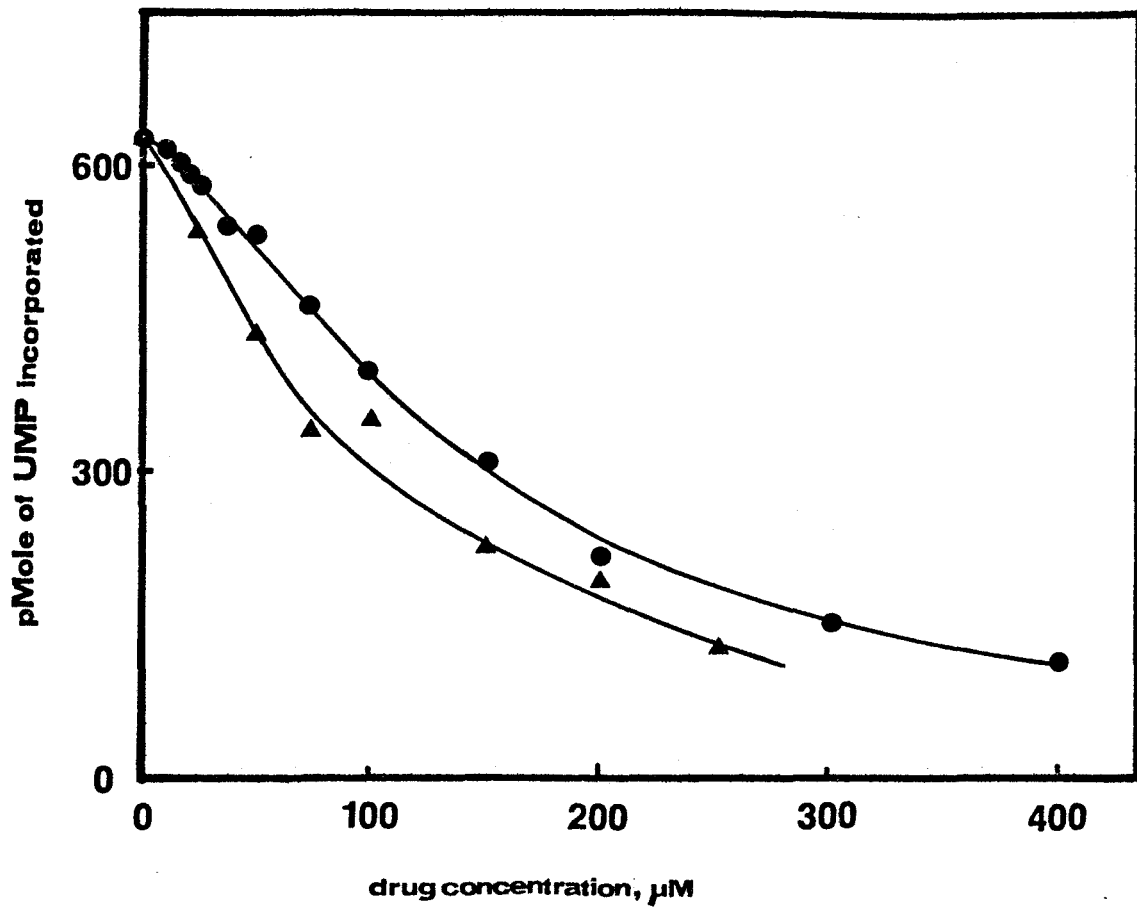
on the basis of the total concentration of drugs present in these solutions (Figures 38). In contrast, Miracil D is an order of magnitude more effective (Figure 37) than the two other derivatives.

This difference between Miracil D and its methyl derivative was expected in view of the results of an earlier investigation (Hirschberg et al., 1968c). Using a similar test system, Hirschberg and his coworkers reported that Miracil D causes a 90 % inhibition of RNA polymerase activity, while methyl-Miracil D is completely ineffective at a drug concentration of $5x10^{-5}$ $\underline{M}$. The minor quantitative differences between these reported results and the results of the present investigation may be due to the differences in assay conditions. Hirschberg and his coworkers used salmon sperm DNA at a concentration of 70 µg/ml, in contrast to calf thymus DNA of 23 µg/ml. Also the assay was performed at pH 7.9, in contrast to a pH 7.0 used for the present experiments.

The above comparison of Miracil D and methyl-Miracil D with respect to their effectiveness as inhibitors of RNA polymerase is obviously based on total drug concentrations. However, since Miracil D and its methyl derivative bind to DNA to different extents, the observed differences toward RNA polymerase may be apparent rather than real and could simply be the result of the different binding capacity of these drugs to DNA.

III.5.3. Comparison of the Effectiveness of Miracil D and Methyl-Miracil D to Inhibit RNA Synthesis

As noted in the previous section, the observed apparent differences in the effectiveness of Miracil D and its methyl derivative in in-

hibiting RNA synthesis may be the result of the differences in their a-

bility to bind to DNA. In order to make the proper comparison, the

inhibition caused by the drugs should be determined as a function of

bound drug concentrations rather than total drugs present in the assay

mixtures. This treatment obviously requires knowledge of the intrinsic

association constants of drugs with DNA under the conditions of RNA

polymerase assays.

As noted previously (see section III.2.4), the binding of

methyl-Miracil D to calf thymus DNA under the conditions of RNA synthe-

sis cannot be accurately determined by the spectrophotometric method

used in this investigation. However, this binding can be estimated in-

directly from absorbance measurements (Figure 30, curve c) carried out

in 0.01 $\underline{M}$ sodium acetate buffer, pH 5.0 using the method outlined in

section II.10.3. Under these conditions, it can be calculated that the

intrinsic association constant K for methyl-Miracil D decreases 5.7-

fold from 1.7×10^5 to 3×10^4 $\underline{M}^{-1}$ as the temperature increases from 25 to

37 $^{\circ}$C. Also from absorbance measurements in 0.01 $\underline{M}$ sodium acetate

buffer, pH 5.0 at ionic strengths of 0.01 and 0.07 $\underline{M}$ (adjusted by the

addition of 1 $\underline{M}$ KCl solution), it is estimated that the intrinsic as-

sociation constant K at 25 $^{\circ}$C decreases 34-fold from 1.7×10^5 to 5×10^3

$\underline{M}^{-1}$ as a result of the increase in ionic strength. Since no binding

whatsoever can be detected at an ionic strength of 0.2 $\underline{M}$, the value of

5×10^3 $\underline{M}^{-1}$ may be assumed to be the upper limit for the association

constant at an ionic strength of 0.2 $\underline{M}$. If the effects of temperature

and ionic strength are asssumed to be additive, then the intrinsic as-

sociation constant of the binding of methyl-Miracil D to calf thymus DNA

under assay conditions cannot be greater than $1.7 \times 10^5/(34 \times 5.7) = 8.8 \times 10^2 \; \underline{M}^{-1}$.

Using the directly obtained value of $1.35 \times 10^4 \; \underline{M}^{-1}$ for the intrinsic association constant of the binding of Miracil D to calf thymus DNA under assay conditions (see section III.2.2) and the value of $8.8 \times 10^2 \; \underline{M}^{-1}$ for the estimated intrinsic association constant of the binding of methyl-Miracil D to calf thymus DNA under assay conditions, the bound drug concentrations and the binding ratios under the conditions of the assay can be calculated as outlined in Appendix B. The synthesis of RNA as a function of the binding ratios for Miracil D and its methyl derivative are presented in Figure 39. Clearly, both Miracil D and methyl-Miracil D, when bound to DNA, inhibit RNA synthesis with equal effectiveness. It may also be noted that the observed inhibitory behaviour of the bound forms of the two drugs parallels their effectiveness in stabilizing DNA against heat denaturation (see section III.4.3). This parallelism of the drugs in the two test systems is further discussed in section IV.5.

III.5.4. Miracil D: An Inhibitor of RNA Chain Initiation and
<u>Elongation</u>

In the enzymatic synthesis of RNA, there are four major steps (Chamberlin, 1974, see section I.6.3): template binding, RNA chain initiation, RNA chain elongation, and termination. An inhibitor can exert its effect on any of these steps. It has been shown that the reciprocal initial velocity $1/v_i$ of the overall reaction (as determined in the present experiments by ^3H incorporation) is linearly dependent on the binding ratio r, if only the elongation step is inhibited (Hyman

Figure 39. The inhibition of RNA synthesis by Miracil D (●) and methyl-Miracil D (○) as the function of the binding ratio r. Enzyme concentration: 10 units/ml, calf thymus DNA concentration: 23 μg/ml, and nucleoside triphosphate concentration: 0.5 mM (each).
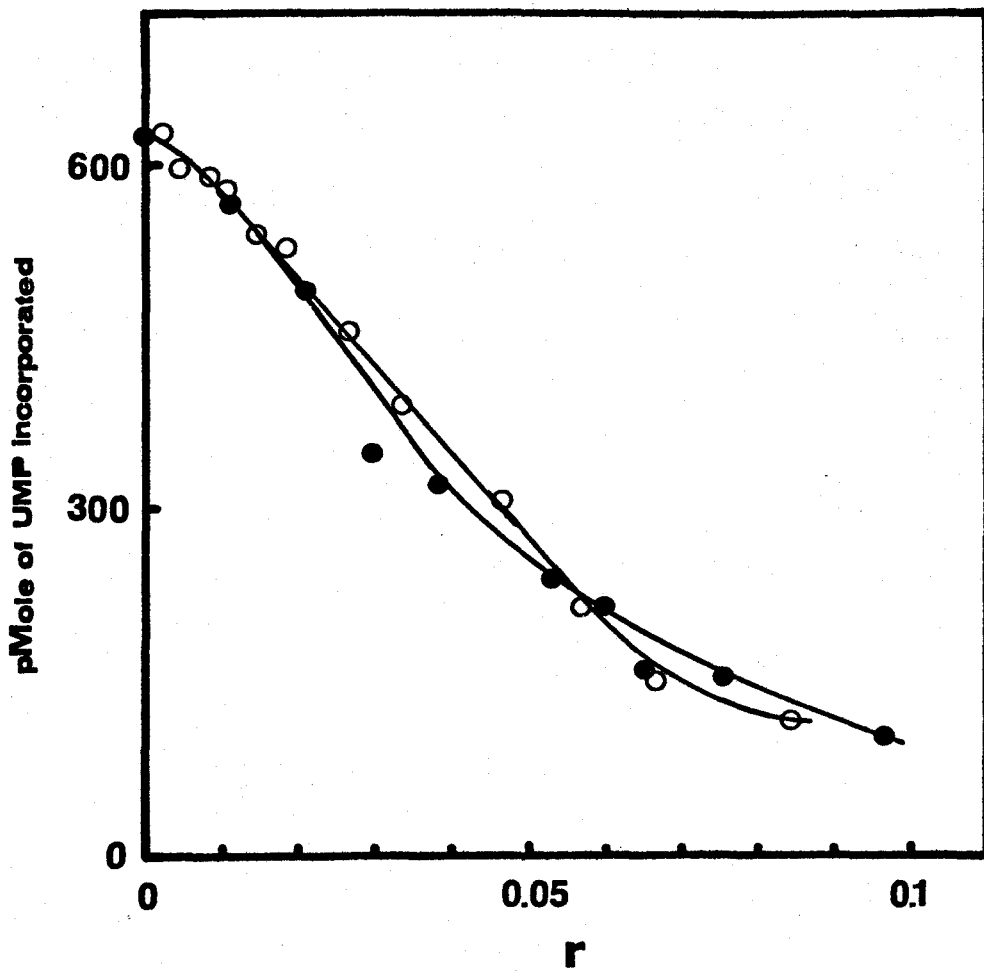
and Davidson, 1970). For Miracil D and its methyl derivative, the dependence of the reciprocal initial velocity $1/v_i$ on the binding ratio r is shown in Figure 40. In the range of binding ratios from 0 to 0.05 a linear relationship is obtained, indicating that the kinetics of inhibition are compatible with the inhibition of the elongation step.

At binding ratios greater than 0.05, however, deviations from linearity are observed. In order to determine whether these deviations are a consequence of inhibition of the initiation of RNA synthesis, the incorporation of both ^{32}P and ^{3}H in RNA were investigated using T2 bacteriophage DNA as the template. Since an RNA molecule retains the γ-phosphate group of the first nucleotide residue involved in its synthesis, the incorporation of γ-[^{32}P]-ATP measures the number of RNA chains synthesized starting with ATP (Richardson, 1973). In contrast, the incorporation of ring labeled [^{3}H]-UTP measures the total amount of RNA synthesized. Preliminary experiments indicated that the rate of RNA synthesis using T2 DNA as template is constant for at least 10 minutes of incubation.

In the case of Miracil D, it is apparent (Figure 41) that the reciprocal initial velocity $1/v_i$ of the total RNA synthesis increases with r up to a binding ratio of about 0.05. At higher r values, the reciprocal initial velocity increases much more rapidly. The incorporation of ^{32}P label, however, remains constant for r values lower than 0.05, indicating that Miracil D does not inhibit initiation. Clearly, the same number of chains is synthesized regardless of the concentration of the inhibitor. For binding ratios greater than 0.05, however, the incorporation of ^{32}P label decreases somewhat. This is an indication

Figure 40. The dependence of the reciprocal initial velocity $1/v_i$ of

RNA synthesis on the binding ratio r in the presence of Miracil D (●)

and methyl-Miracil D (○). Enzyme concentration: 10 units/ml, calf

thymus DNA concentration: 23 μg/ml, and nucleoside triphosphate concen-

tration: 0.5 m$\underline{M}$ (each).
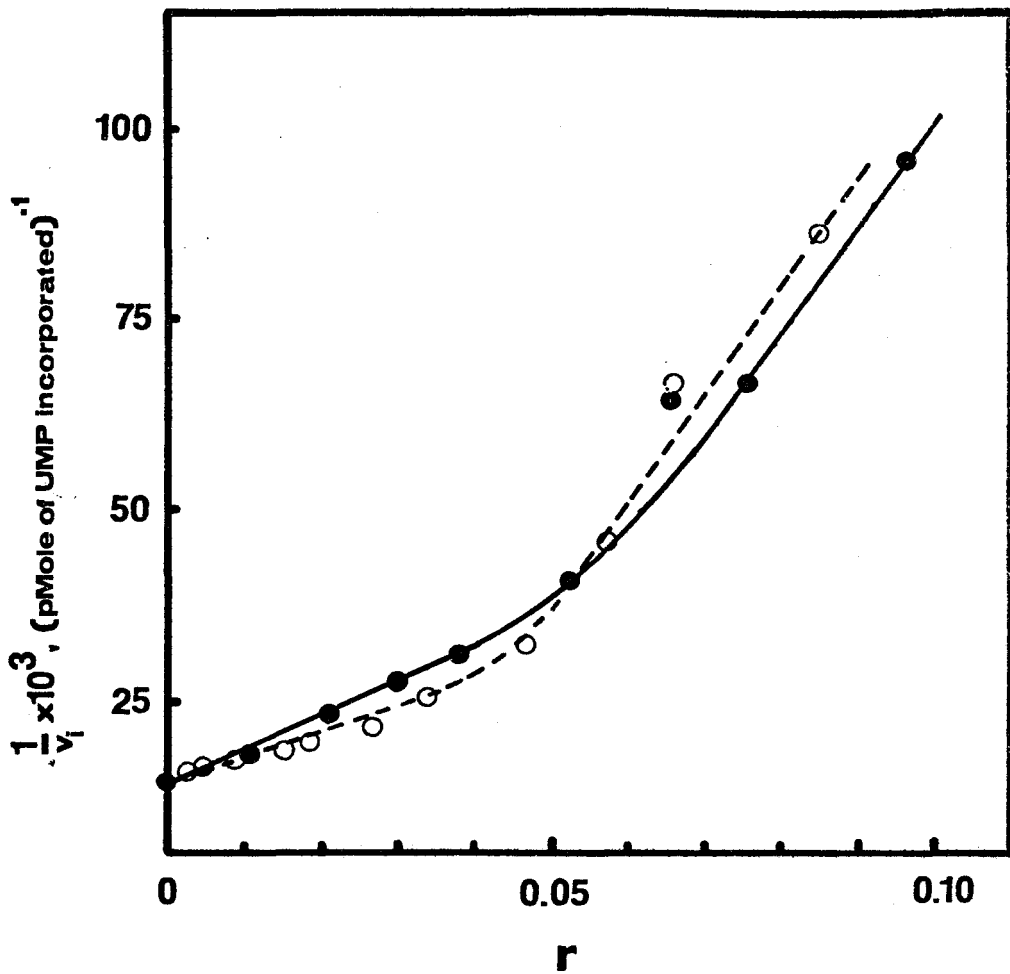
Figure 41. The dependence of the reciprocal initial velocity $1/v_i$ ($\bullet$) and of the initiation ($\blacksquare$) of RNA synthesis on the binding ratio r in the presence of Miracil D. Enzyme concentration: 20 units/ml, T2 DNA concentration: 10 μg/ml, and nucleoside triphosphate concentration: 0.5 m$\underline{M}$ (each).
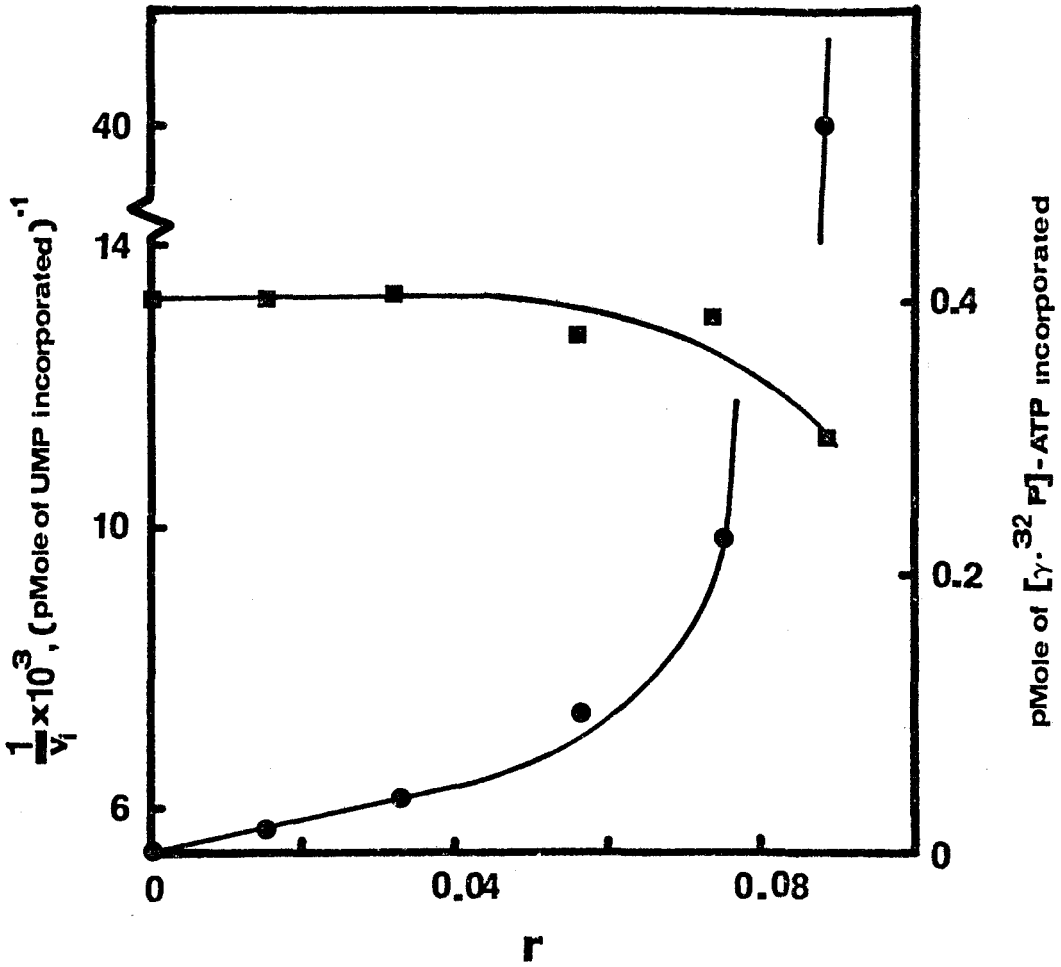
that at higher binding ratios Miracil D interferes also with the in-
itiation step of RNA synthesis. It seems likely, though no experi-
ments were conducted, that methyl-Miracil D behaves similarly.

A good correspondence in the dependences of the reciprocal in-
itial velocity on the binding ratio may be noted for T2 DNA and calf
thymus DNA shown in Figures 40 and 41. Deviations from linearity
start at binding ratios of about 0.05 for both templates.

CHAPTER IV

DISCUSSION

IV.1.   The Structure of the Miracil D-DNA Complex

The binding of Miracil D to DNA takes place through an interca-
lation process as a result of which the drug becomes inserted between
adjacent base pairs of DNA (see section I.6.2). As the case is with
other intercalators, the major forces stabilizing the complex are
probably the result of dipole-dipole, dipole-induced dipole, and
fluctuation dipole-induced dipole (dispersion forces of London) inter-
actions between the planar aromatic Miracil D molecule and the DNA base
pairs (Gersch and Jordan, 1965). Maximum stabilization by dispersion
forces is obtained when the overlapping of molecular orbitals of the
drug and the bases is maximal. This requirement is satisfied only with
the proposed model of Miracil D-DNA complex (Weinstein and Hirschberg,
1971) in which the long axis of the Miracil D molecule is parallel
with those of the base pairs forming the binding site. In this complex
the electrostatic interactions between the side chain of the drug and
the phosphate backbone of DNA are well-accomodated (see section I.6.2),
but the dipole-dipole interactions are not necessarily at their maxi-
mum. Since the dipole moment vectors of the four bases forming the
binding site and of the intercalated Miracil D molecule show into five
different directions, it is hard to predict whether stabilization or
destabilization by dipole-dipole interactions takes place.

It has been shown in the case of proflavine-DNA complexes

158

(Gersch and Jordan, 1965) that permanent dipole moments do not seem to play a decisive role in the orientation of the intercalated drug molecule in the binding sites. Free energy calculations suggest that a hypothetical rotation of intercalated proflavine causes less than 1 Kcal/Mole fluctuation in the ΔG^o of the intercalation process.

IV.2. The Binding of Miracil D to DNA – The Exclusion Model

In the analysis for the interaction of drugs with nucleic acids, certain formulations can serve as useful diagnostic tools in the testing of specific binding models. One of the simplest models for the interaction of small ligand molecules with proteins was developed by Scatchard (Scatchard, 1949). According to this model, if the binding of a ligand molecule to the protein does not influence the binding of other ligand molecules to the same protein molecule, then the binding isotherm has the following form:

$$\frac{r}{c_f} = n \cdot k - k \cdot r \quad ,$$

where r is the binding ratio as previously defined, k is the intrinsic association constant, and n is the number of binding sites for the ligand on the protein molecule. In the Scatchard plot, this isotherm represents a straight line with a slope of $-k$ and with an intercept of $n \cdot k$. The intercept with the r axis is n.

The same approach can be used for the interaction of drug molecules with nucleic acids. In this case the nucleic acid concentration is generally expressed as nucleic acid phosphorous concentration, and, therefore, the intercept with the r axis gives the number of binding

sites for the drug per nucleic acid phosphorous. If all potential intercalating sites were to bind drug molecules, the number of binding sites would be 0.5 per DNA phosphorous. In practice this is not realized. Scatchard plots for drug-nucleic acid interactions take a variety of forms, most often not linear, and the number of binding sites is much less than 0.5, generally ranging between 0.15 and 0.25 (e.g. Waring, 1965; Müller and Crothers, 1968; Peacocke and Skerrett, 1956; Tubbs et al., 1964). Deviations from linearity are generally observed at the higher binding ratios.

In order to overcome the obvious difficulties in the interpretation of curved Scatchard plots, and in order to explain the lower than expected number of binding sites, the exclusion model was introduced (McGhee and von Hippel, 1974). This model is discussed in detail in section II.8.3. The exclusion model was, therefore, selected for analyzing the binding of Miracil D to DNA. The selection of this model was suggested by the fact that, as the case is with other drugs, at saturation only half of the potential DNA binding sites are occupied by Miracil D.

It may be argued that base specificity in binding can also lead to binding in which less than the maximum of potential binding sites are able to participate. In fact, it has been suggested, based on the ability of Miracil D to inhibit DNA dependent RNA polymerase when synthetic DNA templates are used, that Miracil D has a stronger affinity toward adenine residues (Wilson et al., 1972b). Aside from the fact that this evidence is not at all conclusive, about 25 % of the bases in calf thymus DNA are adenine, which suggests that each potential binding

site contains in the average one adenine residue. Hence any preference

of Miracil D for adenine residue, if at all present, could not limit

the maximum number of binding sites to as low a value as 0.25.

Specificity toward base pairs G-C or A-T could also lead to a

decrease in the number of potential binding sites as evidenced in the

case of actinomycins (Müller and Crothers, 1968). Although G-C and A-T

base pairs are equally represented in calf thymus DNA, and could be

responsible for the decreased number of binding sites, this is very un-

likely based on the observations of Haidle and Mandel (private com-

munications to Weinstein and Hirschberg, 1971). These workers tested

the effect of several bacterial DNA's, ranging in base composition from

27 to 69 % G-C content, on their ability to induce spectral shifts in

the spectrum of Miracil D and found no correlation between this proper-

ty and G-C content.

Exclusion does not appear to result from simple mutual steric

interference between bound drug molecules. Since intercalation is ac-

companied by the unwinding of the DNA double helix (Waring, 1970), the

conformation of the binding sites adjacent to an already occupied

binding site differs from the conformation of sites surrounded by un-

occupied adjacent sites. A computerized linked-atom modeling system

was developed by Alden and Arnott to examine the stereochemical re-

quirements for intercalation of planar drugs into DNA (Alden and

Arnott, 1975). All classes of conformational possibilities for ex-

tending the polynucleotide backbone were examined for their ability to

accomodate insertion of a drug into a base-paired region of DNA com-

patible with adjacent regions of DNA while stacking interactions,

steric strain, and non-bonded interatomic contact were optimized. One

conformation was found which proved superior to all others in ability

to satisfy these criteria. This conformation was obtained by the ex-

tension of the backbone by characteristic changes in two torsion angles

to trans values and a change in one sugar puckering to relieve strain

in an adjacent residue. The turn angle distributed over three poly-

nucleotide residues for this most general mode of interaction is 90 $^{\circ}$,

corresponding to a helical unwinding of 18 $^{\circ}$ for DNA. This value is in

good agreement with the unwinding angle of 16.4 $^{\circ}$ discussed in section

I.6.2. It is possible that this conformational change makes the

nearest neighbour sites so stable that binding to them becomes thermo-

dynamically unfavourable. As an alternative, it is also possible that

binding of drug molecules to nearest neighbour sites imposes such a

restriction on the bond angles that the binding sites cannot undergo

the conformational changes necessary to accomodate the intercalated

drug molecule. Independent evidence for the exclusion model is also

obtained from X-ray crystallographic studies the results of which have

suggested that in the ethidium bromide-DNA complex the nearest neighbor

binding sites are excluded from binding (Jain et al., 1973).

Under the conditions of the present binding studies (see section

III.2.1), Miracil D is present as a positively charged monomer (see

section III.1), and, therefore, these studies deal with the interaction

of the monomeric form of the drug with DNA. The intrinsic associ-

ation constant was found to change from 1.2×10^{6} to 4.5×10^{4} $\underline{M}^{-1}$ when the

ionic strength is increased from 0.01 to 0.2 $\underline{M}$. This drastic decrease

of K is consistent with the structure of the Miracil D-DNA complex pro-

posed by Hirschberg (see section I.6.2). In this complex, the terminal
nitrogen atom of the side chain interacts with the negative phosphate
backbone of the DNA. This electrostatic interaction is obviously re-
duced at high ionic strength simply because of the unfavourable compe-
tition between the negative phosphate groups and the more numerous
cations of the buffer for the positive distal nitrogen atom. This is
by no means to say that this electrostatic interaction is completely
abolished at an ionic strength of 0.2 $\underline{M}$. Since the ΔG^o's calculated
for the two intrinsic association constants at 0.01 and 0.2 $\underline{M}$ salt
concentrations (see section III.2.1) are −8.2 (i.e. $-R \cdot T \cdot \ln(1.2 \times 10^6)$)
and −6.3 (i.e. $-R \cdot T \cdot \ln(4.5 \times 10^4)$) Kcal/Mole, respectively, at least 25 %
(i.e. (8.2−6.3)/8.2) of the forces stabilizing the complex in 0.01 $\underline{M}$
sodium acetate buffer, pH 5.0 appear to be electrostatic in character.

IV.3. The Structure of the Methyl-Miracil D-DNA Complex

     Methyl substitution in Miracil D leads to steric hindrance be-
tween the carbonyl oxygen and this substituent, which necessitates the
rotation of the side chain out of the plane of the heterocyclic ring
system (Zilversmit, 1970). The ring system of methyl-Miracil D, how-
ever, remains planar, and there seems to be no reason why the drug
could be prevented from intercalating. CPK model building of the
methyl-Miracil D-DNA complex shows that intercalation is sterically
possible, although the conformation of the side chain may limit some-
what the depth of drug penetration between the base pairs of the double
helix. In this conformation, the interaction between the positive
distal nitrogen atom of the drug and the negative phosphate backbone of
DNA appears to be still possible, but it is not as readily achieved as

with Miracil D. As a result, the electrostatic interactions involved are expected to be reduced which could explain the smaller intrinsic association constant observed for the binding of methyl–Miracil D to DNA. In fact, there is a difference of 1.1 Kcal/Mole (=8.2-7.1) in the ΔG°'s of the binding of Miracil D and methyl–Miracil D to calf thymus DNA in 0.01 $\underline{M}$ sodium acetate buffer, pH 5.0 at room temperature (see sections III.2.1 and III.2.4). The lowered intrinsic association constant compared to Miracil D is certainly not incompatible with the intercalative mode of binding.

The other line of evidence which strongly suggests intercalation of methyl–Miracil D comes from the similarities in the circular dichroism spectra of the DNA complexes formed with Miracil D and methyl–Miracil D. This will be discussed in detail in section IV.4.

As for the applicability of the exclusion model for the binding of methyl–Miracil D to DNA, similar arguments can be advanced as in the case of Miracil D (see section IV.2).

IV.4. The Circular Dichroism of Miracil D–DNA and Methyl–Miracil D–DNA Complexes

Both Miracil D and methyl–Miracil D are optically inactive compounds but, as expected from their intercalative mode of binding (see sections IV.1 and IV.3), they become optically active when bound to DNA (Figures 20 and 24). The dependence of their differential molar extinction coefficients on the binding ratio of the complexes formed (Figures 21, 22, 23, 25, 26, and 27) deviate from those of the majority of other intercalative dyes and drugs discussed in section I.7.2. They deviate from group 1 in that their differential molar extinction

coefficients vary greatly with the binding ratios, and from group 2 that their differential molar extinction coefficients decrease with increasing binding ratios and at low binding ratios they exhibit the maximum circular dichroism. However, 9-aminoacridine resembles the characteristics of Miracil D and methyl-Miracil D complexes (Dalgleish et al., 1969).

Since the distribution of intercalated Miracil D and methyl-Miracil D molecules on DNA is random (except for the nearest neighbour sites due to exclusion), the probability of interaction between intercalated drug molecules is at minimum at low r values. At these r values, however, the observed differential molar extinction coefficients are at their maximum values rather than being zero (in contrast to that of group 2 compounds, see section I.7.2). Therefore, the observed optical activity at low r values is the result of the interaction between these drugs and the asymmetric DNA binding sites (see section I.7.2).

As r increases, the probability of interaction between bound drug molecules increases. Two proposals have been advanced for the mechanism of drug-drug interaction in terms of explaining the resulting optical activity (Dalgleish et al., 1969): (1) exciton interaction between drug molecules mediated through base pairs and (2) alteration of the conformation of neighbouring binding sites as the result of binding. Exciton interactions between identical monomers lead to conservative circular dichroism spectra (Brahms and Brahms, 1970). Since the circular dichroism extrema of the bound drug molecules are located at the same wavelengths as the absorption band maxima (see sections

III.3.1 and III.3.2), the circular dichroism spectra of these drugs must be classified as non-conservative. Therefore, the exciton interaction between bound drug molecules, which is responsible for the optical activity of compounds belonging to group 2 (see section I.7.2) (Jackson and Mason, 1971), can be ruled out (Aktipis and Kindelis, 1973). Therefore, the second mechanism seems likely to describe the circular dichroism characteristics of Miracil D and methyl-Miracil D. The progressive binding of increasing numbers of drug molecules in the vicinity of molecules already bound is expected to alter continuously the conformation of the complex resulting in the lowered differential molar extinction coefficients noted at higher r values.

The quantitative, but not qualitative differences between the circular dichroism of Miracil D-DNA and methyl-Miracil D-DNA complexes could be the result of structural differences of these complexes. As mentioned earlier, in methyl-Miracil D the rotation of the side chain relative to the ring system limits somewhat the depth of penetration of the drug between the base pairs of DNA (see section IV.3). This could lead to a less favourable positioning of the intercalated methyl-Miracil D molecules in the binding site as compared to Miracil D. Since circular dichroism is very sensitive toward changes in molecular conformations, it seems likely that small differences in the positioning of bound drug molecules within the binding site could cause the observed differences in the resulting differential molar extinction coefficients.

In the binding of Miracil D and its methyl derivative to DNA, further drug binding is excluded on the nearest neighbour binding sites

due to an indirect effect of bound drug molecules (see section IV.2).

This exclusion effect in binding extends to only the nearest neighbour

binding sites. However, the effect of binding appears to extend to

sites further away than the nearest neighbour sites as evidenced from

the dependence of the differential molar extinction coefficients on the

binding ratio.

In an analogous manner, the binding of actinomycin was shown to

stabilize binding sites against heat denaturation 15 base pairs away

(Burd et al., 1975). Therefore, the exclusion in binding and the de-

pendence of E_L-E_R on the binding ratio appears to be the result of the

extension of conformational changes beyond the actual site of drug

binding, which means that both binding exclusion and the circular

dichroism properties of these systems are two manifestations of the same

phenomenon.

IV.5. The Inhibition of RNA Synthesis by Miracil D and Methyl-Miracil D

Miracil D inhibits two steps in RNA synthesis: initiation and

elongation (see section III.5.4). Below r values of 0.05, only the

elongation of RNA chains is inhibited, but at binding ratios greater

than 0.05, initiation is inhibited as well.

IV.5.1. The Inhibition of Initiation of RNA Synthesis by Miracil D and Methyl-Miracil D

It is not quite clear why inhibition of initiation comes into

play at an r value of 0.05, but some speculation can be advanced. For

successful initiation to take place, the enzyme must bind to the pro-

moter region on DNA. The bound enzyme molecule occupies about 20 con-

secutive base pairs (Heyden et al., 1975). With respect to the machanism of recognition, the promoter site is selected by a random association with and dissociation from the DNA molecule rather than by selection of promoter region as a result of a sliding movement of the enzyme along the template. In the next step, the enzyme separates the two strands of the template for a length of seven or eight base pairs and assumes the active conformation of the enzyme-template complex (Chamberlin, 1974). With regard to this strand separation, RNA polymerase belongs to the class of melting proteins (von Hippel and McGhee, 1972). Since the drug binding to DNA is a dynamic equilibrium, drug molecules constantly associate with and dissociate from at rates reflected by their rate constants. If drug molecules are bound to the promoter region, they could interfere with the binding of the enzyme. It is believed that a minimum of 12 base pairs is required to insure that a unique sequence of nucleotides (part of the promoter region), which is unlikely to be generated by random assortment of nucleotides, is formed so as to establish a recognition site (Thomas, 1966). Since drug binding by intercalation unwinds and extends the double helix, it appears that intercalated drug molecules distort this unique sequence of 12 base pairs beyond recognition by the enzyme. Therefore, it seems that a drug-free recognition region is necessary for selective binding of the enzyme to the promoter region. With increasing binding ratios, the probability that the recognition region is free of drug molecules obviously decreases. Inhibition of initiation is thus more likely to take place at the higher range of r values, as it has been noted experimentally for Miracil D (see section III.6.4).

In addition to probability considerations, kinetic consider-
ations are also important concerning the inhibition of initiation. The
equilibrium position in the competition of drug and enzyme for the
recognition region overwhelmingly favours the enzyme-template complex
which is characterized by an association constant of about 10^{14} $\underline{M}^{-1}$
(Chamberlin, 1974). Therefore, incubation of drug, template, and
enzyme for longer periods of time and at higher temperatures before the
onset of RNA synthesis would be expected to decrease the inhibition of
initiation. This has been substantiated for ethidium bromide
(Richardson, 1973). Conversely, if drug, template, and enzyme are not
incubated before RNA synthesis started, the inhibition of initiation
would increase relative to the incubated assay. Indeed, actinomycin D,
which is a strong inhibitor of RNA chain elongation (Hyman and Davidson,
1970) and normally does not inhibit initiation, acts as an initiation
inhibitor as well when the drug, the template, and the enzyme are not
incubated for some time before RNA synthesis is started (Maitra et
al., 1967; Sentenac et al., 1968). Although this possibility was not
investigated, it might, therefore, be expected that Miracil D would
become a more effective inhibitor of initiation if the incubation of
drug, template, and enzyme before the onset of RNA synthesis is re-
duced. In the view of the probability and kinetic considerations pre-
sented above, the observation that Miracil D inhibits initiation of RNA
synthesis at r values greater than 0.05 (see section III.5.4) seems to
be the result of two factors: (1) the dissociation rate constant of the
Miracil D-DNA complex and (2) the period of incubation (see section

II.11) of Miracil D, template, and enzyme before the start of RNA
synthesis.

If the only effect of initiation inhibitors is to prevent the
binding of enzyme to the recognition region, then, based on the
considerations above, drugs with low dissociation rates would be the
most likely candidates as inhibitors of initiation. They could be
viewed as retarding the formation of active enzyme-template complex
simply by occupying the recognition region for extended periods of
time.

The actinomycin family is an example of drugs dissociating from
their complexes with DNA at slow rates (Müller and Crothers, 1968).
Although actinomycin D is principally a strong inhibitor of elongation
(Hyman and Davidson, 1970), it can inhibit RNA chain initiation (Maitra
et al., 1967; Sentenac et al., 1968), as mentioned earlier. Therefore,
in the comparison of the relative effectiveness of different drugs as
inhibitors of initiation of RNA synthesis, both initiation and e-
longation inhibitors should be considered, since either type of in-
hibitor can under proper conditions inhibit initiation. At the present
time, the comparison is not possible due to lack of such information.
In addition, the composition of the recognition region could be a
complicating factor, since actinomycin D binds only to G-C base pairs.

The prevention of enzyme binding to the recognition region by
initiation inhibitors is not the only way drugs can interfere with in-
itiation. When the active enzyme-template complex is formed, the two
strands of the template are separated by the bound enzyme for a length
of seven or eight base pairs (see above). Drug molecules bound in the

vicinity of enzyme-template complex can hinder this strand separation

(melting-in). In the case of actinomycin binding to DNA, for instance,

it has been found that binding increases the melting temperature of DNA

regions as far as 15 base pairs away from the actual site of binding

(Burd et al., 1975). This telestabilizing effect could conceivably be

detected by the enzyme, and the rate of melting-in could thus be de-

creased.

In this simplified overview of the mechanism of inhibition of

initiation of RNA synthesis, both the binding and the melting-in steps

can be interfered with by inhibitors. The present experimental data

concerning the initiation inhibition of RNA synthesis by Miracil D (see

section III.5.4) are not adequate to arrive at a firm conclusion

whether Miracil D interferes with the binding or the melting-in (or

both) steps of initiation.

Methyl-Miracil D also inhibits RNA synthesis (see section

III.5.3). If the intrinsic association constant estimated (see section

III.5.3) is essentially correct, then this derivative, when bound to

DNA, is as effective an inhibitor of RNA synthesis as is DNA-bound

Miracil D. Based on the similarity of the dependence of the reciprocal

initial velocity on the binding ratio for both Miracil D and its methyl

derivative (Figure 40), the inhibition of both elongation and initi-

ation is probable for the latter as well, although the inhibition of

initiation by methyl-Miracil D was not investigated separately.

IV.5.2. The Inhibition of Elongation of RNA Synthesis by Miracil D
and Methyl-Miracil D

In order to explain the relative inhibitory effectiveness of
actinomycins as inhibitors of RNA chain elongation, it was proposed
that this effectiveness is related also to their dissociation rate
constants from the drug-template complex (Müller and Crothers, 1968).
According to these authors, as the enzyme moves along the DNA template
in the course of transcription, the enzyme will encounter intercalated
drug molecules. As a result, RNA synthesis comes to a halt, and the
enzyme must wait until the drug dissociates or the enzyme forces the
drug molecule to dissociate. As the next base pair is free of drug,
RNA synthesis can resume. A good correspondence was obtained, when
using different synthetic and natural templates, between the relative
effectiveness of actinomycin D to inhibit elongation and the respective
dissociation rate constants.

However, there are difficulties in extending the above proposal
to every inhibitor of RNA synthesis. Specifically, if we assume an
average chain growth rate of 2.9 nucleotides/sec (Kozlov, 1971) (repre-
senting the incorporation of one nucleotide in 0.34 sec), drug-DNA
complexes with a half-life much shorter than 0.34 sec would not be ex-
pected to appreciably inhibit RNA chain elongation. For ethidium
bromide-calf thymus DNA complexes, a dissociation rate of 138 sec^{-1}
has been determined (Bresloff and Crothers, 1975), which suggests a
half-life of 0.005 sec (=$\log_e 2/138$). This half-life is then about 68
times shorter than the average incorporation time of one nucleotide.
Accordingly, ethidium bromide would not be expected to inhibit RNA chain

elongation. Contrary to expectation, however, it was found that ethidium bromide does inhibit elongation by about 50 % of those RNA molecules whose initiation has not been blocked (Richardson, 1973).

To reconcile this discrepancy, the mechanism of RNA chain elongation should be considered. In the active enzyme-template complex, the two strands of the template are separated for a length of seven or eight base pairs (see above). In the course of transcription, the enzyme continuously separates the two strands of the template in the direction of RNA chain growth, and subsequently the separated strands reform the double helix as the enzyme moves past them. Due to telestabilization of DNA by drugs (see above), it appears that this continuous strand separation can be retarded by drug molecules bound to DNA many sites away from the actual site of RNA synthesis. Consequently, in order for the enzyme to elongate RNA chains uninhibited, it seems that a long stretch of base pairs must be free of drug in the direction of RNA chain growth. At higher binding ratios, this is equivalent to the simultaneous dissociation of a number of inhibitor molecules from the complex within a region of several base pairs extending in front of the enzyme. Therefore, if telestabilization plays an active role in the inhibition of elongation, the half-life of drug-DNA complexes may not be an appropriate measure for judging the expected effectiveness of inhibition. Rather the simultaneous half-life of many complexes should be considered. However, no experimental data are available on the telestabilization of DNA by ethidium bromide and a calculation of an appropriately combined half-life for several complexes would be an extremely complicated task. Therefore, a more

specific explanation as to why ethidium bromide inhibits elongation inspite of the short half-life in the ethidium bromide-template complex (discussed above) cannot be offered at the present time.

The stabilization of DNA in the presence of Miracil D and methyl-Miracil D noted from hyperchromicity studies of both of these complexes (see section III.4.3) indicates that these drugs increase the resistance of DNA against heat denaturation. Since RNA polymerase continuously separates the two strands of DNA in the course of chain elongation, the inhibitory action of the bound forms of the two drugs toward RNA chain elongation (see section III.5.3) should parallel their effectiveness in stabilizing template DNA (see section III.4.3). Indeed, Miracil D and methyl-Miracil D, when bound to DNA, are equally effective in stabilizing DNA against heat denaturation (see section III.4.3) and equally effective in inhibiting RNA polymerase (see section III.5.3).

IV.6. Considerations on the Association and Dissociation Rates of Miracil D, Methyl-Miracil D, and MDMT

As a result of binding to the DNA template, both Miracil D and its methyl derivative inhibit RNA synthesis. Since they are equally effective inhibitors of RNA chain elongation, they may be expected to have similar dissociation rate constants from their complexes with DNA (see previous section). It may be recalled that the intrinsic association constant K of Miracil D with DNA is larger than that of the methyl-Miracil D (see sections III.2.1 and III.2.4, respectively). Also, the intrinsic association constant K for any binary complex is related to the association rate constant k_{ass} and to the dissoci-

ation rate constant k_{diss} through the equation

$$K = \frac{k_{ass}}{k_{diss}} \; .$$

Therefore, it would appear that Miracil D associates with DNA faster than methyl-Miracil D, i.e. $k_{ass,MD} > k_{ass,MMD}$. Consequently, methyl-Miracil D would be expected to have a greater activation energy for association with DNA than Miracil D. This seems to be a reasonable expectation based at least on inspection of the CPK models for the Miracil D-DNA complex relative to that of the methyl-Miracil D-DNA complex (see section IV.3), which suggests that formation of the latter complex may require higher activation energy.

From the present binding studies it also appears that 1-(4-methyl-1,4-diazapentyl)-4-methyl-10-thioxanthene (abbreviated as MDMT) has a smaller intrinsic association constant K_{MDMT} (i.e. equilibrium binding constant) than that (K_{MMD}) of methyl-Miracil D (see section III.2.5). On the basis of the relative magnitudes of these intrinsic association constants (i.e. equilibrium binding constants), the following relationship holds:

$$K_{MMD} > K_{MDMT}$$

or

$$\frac{k_{ass,MMD}}{k_{diss,MMD}} > \frac{k_{ass,MDMT}}{k_{diss,MDMT}} \; .$$

The results presented in Figure 38 indicate that MDMT and methyl-Miracil D inhibit RNA polymerase roughly to the same extent when compared on the basis of total inhibitor concentration present in the as-

say solutions. Since MDMT has a smaller intrinsic association constant
than methyl-Miracil D, it follows that MDMT, if it were compared on the
basis of drug-DNA binding ratios as it should, would have been found to
be a stronger inhibitor of RNA synthesis than methyl-Miracil D. Based
on considerations cited in the preceding section, MDMT should,
therefore, have a lower dissociation rate constant than that of methyl-
Miracil D, i.e. $k_{diss,MDMT} < k_{diss,MMD}$. Consequently,

$$\frac{k_{ass,MDMT}}{k_{diss,MDMT}} > \frac{k_{ass,MDMT}}{k_{diss,MMD}} .$$

From the two unequalities of association to dissociation rates, it
follows that

$$\frac{k_{ass,MMD}}{k_{diss,MMD}} > \frac{k_{ass,MDMT}}{k_{diss,MMD}} .$$

After multiplying by $k_{diss,MMD}$, the relationship $k_{ass,MMD} > k_{ass,MDMT}$
is obtained, indicating that methyl-Miracil D associates with DNA
faster than MDMT.

It is not known at this time whether the formation of the MDMT-
DNA complex is accomplished by intercalation of the MDMT molecule. If
intercalation is involved, this process would require very high acti-
vation energy, since the MDMT molecule is not planar (see section I.2)
and intercalation, similar to that of Miracil D with DNA, would require
that the MDMT molecule become planar. Such a mechanism of complete
intercalation would, therefore, be compatible with the small associa-
tion rate constant predicted above from the results of binding and

inhibition studies.

A completely intercalated MDMT-DNA complex, however, would be expected in analogy to Miracil D and methyl-Miracil D (see sections III.3.1 and III.3.2, respectively) to exhibit optical activity. Although no optical activity was observed experimentally in the case of MDMT-DNA complexes (see section III.3.3), the existence of optical activity for MDMT-DNA complexes cannot be ruled out for the reasons enumerated in section III.3.3.

The possibility that partial intercalation of the MDMT molecule occurs by means of one of the benzene rings should also be considered, but such a mechanism of intercalation appears to be inconsistent with the slow association rate with DNA predicted above. Therefore, a completely intercalated MDMT-DNA complex is proposed, in which the nonplanar MDMT molecule becomes planar as the result of intercalation between adjacent base pairs of the DNA double helix. Of course, other models concerning the structure of MDMT-DNA complex cannot on the basis of the present data be ruled out.

In summary, the following relationships among the intrinsic association constants (K) and the association and dissociation rate constants (k) for Miracil D, methyl-Miracil D, and MDMT are consistent with the molecular structure of these compounds and with the results of the present binding and inhibition studies:

$$K_{MD} > K_{MMD} > K_{MDMT} \ ,$$
$$k_{ass,MD} > k_{ass,MMD} > k_{ass,MDMT} \ , \text{ and}$$
$$k_{diss,MD} = k_{diss,MMD} > k_{diss,MDMT} \ .$$

In conclusion, the binding of Miracil D and methyl-Miracil D to calf thymus DNA was studied by two spectrophotometric methods. Both drugs were found to conform to a model in which two adjacent binding sites cannot be occupied simultaneously. It has also been shown that Miracil D has a greater affinity to native DNA than methyl-Miracil D. However, when bound to DNA, both drugs are equally effective in stabilizing DNA against heat denaturation and inhibiting DNA dependent RNA synthesis.

CHAPTER V

SUMMARY

Miracil D, a schistosomicidal, carcinostatic, and bacteriostatic compound is known to bind to DNA through intercalation. In the resulting complex, the planar heterocyclic ring system of the drug is inserted between adjacent base pairs of the DNA helix, and the positive diethylaminoethylamino side chain of the drug interacts with the negative phosphate backbone of DNA. The circular dichroism measurements in this work suggest that, as a result of the binding, the conformation of the neighbouring binding sites in DNA is also modified. Such a conformational change may prevent the binding of drug molecules to sites which are adjacent to occupied sites. Consequently, when the exclusion in binding to the nearest neighbour sites is taken into account, an intrinsic association constant of 1.2×10^6 $\underline{M}^{-1}$ is obtained in 0.01 $\underline{M}$ sodium acetate buffer, pH 5.0 and at 25 $^\circ$C. We have found that this intrinsic association constant substantially decreases with increasing temperature and ionic strength.

In the case of methyl-Miracil D, the intrinsic association constant (1.7×10^5 $\underline{M}^{-1}$) is lower than that of the binding of Miracil D to DNA. In the former derivative, in contrast to Miracil D, the proximal $-NR_2$ grouping is reported to be non-coplanar with the heterocyclic ring system due to steric interference. The conformation of the proximal nitrogen atom of methyl-Miracil D may thus limit the depth of drug penetration between the base pairs of the DNA double helix, and may,

therefore, reduce the electrostatic interaction between the positive side chain of the drug and the negative phosphate backbone of DNA.

Both Miracil D and methyl-Miracil D are optically inactive but become active when bound to DNA. The circular dichroism bands of Miracil D-DNA and methyl-Miracil D-DNA complexes are located at the absorption maxima and shoulders in the spectra of the bound drugs. The differential molar extinction coefficients of Miracil D-DNA complexes at 337, 347, and 447 nm and of methyl-Miracil D-DNA complexes at 335, 353, and 405 nm decrease as the binding ratio (the ratio of the bound drug concentration to the DNA concentration) increases, indicating that the conformational changes in DNA, due to binding, extend to sites beyond the nearest neighbour binding sites. Based on the non-conservative character of the observed circular dichroism bands, it is suggested that the induced optical activity is the result of the interaction between these drugs and the asymmetric binding sites of DNA.

Miracil D and methyl-Miracil D stabilize DNA against heat denaturation as measured by the increase of the mid-transition temperature of drug-DNA complexes relative to that of native DNA. The drugs are equally effective in this respect when the comparison is made on the basis of binding ratios prevailing at the mid-transition temperature of the complexes. At low binding ratios, the reintercalation of Miracil D in the course of thermal denaturation of DNA is observed, as evidenced from circular dichroism measurements.

Both Miracil D and methyl-Miracil D inhibit DNA dependent RNA polymerase by inactivating the DNA template as a result of drug binding. These intercalators are equally effective in this respect

when the comparison is made at equal binding ratios of drug-DNA complexes. Furthermore, below a binding ratio of 0.05, Miracil D inhibits only the elongation step of RNA synthesis, and the reciprocal initial velocity of elongation is linearly proportional to the binding ratio of the Miracil D-DNA complex. At binding ratios greater than 0.05, however, the initiation of RNA chains is inhibited as well. The equal effectiveness of Miracil D and methyl-Miracil D in inhibiting RNA chain elongation and in stabilizing DNA against heat denaturation suggests that these drugs inhibit RNA polymerase by retarding the strand separation of the DNA template in the course of RNA chain elongation.

BIBLIOGRAPHY

Aizenshtat, Z., Klein, E., Weiler-Feilchenfeld, H., and Bergman, E. D. (1972), "Conformational Studies on Xanthene, Thioxanthene and Acridan," Isr. J. Chem. 10, 753-763

Aktipis, S. and Kindelis, A. (1973), "Optical Properties of the Deoxyribonucleic Acid-Ethidium Bromide Complex. Effect of Salt," Biochemistry 12, 1213-1221

Aktipis, S. and Martz, W. W. (1970), "Circular Dichroism Properties of Ethidium Bromide-Deoxyribonucleic Acid Complexes," Biochem. Biophys. Res. Comm. 39, 307-313

Aktipis, S., Martz, W. W., and Kindelis, A. (1975), "Thermal Denaturation of the DNA-Ethidium Complex. Redistribution of the Intercalated Dye during Melting," Biochemistry 14, 326-331

Alden, C. J. and Arnott, S. (1975), "Visualization of Planar Drug Intercalations in B-DNA," Nucl. Acid Res. 2, 1701-1717

Aroney, M. J., Hoskins, G. M., and Le Fevre, R. W. (1969), "Molecular Polarisability. The Conformations as Solutes of Phenoxanthiin, Xanthene, and Thioxanthene," J. Chem. Soc (B) 980-982

Aroney, M. J., Cleaver, G., and Le Fevre, R. J. W. (1971), "Molecular Polarisability. The Conformations as Solutes of 9,10-Dihydroanthracene, Anthrone, and Xanthone," J. Chem. Soc. (B) 82-85

Bautz, E. K. F. and Dunn, J. J. (1971), "DNA-Cellulose Chromatography of Proteins," Proc. Nucl. Acid Res. 2, 743-747

Blair, D. M. (1958), "Lucanthone Hydrochloride. A Review," Bull. Wld. Health Org. 18, 989-1009

Blake, A. and Peacocke, A. R. (1966), "Extrinsic Cotton Effects of Aminoacridines Bound to DNA," Biopolymers 4, 1091-1104

Blake, A. and Peacocke, A. R. (1968), "The Intercation of Aminoacridines with Nucleic Acids," Biopolymers 6, 1225-1253

Blanz, E. J. and French, F. A. (1963), "A Systematic Investigation of Thioxanthene-9-ones and Analogs as Potential Antitumor Agents," J. Med. Chem. 6, 185-191

Brahms, J. and Brahms, S. (1970), "Circular Dichroism of Nucleic Acids," in "Fine Structure of Proteins and Nucleic Acids," pp.191-270. Edited by Fasman, G. F. and Timasheff, S. N. New York: Marcell Dekker, Inc.

Bresloff, J. L. and Crothers, D. M. (1975), "DNA-Ethidium Reaction Kinetics: Demonstration of Direct Ligand Transfer between DNA Binding Sites," J. Mol. Biol. 95, 103-123

Burd, J. F., Larson, J. E., and Wells, R. D. (1975), "Further Studies on Telestability in DNA," J. Biol. Chem. 250, 6002-6007

Burgess, R. R. (1969), "A New Method for the Large Scale Purification of Escherichia coli Deoxyribonucleic Acid-Dependent Ribonucleic Acid Polymerase," J. Biol. Chem. 244, 6160-6167

Carchman, R. A., Hirschberg, E., and Weinstein, I. B. (1969), "Miracil D: Effect on the Viscosity of DNA," Biochim. Biophys. Acta 179, 158-164

Chamberlin, M. J. (1974), "The Selectivity of Transcription," Ann. Rev. Biochem. 43, 721-775

Chamberlin, M. and Berg, P. (1962), "Deoxyribonuclic Acid-Directed Synthesis of Ribonucleic Acid by an Enzyme from Escherichia coli," Proc. Nat. Acad. Sci. USA 48, 81-94

Crothers, D. M. (1974), "Binding of Small Molecules," in "Physical Chemistry of Nucleic Acids," pp. 253-314. by Bloomfield, V. A., Crothers, D. M., and Tinoco, I., New York: Harper & Row

Dalgleish, D. G., Fujita, H., and Peacocke, A. R. (1969), "Circular Dichroism of Aminoacridines Bound to DNA," Biopolymers 8, 633-645

Dourlent, M. and Helene, C. (1971), "A Quantitative Analysis of Proflavine Binding to Polyadenylic Acid, Polyuridylic Acid, and Transfer RNA," Eur. J. Biochem. 23, 86-95

Gersch, N. F. and Jordan, D. O. (1965), "Interaction of DNA with Aminoacridines," J. Mol. Biol. 13, 138-156

Giovanelli, K. H., Dehler, J., and Hohlneicher, G. (1971), "Zur theoretischen Interpretation der Elektronenspectren einiger mit Akzeptor- und Donatorgruppen substituierter Benzole sowie daraus abgeleiteter Verbindungen," Berichte der Bunsen-Gesellschaft 75, 864-877

Given, P. H., Guha, S., Jones, J. R., and Wedel, R. (1965), "Theoretical Study of Benzologues of 4-Thiapyrone," Nature 206, 184-186

Günnert, R. (1961), "The Structure-Activity Relationship in Several Schistosomicidal Compounds," Bull. Wld. Health Org. 25, 702-706

Hackmann, C., Günnert, R., and Mauss, H. (1949), "Tumor Inhibition Effect of Miracil," Naturwissentschaften 36, 29-33

Haidle, C. W., Brinkley, B. R., and Mandel, M. (1970), "Effect of Miracil D on Marker Frequency Ratio and Cytotoxicity in Bacillus subtilis," J. Bacteriol. 102, 835-842

Hartman, P. E., Berger, H., and Hartman, Z. (1973), "Comparison of Hycanthone ("Etrenol"), Some Hycanthone Analogs, Myxin and 4-Nitroquinoline-1-Oxide as Frameshift Mutagens," J. Pharm. Exp. Ther. 186, 390-398

Hawking, F. and Ross, W. F. (1948), "Miracil D, Its Toxicology, Absorption, and Excretion in Animals and Human Volunteers," J. Pharmacol. 3, 167-173

Hayman, H. J. G. (1962), "Spectrophotometric and Partition Methods of Determining Association Constants of 1:1 Charge-Transfer Complexes," J. Chem. Phys. 37, 2290-2302

Heller, M. J., Tu, A. T., and Maciel, G. E. (1974), "Interaction of Miracil D with Double-Stranded Poly(adenylic Acid)·Poly(uridylic Acid)," Biochemistry 13, 1623-1631

Heyden, B., Nüsslein, C., and Schaller, H. (1975), "Initiation of Transcription within an RNA-Polymerase Binding Site," Eur. J. Biochem. 55, 147-155

Hillman, G. R. and Gibler, W. B. (1975), "Acetylcholine Receptors in Schistosoma mansoni: Visualization and Blockade by Hycanthone," Biochem. Pharmacol. 24, 1911-1914

Hirschberg, E., Brindle, S. D., and Semente, G. (1964), "Development and Properties of Mouse Leukemia L1210 Resistant to Miracil D," Cancer Research 24, 1733-1737

Hirschberg, E., Gellhorn, A., Murray, M. R., and Elslager, E. (1959), "Effects of Miracil D, Amodiaquin, and a Series of Other 10-Thioxanthenones and 4-Aminoquinolines Against a Variety of Experimental Tumors in vitro and in vivo," J. Natl. Canc. Inst. 22, 567-579

Hirschberg, E., Ceccarini, C., Osnos, M., and Carchman, R. (1968a), "Effects of Inhibitors of Nucleic Acid and Protein Synthesis on Growth and Aggregation of the Cellular Slime Mold Dictyostelium discoideum," Proc. Natl. Acad. Sci. USA 61, 316-323

Hirschberg, E., Weinstein, I. B., Carchman, R., and Archer, S. (1968b), "Search for the Carcinostatic Metabolite of Miracil D," Proc. Amer. Assoc. Canc. Res. 9, 30

Hirschberg, E., Weinstein, I. B., Gersten, N., Marner, E., Finkelstein, T., and Carchman, R. (1968c), "Structure-Activity Studies on the Mechanism of Action of Miracil D," Cancer Research 28, 601-607

Hurwitz, J., Furth, J. J., Anders, M., and Evans, A. (1962), "The Role of Deoxyribonucleic Acid in Ribonucleic Acid Synthesis," J. Biol. Chem. 237, 3752-3759

Hyman, R. W. and Davidson, N. (1970), "Kinetics of the in vitro Inhibition of Transcription by Actinomycin," J. Mol. Biol. 50, 421-438

Jackson, K. and Mason, S. F. (1971), "Linear and Circular Dichroism Studies of DNA-Monoaminoacridine Complexes," Trans. Farad. Soc. 67, 966-989

Jain, S. C., Tsai, C. C., and Sobell, H. M. (1973), "Visualization of Drug-Nucleic Acid Interactions at Atomic Resolution: Unifying Structural Concepts in Understanding Drug-DNA Interactions," Biophys. J. 17, 59a

Kikuth, W. and Gönnert, R. (1948), "Experimental Studies on the Therapy of Schistosomiasis," Ann. Trop. Med. Parasit. 42, 256-267

Kikuth, W., Gönnert, R., and Mauss, H. (1946), "Miracil, ein neues Chemotherapeuticum gegen die Darmbilharziose," Naturwissentschaften 33, 253

Kleinwächter, V., Balcarova, Z., and Bohacek, J. (1969), "Thermal Stability of Complexes of Diaminoacridines with Deoxyribonucleic Acids of Varying Base Content," Biochim. Biophys. Acta 174, 188-201

Klotz, I. M. and Rosenberg, R. M. (1972), "Chemical Thermodynamics," 3rd ed. Menlo Park, Cal.: W. A. Benjamin, Inc.

Kozlov, Y. V. (1971), "Kinetics of the Initiation and Growth of RNA Chains at High and Low Ionic Strengths," Mol. Biol. (Russian) 5, 126-132

Lamm, M. E. and Neville, D. M. (1965), "The Dimer Spectrum of Acridine Orange Hydrochloride," J. Phys. Chem. 69, 3872-3877

Lazurkin, Y. S., Frank-Kamenetskii, M. D., and Trifonov, E. N. (1970), "Melting of DNA: Its Study and Application as a Research Method," Biopolymers 9, 1253-1306

Lea, M. A., Miller, S., Mackauf, I., Hirschberg, E., and Morris, H. P. (1972), "Action of Miracil D and Related Compounds and DNA and RNA Synthesis in Regenerating Liver and Hepatomas," Int. J. Cancer 9, 484-489

Lerman, L. S. (1961), "Structural Considerations in the Interaction of DNA and Acridines," J. Mol. Biol. 3, 18-30

Mahler, H. R., Kline, B., and Mehrotra, B. D. (1964), "Some Observations on the Hypochromism of DNA," J. Mol. Biol. 9, 801-811

Maitra, U., Nakata, Y., and Hurwitz, J. (1967), "The Role of Deoxyribonucleic Acid in Ribonucleic Acid Synthesis," J. Biol. Chem. 212, 4908-4918

Martz, W. W., and Aktipis, S. (1971), "A System for Automatic Temperature-Programmed Recording of Circular Dichroism and Optical Rotatory Dispersion," Anal. Biochem. 39, 327-332

Mauss, H. (1948), "Uber basisch substituierte Xanthon- und Thioxanthone-Abkömmlinge; Miracil, ein neues Chemotherapeuticum," Chem. Ber. 81, 19-31

McGhee, J. D. and von Hippel, P. H. (1974), "Theoretical Aspects of DNA-Protein Interactions: Co-operative and Non-co-operative Binding of Large Ligands to a One-dimensional Homogeneous Lattice," J. Mol. Biol. 86, 469-489

Müller, W. and Crothers, D. M. (1968), "Studies of the Binding of Actinomycin and Related Compounds to DNA," J. Mol. Biol. 35, 251-290

Munro, D. C. (1961), "Physicochemical Properties of Some Chemotherapeutic Thioxanthones," J. Chem. Soc. 5381-5384

Nakamoto, T., Fox, C. F., and Weiss, S. B. (1964), "Enzymatic Synthesis of Ribonucleic Acid," J. Biol. Chem. 239, 167-174

Peacocke, A. R. and Skerrett, J. N. H. (1956), "The Interaction of Aminoacridines with Nucleic Acids," Trans. Farad. Soc. 52, 261-279

Rabinowitch, E. and Epstein, L. F. (1941), "Polymerization of Dyestuffs in Solution. Thionine and Methylene Blue," J. Amer. Chem. Soc. 63, 69-78

Richardson, J. P. (1973), "Mechanism of Ethidium Bromide Inhibition of RNA Polymerase," J. Mol. Biol. 78, 703-714

Rosi, D., Peruzotti, G., Dennis, E. W., Berberian, D. A., Freele, H., Tullar, B. F., and Archer, S. (1967), "Hycanthone, a New Active Metabolite of Lucanthone," J. Med. Chem. 10, 867-876

Rubenstein, I., Thomas, C. A., and Hershey, A. D. (1961), "The Molecular Weights of T2 Bacteriophage DNA and Its First and Second Breakage Products," Proc. Natl. Acad. Sci. USA 47, 1113-1122

Scatchard, G. (1949), "The Attractions of Proteins for Small Molecules and Ions," Ann. New York Acad. Sci. 51, 660-672

Schildkraut, C. and Lifson, S. (1965), "Dependence of the Melting Temperature of DNA on Salt Concentration," Biopolymers 3, 195-208

Scholtan, W. (1959), "Kolloidchemische Eigenschaften von Salzen basisch substituierter Xanthon- und Thioxanthonderivative," Kolloid-Zeitschrift 170, 19-29

Sentenac, A., Simon, E. J., and Fromageot, P. (1968), "Initiation of Chains by RNA Polymerase and the Effects of Inhibitors Studied by a Direct Filtration Technique," Biochim. Biophys. Acta 161, 299-308

Sharp, T. M. (1951), "A New Synthesis of Lucanthone (Miracil D, Nilodin)," J. Chem. Soc. 2961-2963

Sreevalsan, T. (1973), "Isolation of Single-Stranded Viral Ribonucleic Acids," Meth. Mol. Biol. 4, 64-92

Thomas C. (1966), "Recombination of DNA Molecules," Progr. Nucl. Acid Res. 5, 315-337

Thomas, C. A. and Abelson, J. (1966), "The Isolation and Characterization of DNA from Bacteriophage," in "Procedures in Nucleic Acid Research," vol. 1, pp. 553-561. Edited by Cantoni, G. L. and Davies, D. R. New York: Harper and Row Publishers

Tsai, C. C., Jain, S. C., and Sobell, H. M. (1975), "X-Ray Crystallographic Visualization of Drug-Nucleic Acid Intercalative Binding: Structure of an Ethidium-Dinucleoside Monophosphate Crystalline Complex, Ethidium: 5-Iodouridyl(3'-5')Adenosine," Proc. Natl. Acad. Sci. USA 72, 628-632

Tubbs, R. K., Ditmars, W. E., Van Winkle, Q (1964), "Heterogeneity of the Interaction of DNA with Acriflavine," J. Mol. Biol. 9, 545-557

von Hippel, P. H. and McGhee, J. D. (1972), "DNA-Protein Interactions," Ann. Rev. Biochem. 41, 231-300

Waring, M. J. (1965), "Complex Formation between Ethidium Bromide and Nucleic Acids," J. Mol. Biol. 13, 269-282

Waring, M. J. (1970), "Variation of the Supercoils in Closed Circular DNA by Binding of Antibiotics and Drugs: Evidence for Molecular Models Involving Intercalation," J. Mol. Biol. 54, 247-279

Waring, M. J. (1973), "Interaction of Indazole Analogs of Lucanthone and Hycanthone with Closed Circular Duplex-Deoxyribonucleic Acid," J. Pharm. Exp. Ther. 186, 385-389

Weinstein, I. B., Carchman, R., Marner, E., and Hirschberg, E. (1967), "Miracil D: Effects on Nucleic Acid Synthesis, Protein Synthesis, and Enzyme Induction in Escherichia coli," Biochim. Biophys. Acta 142, 440-449

Weinstein, I. B., Chernoff, R., Finkelstein, I., and Hirschberg, E. (1965), "Miracil D: An Inhibitor of Ribonucleic Acid Synthesis in Bacillus subtilis," Mol. Pharmacol. 1, 297-305

Weinstein, I. B. and Hirschberg, E. (1971), "Mode of Action of Miracil D," Progr. Mol. Subcell. Biol. 2, 232-246

Wilson, R. G., Bodner, R. H., and MacWorther, G. E. (1975), "Inhibition of Macromolecular Synthesis in L1210 Mouse Leukemia Ascites Cells by Hycanthone," Biochim. Biophys. Acta 378, 260-268

Wilson, R., Church, J., Bodner, R., Sylvain, N., and Hirschberg, E. (1972a), "The Effect of Miracil D and Analogs upon Nucleic Acid Synthesis in Leukemia L1210 Cells," Proc. Amer. Assoc. Canc. Res. 13, 76

Wilson, R. G., Church, J. A., and Sylvain, N. P. (1972b), "The Effect of Miracil D upon the Template Properties of Polynucleotides for a Bacterial RNA Polymerase," Biochim. Biophys. Acta 277, 564-566

Zilversmit, R. (1970), "Thioxanthenones: Structural Differences between Lucanthone and Its N-Methyl Derivative," Mol. Pharmacol. 6, 172-177

Zilversmit, R. (1971), "Thioxanthenones. II. Studies on the Hydrogen-Bonding Capacity of Lucanthone," Mol. Pharmacol. 7, 674-682

APPENDIX A

APPENDIX A

A Proposed Model for the Structure of Miracil D Dimers

in Aquaeous Media

Dyes, which are generally derivatives of planar heterocyclic aromatic rings, have long been known to form molecular aggregates in aquaeous solutions (Rabinowitch and Epstein, 1941). Aggregation is generally accompanied by spectral changes and under certain circumstances these spectral changes can be used to quantitate the aggregation process. The molecules in the aggregates are placed with their planes parallel to one another like coins in a stack. The aggregate is stabilized by dipole-dipole, dipole-induced dipole interactions and London dispersion forces. Charges located within the molecules generally can destabilize the aggregate.

For Miracil D, a stacked dimer structure can also be postulated which produces maximum stabilization by dispersion forces. Four major "stacked" arrangements are possible in which the long molecular axes are parallel to one another. Only two out of these four arrangements place the molecular dipoles in an opposing arrangement favourable for dipole-dipole interactions. In order to obtain maximum separation of the positive charges carried on the diethylaminoethylamino side chain of the Miracil D molecule, which could destabilize the dimer, the dimer with diagonally located side chains should be considered as the most probable structure for Miracil D dimers in 0.01 and 0.2 $\underline{M}$ sodium acetate buffers, pH 5.0 (Figure 42).

Figure 42. A dimer structure proposed for Miracil D in aquaeous solutions.
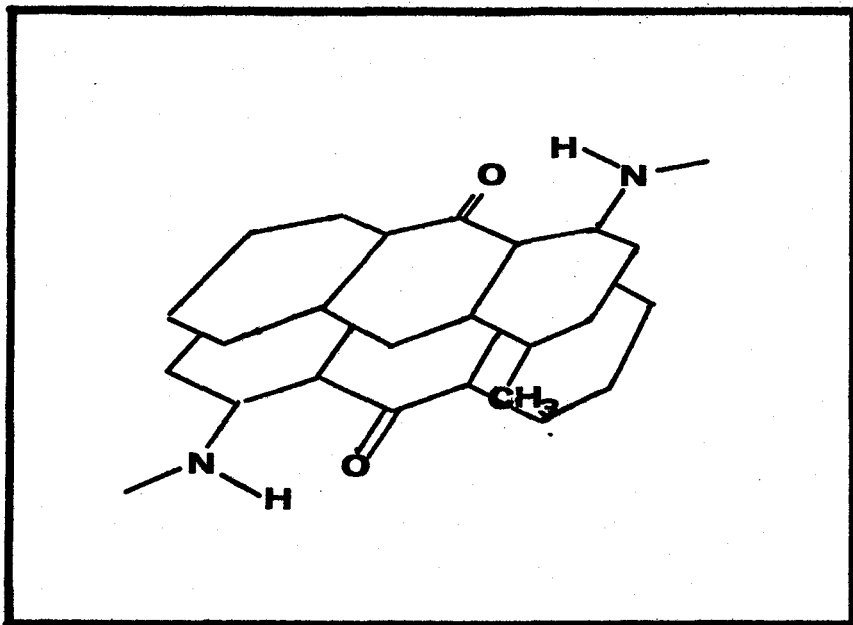
The experimental results obtained in these studies are consistent with the postulated dimer structure in two respects. First, the positively charged side chains are placed at a distance in the dimer that reduces the electrostatic repulsion between them to a negligible level. Therefore, changes in the ionic strength should not be expected to influence the stability of the dimer as a result of shielding of the electric charges. Indeed, the experimentally determined dimerization constants in 0.01 and 0.2 $\underline{M}$ sodium acetate buffers, pH 5.0 are found to be independent of ionic strength (see section III.1). Secondly, it may be noted that upon dimerization, the monomeric form of Miracil D is transferred from a completely aquaeous environment to an environment in which only one face of the molecule is exposed to the aquaeous phase while the other face being placed into contact with a hydrophobic medium. This environmental change is accompanied by a red shift of the absorption peak at 330 nm as expected. A similar red shift in this absorption maximum of Miracil D is observed upon transfer of the drug from polar to non-polar solvents (Zilversmit, 1971).

APPENDIX B

The Calculation of the Binding Isotherm

for the Exclusion Model

For the calculation of the binding isotherms of the exclusion model, a computer program was used, written in CPS PL/I language. The program is shown below:

```
 1.            GET LIST(N);
 2.            DECLARE A(N) CONTROLLED ,DNA(N) CONTROLLED ,R(N)
CONTROLLED ,ROCF(N) CONTROLLED ,AC(N) CONTROLLED;
 3.            IF ALLOCA(A) THEN FREE A,DNA,R,ROCF,AC;
 4.            ALLOCATE A,DNA,R,ROCF,AC;
 5.            GET LIST(A,DNA,CT);
 6.            GET LIST(AF,AB);
 7.    NEWK:   GET LIST(K);
 8.            PUT LIST('ASSOCIATION CONSTANT            =',K);
 9.            PUT LIST('ABSORBANCE OF FREE DRUG         =',AF);
10.            PUT LIST('ABSORBANCE OF BOUND DRUG        =',AB);
11.            PUT LIST('TOTAL DRUG CONCENTRATION        =',CT);
12.            DO I=2 TO N;
13.            R(I)=(AF-A(I))*CT/(AF-AB)/DNA(I);
14.            ROCF(I)=(AF-A(I))/(A(I)-AB)/DNA(I);
15.            END;
16.            /**/;
17.            DO I=2 TO N;
18.            CALL CALCA(K,CT,DNA(I),AF,AB,X);
19.            AC(I)=X;
20.            END;
21.            DO I=2 TO N;
22.            PUT LIST('');
23.            PUT LIST('');
24.            PUT LIST('                    SAMPLE #',I);
25.            PUT LIST('');
26.            CALL CALCA(K,CT,1.015*DNA(I),AF,AB,ACDU);
27.            CALL CALCA(K,CT,.985*DNA(I),AF,AB,ACDL);
28.            PUT LIST('LOWER ABS. LIMIT        =',ACDU-.003);
29.            PUT LIST('UPPER ABS. LIMIT        =',ACDL+.003);
30.            PUT LIST('ABSORBANCE OBSERVED     =',A(I));
31.            IF A(I)>ACDU-.003&A(I)<ACDL+.003 THEN PUT LIST ('
               IN RANGE'); ELSE PUT LIST('                    NOT
IN RANGE');
```

```
32.                PUT LIST('R OBSERVED              =',R(I));
33.                PUT LIST('R/CF OBSERVED           =',ROCF(I));
34.                PUT LIST('R THEORETICAL           =',(AF-AC(I))*CT
/(AF-AB)/DNA(I));
35.                PUT LIST('R MAX. DUE TO ERROR     =',(AF-ACDU+.003)*
CT/(AF-AB)/DNA(I));
36.                PUT LIST('R MIN. DUE TO ERROR     =',(AF-ACDL-.003)*
CT/(AF-AB)/DNA(I));
37.                PUT LIST('R/CF THEORETICAL        =',(AF-AC(I))/
(AC(I)-AB)/DNA(I));
38.                PUT LIST('R/CF MAX. DUE TO ERROR =',(AF-ACDU+.003)/
(ACDU-.003-AB)/DNA(I));
39.                PUT LIST('R/CF MIN. DUE TO ERROR =',(AF-ACDL-.003)/
(ACDL+.003-AB)/DNA(I));
40.                PUT LIST('EXP. DNA CONC.          =',DNA(I));
41.                END;
42.    CALCA:     PROCEDURE (KP,CTP,DNAP,AFP,ABP,AP);
43.                ALPHA=(-16*KP*CTP-8*KP*DNAP-4)/16/KP/DNAP;
44.                BETA=(8*KP*CTP+KP*DNAP+2)/16/KP/DNAP;
45.                GAMMA=-CTP/16/DNAP;
46.                IF BETA<3/16 THEN RUP=4*BETA/3; ELSE RUP=.25;
47.                RLP=0;
48.                COUNT=1;
49.    HALF:      RP=.5*(RLP+RUP);
50.                D=RP**3+ALPHA*RP**2+BETA*RP+GAMMA;
51.                IF D=0 THEN GO TO EXIT;
52.                IF D>0 THEN RUP=RP;
53.                IF D<0 THEN RLP=RP;
54.                IF COUNT>30 THEN GO TO EXIT;
55.                COUNT=COUNT+1;
56.                GO TO HALF;
57.    EXIT:      AP=AFP-(AFP-ABP)*RP*DNAP/CTP;
58.                END CALCA;
59.                STOP;
```

Storage area for the experimental data and the calculated

quantities of N samples is allocated in instructions 1 through 4. Ab-

sorbances (A), nucleic acid concentrations (DNA), total drug concen-

tration (CT), absorbances of free (AF) and bound (AB) drug are re-

quested in instructions 5 and 6. The experimental values of r (R) and

r/c_f (ROCF) of the samples are calculated in instructions 12 through

15. The theoretical absorbance (AC) of the samples with the arbi-

trary association constant (K), which is requested in instruction 7,

are calculated in instructions 17 through 20 using the internal procedure CALCA. The theoretical absorbance is calculated on the basis of the actual nucleic acid concentration. An error of 1.5 % in nucleic acid concentration is assumed, and the absorbances (ACDU and ACDL) corresponding to 1.5 % and -1.5 % errors are calculated in instructions 26 and 27.

Since the error of absorbance measurements is superimposed on the error in nucleic acid concentrations, an error of 0.003 in absorbance is taken into account at this point (ACDU-0.003 and ACDL+0.003). If the experimental absorbance falls between these two limits, IN RANGE is printed in instruction 31. The values of r and r/c_f corresponding to these absorbance limits and to the theoretical absobance are calculated in instructions 34 through 39.

The internal procedure CALCA consists of instructions 42 through 58. This procedure calculates the zero place of a polynomial of third degree in the $0 < RP < 0.25$ range. The notation of variables is the same as those in Appendix C, except that P's are added to the end of the variable names (in instructions 42 through 58) to signify that they are used in the internal procedure CALCA.

In the approximation of the zero place, the method of interval bisection is used. According to this method, the interval, in which the zero place is located, is halved and that half is selected as the basis of the next approximation step, for which the polynomial at the endpoints of the selected interval has opposite signs. The halving is repeated 30 times, so that the value of RP is determined with an accuracy of at least $0.25/2^{30}=2.3 \times 10^{-10}$. The analytical form of the poly-

nomial, and the existence and uniqueness of the zero place in the [0,0.25] interval are discussed in Appendix C.

Different values of K can be examined as to whether they fit the experimental points within experimental error or not by executing instructions 7 through 59.

APPENDIX C

Mathematical Proof for the Existence and Uniqueness of the Solution

of Binding Isotherm for the Exclusion Model

The binding of ligands to nucleic acids, when binding to the nearest neighbour sites is not allowed, can be described by equation

$$\frac{r}{c_f} = K \cdot \frac{(1-4\cdot r)^2}{2\cdot(1-2\cdot r)} \quad , \tag{4}$$

where the binding ratio r is defined as

$$r = \frac{c_b}{[P]} \quad , \tag{3}$$

and c_f and c_b are the molar concentrations of free and bound ligands, K is the intrinsic association constant, and [P] is the nucleic acid concentration (McGhee and von Hippel, 1974). Since for the total drug concentration c_t we have

$$c_t = c_f + c_b \quad ,$$

using the definition of the binding ratio r, c_f can be expressed as

$$c_f = c_t - r \cdot [P] \quad .$$

Substitution of c_f into equation (4) produces the following relationship:

$$\frac{r}{c_t - r \cdot [P]} = K \cdot \frac{(1-4 \cdot r)^2}{2 \cdot (1-2 \cdot r)} \ .$$

By defining α, β, and γ as

$$\alpha = - \ \frac{16 \cdot K \cdot c_t + 8 \cdot K \cdot [P] + 4}{16 \cdot K \cdot [P]} \ ,$$

$$\beta = \frac{8 \cdot K \cdot c_t + K \cdot [P] + 2}{16 \cdot K \cdot [P]} \ , \text{ and}$$

$$\gamma = - \ \frac{c_t}{16 \cdot [P]} \ ,$$

the binding isotherm can be written as a cubic equation of the form

$$r^3 + \alpha \cdot r^2 + \beta \cdot r + \gamma = 0.$$

In the interpretation of binding studies on the basis of this exclusion model, it is necessary to determine the value of r for given sets of K, c_t, and [P]. Since the calculation of the roots of this cubic equation by the Cardano formula is complex, a straightforward numerical approximation was developed. For the successful application of this numerical approximation, it was necessary to analyze the cubic equation itself.

Defining the f(r) polynomial by

$$f(r) = r^3 + \alpha \cdot r^2 + \beta \cdot r + \gamma \ ,$$

solving the cubic equation is equivalent to finding the zero places of the f(r) polynomial. Since only those r values, for which $0 \leq r \leq 0.25$,

have real physical meaning, solutions may be restricted to the [0,0.25] interval. At the endpoints of this interval $f(0)=-c_t/(16\cdot[P])$ and $f(0.25)=1/(64\cdot K\cdot[P])$. The values of c_t, K, and [P] are positive numbers, therefore, $f(0)<0$ and $f(0.25)>0$, i.e. the $f(r)$ polynomial changes sign in the [0,0.25] interval. The $f(r)$ polynomial is continuous for any r and, according to Bolzano's theorem, an r for which $f(r)=0$, where $0<r<0.25$, should exist. This assures that the $f(r)$ polynomial has at least one zero place in the interval of interest.

That there is no more than one zero place will be proven below. For this purpose, three cases will be distinguished on the basis of the value of β. The value of β determines whether the local extrema are maxima or minima. (The apostrophe will denote differentiation with respect to r.)
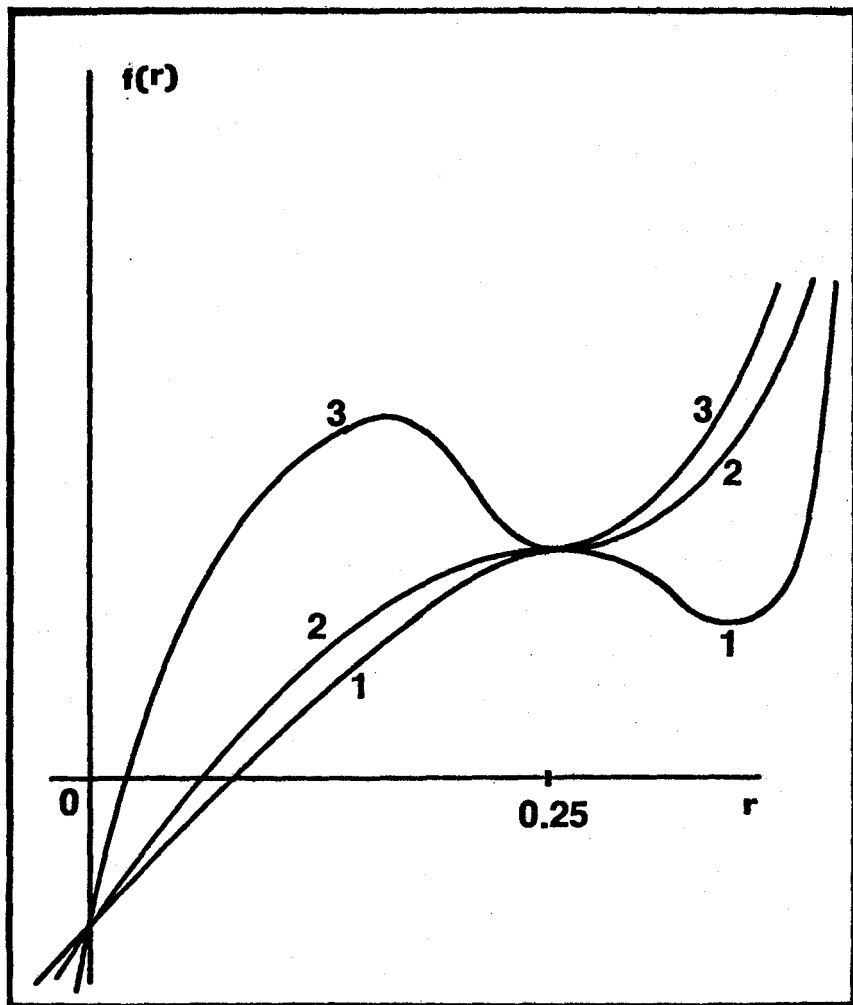
Case 1: $\beta>3/16$

Since $f'(0.25)=0$ and $f''(0.25)=-4\cdot\beta+3/4<0$, the polynomial exhibits a local maximum at r=0.25. Since $f'(4\cdot\beta/3)=0$ and $f''(4\cdot\beta/3)=4\cdot\beta-3/4>0$, the $f(r)$ polynomial exhibits a local minimum at $r=4\cdot\beta/3>0.25$. These extrema are separated by an inflection point at $r=2\cdot\beta/3+1/8>0.25$. Since $f'(r)=3\cdot(1-4\cdot r)\cdot(4\cdot\beta/3-r)/4$, and each term is positive if r<0.25, then $f'(r)>0$ if r<0.25. Therefore, $f(r)$ is monoton increasing in the [0,0.25] interval. Hence $f(r)$ cannot have more than one zero place in the interval of interest (Figure 43, curve 1).

Case 2: $\beta=3/16$

The $f(r)$ polynomial has no local extrema but exhibits an inflection point at r=0.25 because $f''(0.25)=0$. Since $f'(r)=3\cdot(1-4\cdot r)^2/16>0$ for any r, $f(r)$ is monoton increasing for any r. Hence $f(r)$ cannot have

Figure 43. Schematic representation of the f(r) polynomial for different values of β as parameter. (1) β>3/16, (2) β=3/16, and (3) β<3/16 (see text for details).

more than one zero place in the [0,0.25] interval (Figure 43, curve 2).

Case 3: $\beta < 3/16$

Since $f'(4 \cdot \beta/3)=0$ and $f''(4 \cdot \beta/3)=4 \cdot \beta-3/4<0$, the $f(r)$ polynomial exhibits a local maximum at $r=4 \cdot \beta/3<0.25$. Since $f'(0.25)=0$ and $f''(0.25)=-4 \cdot \beta+3/4>0$, the $f(r)$ polynomial exhibits a local minimum at $r=0.25$. At this local minimum the polynomial is still positive because $f(0.25)=1/(64 \cdot K \cdot [P])$. The extrema are separated by an inflection point at $r=2 \cdot \beta/3+1/8<0.25$. Since $f'(r)=3 \cdot (1-4 \cdot r) \cdot (4 \cdot \beta/3-r)/4$, the $f(r)$ polynomial is monoton increasing when $r<4 \cdot \beta/3$ (before the local maximum), is monoton decreasing when $4 \cdot \beta/3<r<0.25$ (between the two extrema), and is monoton increasing again when $r>0.25$ (after the local minimum). Consequently, there is only one zero place in the $[0,4 \cdot \beta/3]$ interval. Although $f(r)$ is monoton decreasing in the $[4 \cdot \beta/3,0.25]$ interval, there is no zero place in this interval because the polynomial is still positive at the minimum. Hence there is only one zero place in the [0,0.25] interval (Figure 43, curve 3).

It can be concluded that there is one and only one zero place in the [0,0.25] interval regardless of the value of β.

APPROVAL SHEET

The dissertation submitted by Laszlo Bodoni has been read and approved by the following Committee:

Dr. Stelios Aktipis, Director
Professor, Biochemistry, Loyola

Dr. Mary Ellen Druyan
Assistant Professor, Biochemistry, Loyola

Dr. Allen Frankfater
Associate Professor, Biochemistry, Loyola

Dr. Eugene O. Major
Assistant Professor, Microbiology, Loyola

Dr. Harvey W. Posvic
Associate Professor, Chemistry, Loyola

The final copies have been examined by the director of the dissertation and the signature which appears below verifies the fact that any necessary changes have been incorporated and that the dissertation is now given final approval by the Committee with reference to content and form.

The dissertation is therefore accepted in partial fulfillment of the requirements for the degree of Doctor of Philosophy.

January 30, 1978
Date

Director's Signature